Minimizing the Impact of Resonances in Low Voltage Grids by Power Electronics based Distributed Generators

PROEFSCHRIFT

ter verkrijging van de graad van doctor aan de
Technische Universiteit Eindhoven, op gezag van de
rector magnificus, prof.dr.ir. C.J. van Duijn, voor een
commissie aangewezen door het College voor
Promoties in het openbaar te verdedigen
op maandag 18 april 2011 om 16.00 uur

door

Petrus Jacobus Marie Heskes

geboren te ’s-Gravenhage

Dit proefschrift is goedgekeurd door de promotor:

prof.ir. W.L. Kling

Copromotor:
Univ.-Prof.Dr.-Ing. J.M.A. Myrzik

The work leading to this thesis was supported by the Energy Research Centre of the Netherlands (ECN) and the EOS-LT program of Agentschap NL.

Printed by: Printservice Technische Universiteit Eindhoven.
Cover design by: Paul Verspaget Grafische Vormgeving-Communicatie.

A catalogue record is available from the Eindhoven University of Technology Library.

ISBN: 978-90-386-2456-3

Promotor:

prof.ir. W.L. Kling, Technische Universiteit Eindhoven

Copromotor:

Univ.-Prof.Dr.-Ing. J.M.A. Myrzik, Technische Universiteit Dortmund

Core committee:

Univ.-Prof.Dr.-Ing. A. Monti, RWTH Universiteit Aken

dr.ir. P. Bauer, Technische Universiteit Delft

dr.ir. P. Ribeiro, Technische Universiteit Eindhoven

Other members:

prof.dr. E.A. Lomonova, Technische Universiteit Eindhoven

ir. M.J.J. Scheepers, Energieonderzoek Centrum Nederland

prof.dr.ir. A.C.P.M. Backx (chairman), Technische Universiteit Eindhoven

Minimizing the Impact of Resonances in Low Voltage Grids by Power Electronics based Distributed Generators

Summary

Today's Distributed Generators (DG) and load appliances are increasingly build up with power electronics. This trend is expected to grow further in the future. Also developments are ongoing to improve the performance and efficiency of grid components by means of power electronics and several grid components might be replaced by power electronics based versions in the future. One of the nice properties of power electronics based grid components is the possibility of voltage control. This feature is very welcome to keep voltage levels within prescribed limits while implementing large numbers of DG. Load appliances often use internal circuits that work on a controlled direct voltage level and this is achieved by using power electronics. In this way the performance of such appliances is much higher today than in the past. Besides this and other advantages, disadvantages will also show up. The disadvantages that are studied in this thesis are the increased harmonics caused by resonances and oscillatory voltages caused by non-linear constant power loads.

Beside existing resonances in the grid, new ones will be added by large numbers of capacitances used in Electro Magnetic Interference (EMI) filters of power electronics based appliances. These capacitances can interact with inductances in the grid and bring significant resonances that can amplify harmonic currents and voltages to a high level, even in the lower harmonic frequency range.

Oscillatory voltages can be caused by improper stabilization actions. Stabilization of a voltage level on a load in an active way, thus by making use of a power electronics converter, brings a constant power load to the grid. This kind of load behaves as a negative differential impedance which can contribute to an oscillatory grid voltage.

The proposed solution in this thesis for minimizing the impact of resonances caused by parallel capacitances in the grid is a combination of two so called ancillary services, namely Virtual Parallel Capacitance Reduction (VPCR) and Virtual Resistive Harmonic Damping (VRHD). VPCR is an ancillary service that let a power electronics converter generate a current to compensate currents through the capacitances placed in parallel with the grid, for a frequency range that includes the fundamental and a number of harmonics. VRHD is an ancillary service that gives a power electronics converter a resistive behavior for a number of harmonics. This action will bring extra damping to resonances in the grid.

Especially the combination of both VPCR and VRHD is an approach that is very effective for minimizing the impact of resonances in the Low Voltage (LV) distribution grid. This combination provides two measures. Firstly VPCR with its compensation current causes the effect that a resonance is virtually shifted towards a higher frequency value, in the range where the propagation is limited. Secondly VRHD damps the resonance peak to a lower level.

VPCR and VRHD can be implemented in appliances with a power electronics interface directly coupled to the grid and in inverters for DG. They do not need a series regulator, because these services are shunt based and acting as active shunt filters. This thesis studies the implementation of VPCR and VRHD in inverters for DG.

It has been noticed in various situations in the Netherlands that concentrations of large numbers of EMI filter capacitors of Photovoltaic (PV) systems can bring problematic resonances to the distribution grid. In these cases, large numbers of small inverters for PV systems were connected to the grid which resulted in a high level of harmonic voltage distortion caused by these grid resonances. Studies showed that the parallel output capacitor of inverters for PV systems is relatively high and on an average can triple the total parallel capacitance value at the Point of Connection (PoC) of a dwelling. Another development that increases the total number of capacitors connected to the grid is that appliances are not galvanically isolated from the grid anymore in the switched-off mode. In this mode the appliance goes to an idle state and the EMI filter capacitor remains connected.

To master the transition towards a more decentralized generation, knowledge about the harmonic interactions and minimizing the impact of resonances is very important. Research on this is needed to separate causes and effect in situations of insufficient quality of the grid voltage, and to come to the right measures to handle these problems.

The research in this thesis deals with the harmonic interaction and minimizing of the impact of resonances in a future situation with large numbers of power electronics based load appliances and DG. Based on the problem definition above, the general objective of this thesis is defined as:

> Investigate the possibilities to minimize the impact of resonances and harmonic distortions by using ancillary functionalities of the power electronics inverters of DG that are connected to the LV distribution grid.

The research work is performed by means of computer simulations and laboratory validation. The most important contribution of the work is the development of a control strategy for the grid connected DG inverters which minimizes harmonic voltage pollution. An important element of the work was the building and programming of a versatile inverter with a Digital Signal Processor (DSP) structure, used for validation of the laboratory set-ups. With this versatile inverter, various control strategies could be implemented to minimize harmonic voltage pollution.

The contributions of this thesis can be summarized as follows:

- a detailed description of the basic concept of harmonic interaction and grid resonances to separate cause and effect,
- the development of a grid impedance spectrum measurement system for the estimation of grid resonances,
- the development of computer models and simulations of a small grid and inverters for DG with the ancillary service functions VPCR and VRHD to study grid resonances,
- a versatile hardware model of an inverter with a DSP control is build and the ancillary service functions VPCR and VRHD to minimize the effect of grid resonances are implemented,
- laboratory validation is performed of computer model simulations of inverter hardware with the ancillary services,

- computer simulations are done of a distribution system with grid resonances and inverters with ancillary services.

The main conclusions are described below.

Oscillatory voltages caused by the interaction between voltage control systems and constant power loads are only expected at sub harmonic frequencies. A possible solution for these oscillations can be found in adjusting the parameters of voltage control systems.

Results of the validated simulations show that the studied ancillary services perform as expected, especially the combination of two described ancillary services VPCR and VRHD is a strong measure to minimize the impact of resonances in the harmonic frequency range, in the LV distribution grid. These services produces the effect of a virtual resonance shift towards a higher harmonic frequency range where the propagation is limited, and damp resonance peaks to a lower level.

Results from simulated and practical measurements show that the grid impedance spectrum measurement system can work well by injecting a very low measurement current. The system is capable of operating under polluted grid voltages.

Samenvatting

Tegenwoordig zijn Decentrale Generatoren (DG) en verbruikstoestellen steeds meer opgebouwd met vermogenselektronica. Het is te verwachten dat deze trend zich verder doorzet in de toekomst. Ook zijn er ontwikkelingen gaande om de prestatie en efficiëntie te verbeteren van netcomponenten door toepassing van vermogenselektronica en diverse netcomponenten worden mogelijk vervangen door vermogenselektronische versies in de toekomst. Een van de aantrekkelijke eigenschappen van vermogenselektronische netcomponenten is de mogelijkheid van spanningsregeling. Deze eigenschap is zeer welkom om spanningsniveaus binnen de voorgeschreven grenzen te houden als grote aantallen DG geïmplementeerd worden. Verbruikstoestellen gebruiken vaak interne schakelingen die werken op een gecontroleerd gelijkspanningsniveau en dit wordt bereikt door toepassing van vermogenselektronica. Op deze manier is de prestatie van dergelijke apparaten vandaag de dag veel hoger dan in het verleden. Naast dit en andere voordelen, zijn er ook nadelen. De nadelen die bestudeerd zijn in dit proefschrift zijn de toenemende harmonischen veroorzaakt door resonanties en oscillerende spanningen ten gevolge van niet-lineaire constant-vermogen-belastingen.

Naast bestaande resonanties in het net, zullen er nieuwe toegevoegd worden door de grote aantallen capaciteiten, die gebruikt worden in Electro Magnetische Interferentie (EMI) filters van vermogenselektronische toestellen. Deze capaciteiten kunnen wisselwerken met inducties in het net en behoorlijke resonanties veroorzaken die harmonische stromen en spanningen kunnen versterken naar een hoog niveau, zelfs in het lagere harmonische frequentiegebied.

Oscillerende spanningen kunnen veroorzaakt worden door ongepaste stabilisatie-acties. Stabilisatie van een spanningsniveau op een belasting op een actieve manier, dus door gebruik te maken van een vermogenselektronische omvormer, zorgt voor een constant-vermogen-belasting op het net. Dit soort belasting gedraagt zich als een negatieve differentiaalimpedantie die kan bijdragen aan een oscillerende netspanning.

De voorgestelde oplossing in dit proefschrift om het effect van resonanties, veroorzaakt door de parallelle capaciteiten in het net, te minimaliseren, is een combinatie van twee zogenaamde aanvullende diensten, namelijk Virtual Parallel Capacitance Reduction (VPCR) en Virtual Resistive Harmonic Damping (VRHD). VPCR is een aanvullende dienst die vermogenselektronische omvormers een stroom laat genereren om de stromen door de capaciteiten parallel aangesloten op het net te compenseren, voor een frequentieband die de grondfrequentie en een aantal harmonischen omvat. VRHD is een aanvullende dienst die vermogenselektronische omvormers het gedrag van een weerstand geeft voor een aantal harmonischen. Deze actie zal voor extra demping zorgen van de resonanties in het net.

Met name de combinatie van zowel VPCR en VRHD is een aanpak die erg effectief is om de gevolgen van resonanties in het laagspanningsnet (LS) te minimaliseren. Deze combinatie voorziet in twee maatregelen. Ten eerste, VPCR met zijn compensatiestroom veroorzaakt het effect dat een resonantie virtueel verschoven wordt naar een hogere frequentiewaarde, in het gebied waar de voortplanting beperkt is. Ten tweede, VRHD dempt de resonantiepiek naar een lager niveau.

VPCR en VRHD kunnen geïmplementeerd worden in toestellen met een vermogenselektronische interface, die direct gekoppeld zijn aan het net, en in omvormers voor DG. Ze hebben geen serieregelaar nodig, omdat deze diensten gebaseerd zijn op parallelwerking en zich gedragen als parallel geschakelde actieve filters. Dit proefschrift bestudeert de toepassing van VPCR en VRHD in omvormers voor DG.

Het is waargenomen in verschillende situaties in Nederland dat concentraties van grote aantallen EMI filter condensatoren van photovoltaïsche (PV) systemen problematische resonanties in het distributienet kunnen veroorzaken. In deze situaties waren grote aantallen kleine omvormers voor PV systemen verbonden met het net, wat resulteerde in een hoog niveau van harmonische spanningsvervorming veroorzaakt door deze netresonanties. Studies hebben aangetoond dat de parallelle uitgangscondensator van de omvormers voor PV systemen relatief groot is en gemiddeld genomen de totale parallelle capaciteitswaarde op het aansluitpunt van een woning kan verdrievoudigen. Een andere ontwikkeling die het totale aantal condensatoren verbonden aan het net vergroot, is dat toestellen niet meer galvanisch gescheiden worden van het net in de uitgeschakelde toestand. In deze situatie gaat het toestel naar een rust-toestand en de EMI filter condensator blijft verbonden.

Om de transitie naar een meer gedecentraliseerde opwekking te beheersen, is kennis nodig van de harmonische interacties en is het minimaliseren van de gevolgen erg belangrijk. Onderzoek hiernaar is nodig om oorzaak en gevolg te onderscheiden in situaties van onvoldoende kwaliteit van de netspanning en om te komen tot de juiste maatregelen om deze problemen aan te pakken.

Het onderzoek in dit proefschrift handelt over harmonische interacties en het minimaliseren van de gevolgen van resonanties in een toekomstige situatie met grote aantallen vermogenselektronische belastingen en DG. Gebaseerd op bovenstaande probleemstelling, is het algemene doel van dit proefschrift gedefinieerd als:

> Onderzoek de mogelijkheden om de gevolgen van resonanties en harmonische vervormingen te minimaliseren door gebruik te maken van aanvullende diensten van de vermogenselektronische omvormers van DG aangesloten op het laagspanningsdistributienet.

Het onderzoek is uitgevoerd door middel van computersimulaties en laboratorium validaties. De meest belangrijke bijdrage van dit werk, is de ontwikkeling van een regelstrategie voor netgekoppelde DG-omvormers die de harmonische spanningsvervuiling minimaliseren. Een belangrijk element van het werk was het bouwen en programmeren van een universele omvormer met een Digitale Signaal Processor (DSP) structuur, die gebruikt is voor validatie van de laboratorium opstellingen. Met deze universele omvormer konden diverse regelstrategieën geïmplementeerd worden om de harmonische spanningsvervuiling te minimaliseren.

De bijdragen van dit proefschrift kunnen als volgt samengevat worden:

- een gedetailleerde beschrijving van het basisconcept van harmonische interacties en netresonanties, om gevolg en effect te scheiden,
- de ontwikkeling van een netimpedantiespectrum-meetsysteem voor het bepalen van netresonanties,
- de ontwikkeling van computermodellen en simulaties van een klein net en omvormers voor DG, met de aanvullende functies VPCR en VRHD, om netresonanties te bestuderen,
- een universeel hardware model van een omvormer met een DSP besturing is gebouwd en de aanvullende functies VPCR en VRHD, om het effect van netresonanties te minimaliseren zijn geïmplementeerd,

- laboratorium validatie is uitgevoerd van de computer model simulaties van de omvormer hardware met de aanvullende diensten,
- computer simulaties zijn gedaan van een distributiesysteem met netresonanties en omvormers met aanvullende diensten.

De belangrijkste conclusies zijn hieronder beschreven.

Oscillerende spanningen veroorzaakt door de interactie tussen spanningsregelsystemen en constant-vermogens-belastingen worden alleen verwacht bij subharmonische frequenties. Een mogelijke oplossing voor deze oscillaties kan gevonden worden in de afstelling van de parameters van spanningsregelingen.

Resultaten van de gevalideerde simulaties tonen aan dat de bestudeerde aanvullende diensten naar verwachting presteren, met name de combinatie van de twee beschreven aanvullende diensten VPCR en VRHD, is een sterke maatregel om de gevolgen van resonanties in het LS-distributienet, in het harmonische frequentiegebied, te minimaliseren. Deze diensten produceren het effect van een virtuele resonantieverschuiving naar een hoger harmonisch frequentiegebied waar de voortplanting gelimiteerd is, en dempen resonantiepieken naar een lager niveau.

Resultaten van gesimuleerde en praktische metingen tonen aan dat het netimpedantiespectrum-meetsysteem goed kan werken door zeer lage meetstromen te injecteren. Het systeem is in staat te werken onder vervuilde netspanningen.

Contents

Chapter 1

Introduction

This chapter shortly describes the impact of important changes in the electricity grid towards the future with special focus on the connected appliances. This motivates the research in this field. The specific research objectives, questions and approach of this thesis are described and also the relation with international research and a national long-term research program. An outline of the thesis is included in this chapter.

1.1 Background and problem definition

New technologies such as smart systems to optimize energy use, will greatly increase energy efficiency and lead to savings in the consumption of electrical energy. But beside these energy saving technologies, new electricity usage such as electric vehicle battery charging systems will become more popular. Therefore the total electrical energy use at the end of the 21st century, will be much higher than today [WEC 04], [Mee 08].

One of the European Commission's 20-20-20 policy targets is to have 20% of the total energy consumption from renewable sources in the year 2020. As electricity will have a main share in this development, Distributed Generation (DG) with local wind and Photovoltaic (PV) energy sources is expected to grow to large numbers integrated in the electricity grid.

This situation is totally different from today. DG will affect voltage control and protection because of the possibility of a reverse energy flow. Voltage levels in a distribution grid can rise in situations of a local surplus of generation [Cob 07]. Protection can also be affected in these situations, e.g. response times to clear a fault can be problematically increased [Cos 10]. New components will be integrated to control demand and supply, power flow, voltage stability and the quality of the voltage.

In general, the electricity grid that will conduct the future energy supply will need to be able to integrate a large share of renewables. These sources can be centralized in large-scale offshore wind farms and concentrated solar systems as well as in a distributed form like large numbers of small PV and micro Combined Heat and Power (μCHP) installations.

1.1.1 Impact of power electronics based DG and appliances

Beside the mentioned developments, DG and load appliances are increasingly build up with power electronics. This trend is expected to grow further in the future. At this moment also developments are ongoing to improve the performance of grid components by means of power electronics. Several grid components in the future might be replaced by power electronics based versions. One of the major properties of power electronics based grid components is the possibility of automated voltage control. This feature is very welcome to keep voltage levels within prescribed limits while implementing large numbers of DG. Load appliances often use internal circuits that work on a controlled direct voltage level which can be achieved by using power electronics. In this way performance of appliances can be much higher today than in the past. Beside this and other advantages, disadvantages will also show up. The disadvantages that are studied in this thesis are amplified harmonics caused by resonances and oscillatory voltages caused by constant power loads.

1.1.2 Oscillatory voltages

One specific disadvantage of the use of power electronics is the Constant Power Load (CPL) behavior which introduces a Negative Differential Impedance (NDI). This CPL behavior is caused by stabilization of a voltage level on a load in an active way, thus by making use of a power electronics converter. Large numbers of CPLs can be the cause of an oscillatory grid voltage [Mol 08], [Ema 04]. This thesis proposes a solution to reduce oscillatory voltages by changing the voltage control parameters.

1.1.3 Resonances

Another disadvantage of the use of power electronics is caused by the interaction of output capacitors of power electronics based appliances at one hand and grid inductances at the other hand. This interaction can add problematic resonances to the grid. Large numbers of parallel capacitances used in Electro Magnetic Interference filters (EMI-filters) of power electronics based appliances and inverters for DG can bring resonances in the grid that can amplify harmonic currents and voltages to a high level, even in the lower harmonic frequency range. Concentrations of large numbers of EMI-filter capacitors of PV systems can bring problematic resonances which already have been noticed in various situations, under which some demonstration projects in the Netherlands [End 01], [Ens 04], [Hes 05], [Kot 05], [Lis 06]. In these projects, large numbers of small inverters for PV systems were connected to the Low Voltage (LV) grid which resulted in a high level of harmonic voltage distortion caused by the interaction of non-linear loads and these grid resonances. Studies showed that the parallel output capacitor of the inverters for PV systems is relatively high and on average can triple the total parallel capacitance at the Point of Connection (PoC). Another development that increases the total number of capacitors connected to the grid is that appliances are not galvanically isolated from the grid anymore in the switched-off mode. In this mode the appliance goes to an idle state and the EMI-filter capacitor remains connected. This thesis proposes a solution to minimize the impact of these added resonances by implementing extra control loops on power electronics inverters for DG.

1.1.4 Ancillary services to minimize the impact of resonances

The proposed solution in this thesis for the minimization of the impact of resonances because of parallel capacitances in the grid is a combination of two so called ancillary services, namely Virtual Parallel Capacitance Reduction (VPCR) and Virtual Resistive Harmonic Damping (VRHD). VPCR is a service that let a power electronics converter generate an extra current to compensate currents through capacitances placed in parallel with the grid, for a frequency range that includes the fundamental and a number of harmonics. VRHD is a service that gives the power electronics converter a resistive behavior for a number of harmonics. This action will bring extra damping to resonances in the grid.

Especially the combination of both VPCR and VRHD is an approach that is very effective for minimizing the impact of resonances in the LV distribution grid.

1.2 Objective and research questions

1.2.1 Introduction

To master the transition towards the future electricity supply, knowledge about the harmonic interactions and minimizing the impact of resonances is very important. Research on this is needed to separate causes and effect in situations of insufficient quality of the grid voltage, and to come to the right measures to handle these problems. Management systems to control generation and loads will be indispensable and in spite of all these changes, stability of the system and quality of the grid voltage must be sustained.

The research described in this thesis focuses on the quality of the grid voltage at a Point of Common Coupling (PCC) in the LV distribution grid and also at the PoC between the Distribution System Operator (DSO) and the customer as illustrated in Figure 1.1. The work will show possibilities to improve the quality of the grid voltage in expected future situations, by means of ancillary services in power electronics based DG. These ancillary services can also be implemented in home appliances with a power electronics converter that is directly coupled the grid.

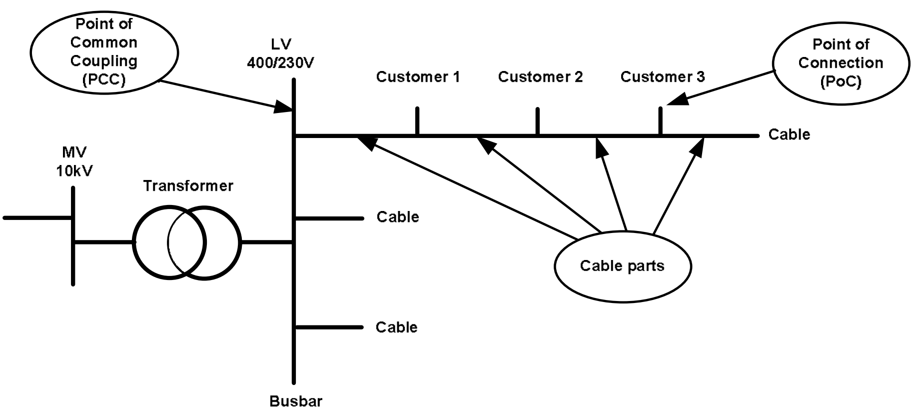

Figure 1.1: Example of a LV distribution grid, one PCC and one PoC example is depicted.

1.2.2 Objective and research questions

Based on the problem definition of section 1.1, the general objective of this thesis is defined as:

> *Investigate the possibilities to minimize the impact of resonances and harmonic distortions by using ancillary functionalities of the power electronics inverters of DG that are connected to the LV distribution grid.*

From this objective, the following research questions have been derived:

- How can the harmonic interaction be represented and analyzed?

- How to develop a method to estimate the sensitiveness of the grid for harmonic voltage pollution?
- How can stabilization against grid voltage fluctuations, by power electronics converters cause an oscillatory grid voltage and how to minimize this effect?
- How to develop an inverter for DG with ancillary services, to minimize the effect of grid resonances that can cause harmonic voltage distortion?
- Can large numbers of power electronics based DG in a LV distribution grid virtually compensate parallel capacitances and damp resonances?

1.2.3 Relation with other research

1.2.3.1 Harmonic reduction

This thesis research focuses on the minimization of the harmonic distortion by active filters that are integrated in power electronics based DG. Solutions with a shunt active filter are considered because this type of filter can be implemented in a grid connected power electronics inverter. Small inverters for DG, up to about 5 kW, often make use of fast switching semiconductors. This makes the inverter capable of controlling its output current not only for the fundamental frequency, but also in the harmonic frequency range.

This limitation to only use shunt active filters in a distribution grid has a drawback. Harmonics from non-linear loads in the Medium Voltage (MV) grid should not be handled with only shunt active filters in the LV grid (see Chapter 2). For these so called background harmonics, an optimal solution would be the integration of series-active and shunt-active filters [Fuj 98a].

A very attractive way to reduce harmonic distortion is the use of resistive impedance for harmonics. A number of papers like [Ryc 02], [Gus 07] recommend that polluting loads like diode-capacitor rectifiers should have an electronics front-end with a Power Factor Corrector (PFC) and that these PFCs should have a resistive impedance for harmonics. This approach will damp harmonics and is also very effective for damping of resonances in the grid. Further this is easy to implement in all kinds of grid situations because there is no need to measure grid parameters, only the grid voltage at the output connectors of the PFC itself must be measured. This damping system can be implemented in inverters for DG [Ryc 05b] and in bidirectional full-bridge AC-DC converters [Ryc 06] as well.

There is however a contradiction in the needed counter-measure for background harmonics and harmonics from non-linear loads in the distribution grid, therefore the harmonic damping must be limited to avoid wrong compensation of background harmonics (see Chapter 2). This wrong compensation can result in excessive harmonic currents through the distribution transformer, lines and cables. The best solution for the reduction of background harmonics, is to tackle the problem at the source, for example a harmonic shunt compensator nearby a disturbing load, that is causing harmonic pollution in surrounding distribution grids. But when sufficient compensation of the disturbing load locally cannot be performed, a possible solution then could be the implementation of active filters on substation level [Aka 05]. Both solutions will possibly work very well together. Research on combinations of filters can be found in [Fuj 98a], [Fuj 98b] and [Aka 96].

In the harmonic reduction technique for compensation of background distortion with an active filter on substation level, probably also a series active filter will be needed [Aka 05]. In [Aka 96] is explained that series and shunt active filters are "dual" to each other, therefore the combination of these two can bring a total package for:

- background compensation because of harmonic isolation between the sub-transmission system and the distribution system by the series active filtering,
- damping of the amplification (resonances) of voltage harmonics in a distribution feeder by the shunt active filtering,
- harmonic current compensation by the shunt active filtering.

The last item "harmonic current compensation" may not be needed if a remainder harmonic distortion is allowed. A series active filter can be used then for background compensation and a shunt active filter acting as a resistive harmonic impedance for damping of harmonics and resonances. The first one can be placed at the MV/LV substation and the latter one can be integrated in LV inverters for DG.

The integration of a series and a shunt active filter in one filter that is located at the MV/LV substation, would be a solution to implement for the DSO. This solution is however in contradiction with the conclusion of paper [Aka 97], that states that the best location is not the beginning terminal but the end terminal of the primary line in the feeder, and also in contradiction with [Aka 99] which recommends an active filter that acts as a harmonic termination resistor at the end of the power distribution line. However if the first priority is the damping of possible resonances in the grid and the second priority the reduction of harmonics, a new approach is needed. Such a new approach in priority settings holds for future grids with increasing numbers of capacitive loads, were possible resonances in the grid is a real threat and reduction of this has a high priority [Cob 07]. Paper [Jin 02] discusses the optimal damping impedance and compares it to the characteristic impedance of a line, Z_0. Paper [Ryc 06] discusses that the magnitude of the resistive harmonic impedance must be independent of the fundamental impedance magnitude, i.e. the resistive harmonic impedance must be a constant value. Recommended are values in between 0.5 to 2 times the equivalent resistance that would draw the rated power of the appliance that offers this service, from the grid. In paper [Ryc 02] is shown that the required shunt harmonic impedance does not necessarily have to be limited to purely resistive values.

1.2.3.2 Measurement system

One method to measure the harmonic impedance of a LV distribution grid, is based on double phase locked amplifiers [Vis 05]. Results of this system can be good, however a disadvantage is the measurement of only one frequency at a time.

In the paper [Kar 05] Fourier-based methods are discussed and reminds readers that Fourier-based methods can only detect integer multiples of the base frequency. It also discusses the low accuracy when estimating small (weak) frequency components which are masked by large near-by frequency components or high noise levels.

Measurement systems, based on Fourier transformation or based on a phase locked principal can only work well if during the averaging time the input signal is constant and periodical. In practice, voltage and current harmonics are time-variant because of continual changes in load conditions, and to some extent in system configuration [Bag 02]. In [Bag 98] several approaches are presented, that have been proposed in recent years, to improve the accuracy of measuring harmonic magnitudes in time varying conditions. Measurement of time varying signals is an active research area in signal processing techniques [Rib 09]. Paper [Bag 98] also discusses typical variations of harmonic signals, from recorded data at two different industrial sites. It can be seen that the Total Harmonic Distortion (THD) can be constant for about a few minutes, this will be long enough for a complex impedance measurement, however sudden changes also can happen; a measurement system must be able to cope with this.

1.2.3.3 Cooperative control

Paper [Jin 03] proposes cooperative control with a communication link of multiple active filters. This paper discusses with a number of references, that independent control might make multiple active filters produce unbalanced compensating currents. In paper [Jin 02] the first step in cooperative control with a communication link of multiple active filters was made. In this thesis cooperative control of multiple inverters without a communication link will be studied for damping harmonics in LV distribution grids.

1.3 Approach

The research work is performed by means of computer simulation and laboratory validation, based on a theoretical fundament. The most important part of the work is the development of a control strategy for grid connected DG, that minimizes harmonic voltage pollution. Another important part of the work is the building and programming of a versatile inverter with a Digital Signal Processor (DSP) structure, used for validation in laboratory set-ups. With this versatile inverter, various control strategies can be implemented to minimize harmonic voltage pollution.

The work of this thesis can be summarized as follows:

- a detailed description of the basic system of harmonic interaction and grid resonances will be made to separate cause and effect,
- a grid impedance spectrum measurement system will be developed for the estimation of the potential to increase harmonic voltage pollution by power electronics based load appliances and DG inverters,
- computer models will be developed and simulations will be done of a small grid and inverters for DG with the ancillary service functions VPCR and VRHD to study grid resonances,
- a versatile hardware model of an inverter with a DSP control will be build and the ancillary service functions VPCR and VRHD will be implemented to minimize the effect of grid resonances,
- laboratory validation of computer model simulations of inverter hardware with the ancillary services will be performed,
- a distribution systems with grid resonances and inverters with ancillary services to minimize this will be computer simulated.

1.4 Relation to the EOS-LT project KTI

The research presented in this thesis has been performed within the framework of the EOS-LT project KTI (in Dutch "Kwaliteit van de spanning in Toekomstige Infrastructuur"). The project is related to the quality of the voltage in future infrastructure and aims to answer essential research questions in this respect. This project is subsidized by the Long Term Energy Research Program, (in Dutch “Energie Onderzoek - Subsidie Lange Termijn, EOS-LT) from Agentschap NL (former SenterNovem), an agency of the Dutch Ministry of Economical Affairs. The program wants to extend new energy technology, and aims to stimulate research in this field with a long term horizon, i.e. introduction to the market is further away than 10 years. Results need to contribute to energy efficiency and sustainable energy in the Netherlands and needs to improve knowledge in this field.

1.4.1 Structure

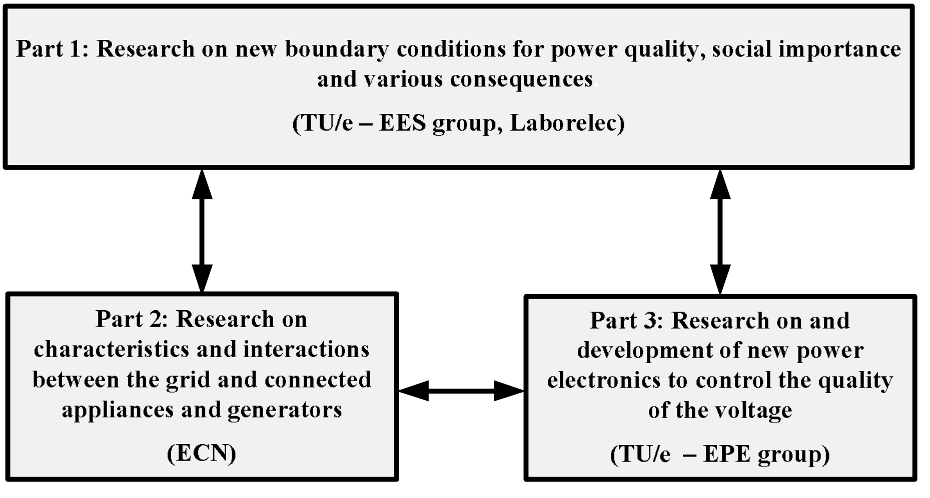

Figure 1.2: Structure of the KTI project.

Figure 1.2 gives an overview of the structure of the KTI project. The project is divided into three parts, being:

1. Research on new boundary conditions, social aspects and responsibilities. The EES group of the Eindhoven University of Technology (TU/e – EES group) and Laborelec are responsible for this part.

The research in this part addresses the needs of grid operators, customers, manufacturers and legislators, and will make clear which developments are expected and how responsibilities must be adjusted to guarantee control over the quality of the voltage in a future infrastructure. This must lead to an economic optimum for future grids, installations and appliances.

2. Research on characteristics and interactions between the grid and connected appliances and generators. The Energy Research Centre of the Netherlands (ECN) is responsible for this part.

   In this part, analysis of interactions between grid, installations, appliances and generators are performed. Studied is the today's behavior of installations and appliances and the needed behavior in a future infrastructure, to control the quality of the voltage. Special point of attention is the effect of ancillary services provided by power electronics, to improve the quality of the voltage at the PoC.

3. Research on and development of new power electronics to control the quality of the voltage. The EPE group of the Eindhoven University of Technology (TU/e – EPE group) is responsible for this part.

   The research in this part focuses on new power electronics with the possibility to control the quality of the voltage in a way that appliances of users can function well under various voltage quality conditions.

Part 2 was the basis of the work that was done for this thesis.

1.5 Thesis outline

Chapter 1 Introduction

Two power quality issues are studied in this thesis which may become more important in future electricity grids with large numbers of power electronics based DG and load appliances. An overview of the context is given in Figure 1.3.

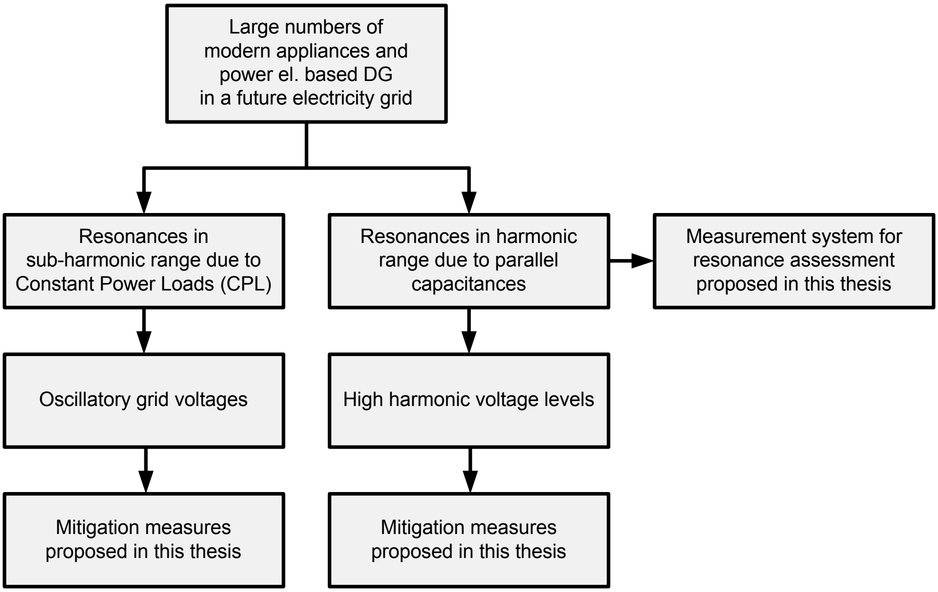

Figure 1.3: Overview of the studied power quality problems in this thesis.

The objective and research questions that are covered by this thesis are described and also the relevance with related international research is discussed.

Chapter 2 Harmonic interaction

The phenomenon of harmonic interaction is explained. Fundamental ways to reduce harmonics are discussed, e.g. reduction of resonances, damping of harmonics and compensation of harmonics. Attention is paid to the reduction of resonances, as this can be provided as an ancillary service of an inverter for DG in this thesis.

Chapter 3 Impedance measurement for PQ indication

A way to estimate the sensitivity of the grid to disturbances in the field of PQ is presented via a complex harmonic impedance spectrum measurement system. This system performs on-line impedance measurements in the electricity grid and is designed for implementation in the DSP control system of power electronics based DG.

Chapter 4 Modern appliances with constant power

The non-linear constant power load nature of power electronics based appliances and their effect on the quality of the grid voltage is explained. It is discussed that stabilization against grid voltage fluctuations by a power electronics converter can lead to a negative differential impedance which can cause an oscillatory grid voltage.

Chapter 5 Ancillary services for harmonic reduction

Computer simulations with a laboratory validated inverter model will give insight in the effect of the two ancillary services VPCR and VRHD that are implemented. These ancillary services can minimize the effect of resonances and reduce harmonic voltages in LV distribution systems.

Chapter 6 Extensive simulation of a distribution grid

Two large-scale computer simulation set-ups of a LV distribution grid with the validated inverter models of Chapter 5 implemented are discussed. In the first simulation 200 pieces of these inverters are placed in homes and virtually compensating their own output capacitances by means of VPCR. In the second simulation 100 pieces of these inverters are placed in homes and virtually compensating external capacitive loads as well. Also VRHD is applied to the inverter models. Impedances under various conditions, representing the total power system at the substation's LV busbar, are observed and discussed.

Chapter 7 Conclusions and recommendations

Conclusions are drawn and contributions are given related to the total work of this thesis. Recommendations for follow-up work are also made.

Chapter 2

Harmonics and grid resonances

In this chapter attention is paid to harmonic currents and voltages in Low Voltage (LV) distribution grids as well as the effect that grid resonances can have on the resultant harmonic distortion. Techniques for active damping of harmonics and minimizing the impact of resonances are discussed; these techniques are further elaborated in this thesis as ancillary services of power electronics based Distributed Generation (DG).

2.1 Harmonics in an electricity distribution grid

Harmonics are sinusoidal components of voltages or currents with a frequency equal to an integer multiple of the fundamental frequency. Frequency components below the fundamental or non-integer multiples of the fundamental are called sub-harmonics and inter-harmonics respectively. The most important causes of harmonic currents in a distribution grid are non-linear loads and equipment [Std 03].

In this thesis attention is given to harmonics in the range of the standard for the quality of the voltage, i.e. below 2000Hz for a grid with a 50Hz fundamental [Std 01]. One important remark in this standard is that harmonics higher than the 25th are usually small, but largely unpredictable because of resonance effects.

2.1.1 Character of linear and non-linear loads

A load is called to be linear if Z_{load} is linear. This is valid if (2.1), (2.2) and according to the superposition rule also (2.3) holds [Coo 72]:

$$V_1 = I_1 Z_{load} \tag{2.1}$$

$$V_2 = I_2 Z_{load} \tag{2.2}$$

$$(V_1 + V_2) = (I_1 + I_2) Z_{load} \tag{2.3}$$

In general a linear system can be modeled as the sum of independent linear subsystems for each harmonic frequency. These linear subsystems are independent because the n^{th} harmonic voltage only affects the n^{th} harmonic current. With a non-linear system, the n^{th} harmonic voltage affects a number of harmonic currents, and therefore the subsystems are not independent [Bos 06].

2.1.1.1 Modeling of non-linear loads

Non-linear loads draw currents from the grid which in turn can be decomposed into a number of harmonic currents. These harmonic currents can be considered in many situations independent of other loads and the specific grid. Therefore, to facilitate calculations, a non-linear load can be modeled as a combination of harmonic current sources in parallel with the fraction of the load which is linear and one single source for each harmonic. The sign of the harmonic current sources is so defined that harmonic current flows into the grid and the fundamental current into the linear part of the load. Figure 2.1 gives the model of a linear and non-linear load [Std 03], [Col 99].

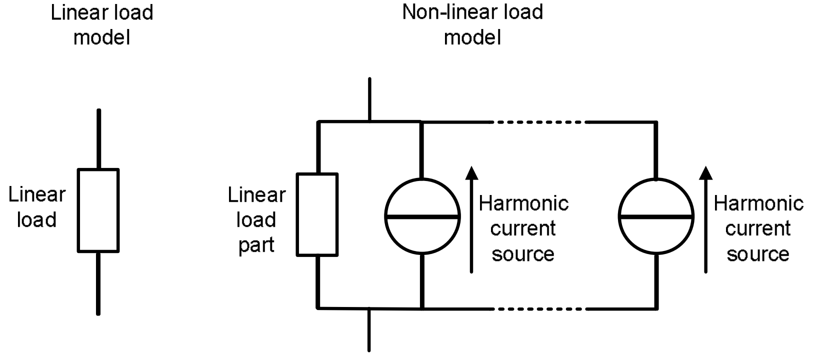

Figure 2.1: Model of a linear and a non-linear load.

Using the parallel representation of a linear load and a current source as depicted in Figure 2.1 generally is not sufficient to model a non-linear load that is working under various circumstances [Pom 07]. This is only the case for small changes around a specific operating point and under an applied grid voltage with a specific pollution. Saturation aspects and the amount of pollution of the grid voltage can have effect on the harmonic current emission, this should be taken into account while modeling non-linear loads. So for each operating point and each applied voltage shape, a new model might be needed. The sensitiveness to various voltage shapes is especially true for loads that use the combination of a diode rectifier and buffer capacitor in its front-end. A so called “Harmonic fingerprint” can be used to model non-linear loads that are fed by a grid voltage that is polluted with various harmonic voltages and levels [Cob 07].

The model depicted in Figure 2.1 makes use of a Norton equivalent circuit, this can be replaced in a Thevenin equivalent circuit as well. Thevenin equivalent circuits, i.e. a series connection of a linear load and a voltage source are generally used if the impedance in the model has a low value compared to other impedances in the observed system. An example of this is the modeling of harmonic sources in a Medium Voltage (MV) grid that penetrate into the LV grid, i.e. background harmonics. Impedance levels in the MV grid, transferred to equivalent levels in the LV grid have a very low value compared to other impedances in the LV distribution grid. A Thevenin equivalent circuit is often used to model harmonics from the MV grid that penetrates into the LV grid (background harmonics).

Because throughout this thesis only small signal analysis are performed under steady-state conditions, the load model as depicted in Figure 2.1 is used.

2.1.2 Effect of the grid impedance

Harmonic currents are transferred into harmonic voltages via grid impedances, so through impedances of sources, loads and grid components harmonic interaction can take place. Figure 1.1 gave an example of a LV distribution grid. All cable parts and also the distribution transformer have impedance, the dominating impedance in this is the distribution transformer with its inductive character [Std 03]. Grid impedances for harmonic frequencies up to the 25^{th} harmonic increase with the harmonic number [Old 04]. Therefore, the connected loads in the LV distribution system have a significant effect on the local grid impedance for this frequency range.

The effect of loads on the distribution grid becomes more important as more power electronics based loads with a filter capacitor in parallel at the output terminals are connected. Modern home appliances often use an electronic power supply which transfers the alternating grid voltage into a direct voltage for internal use. Power supplies with their fast switching voltage levels have the potential to put high frequency disturbances into the grid, i.e. conducted Electro Magnetic Interference (EMI). To avoid this, an EMI filter at the output is used. It is this EMI filter located in between the electricity grid and the home appliance that places a parallel capacitance on the grid. Although these parallel capacitances of home appliances are small, the large number of such loads and also DG causes the aggregate parallel capacitance in a distribution grid to rise to a high level. Parallel capacitances and inductive grid impedances can come into resonances. These resonances can be seen as parallel or series resonances. Especially when the aggregate parallel capacitance in a distribution grid is big, a possible resonance can lie in the harmonic frequency range below the 25^{th} harmonic [Ens 04].

Parallel resonances in the LV grid can make the impedance around the resonance frequency rise to a much higher level. Harmonic currents that lie in the frequency range of the resonance peak can then be transferred into problematic high harmonic voltage levels. Therefore these resonances are a real threat for power quality.

Series resonances in the LV grid can bring a low impedance path for background harmonics, i.e. harmonic voltages in the MV grid causes harmonic currents into the LV grid. These harmonic currents will flow through the distribution transformer and can have unwanted effects in this component [Std 03]. Beside this, at the LV busbar harmonic voltages can rise to a high level.

Figure 2.2 gives an impression of the impedance as function of the frequency of a parallel and series resonance.

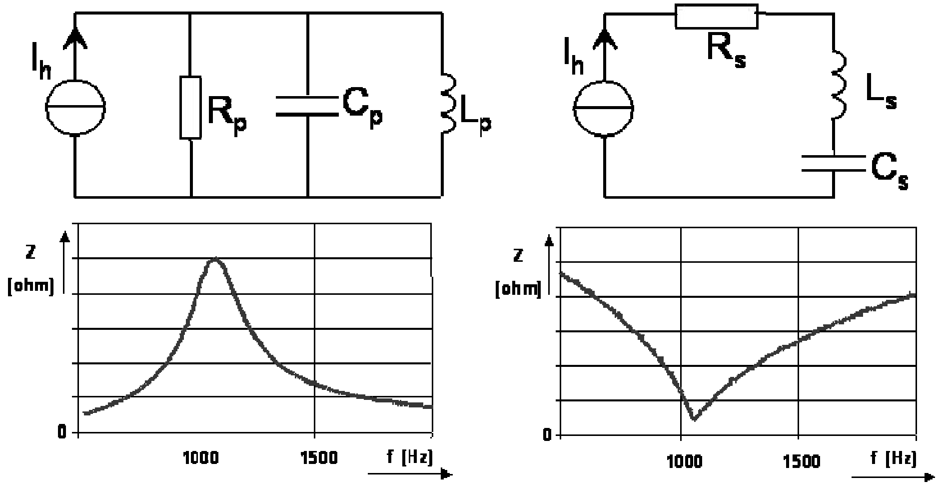

Figure 2.2: Impedance as function of the frequency of a parallel and a series resonance.

Figure 2.3 gives a measurement result of the harmonics in the voltage at one of the substation feeders of a LV distribution grid with a large number of inverters for DG. Two fairly high harmonic levels can be noticed at the 11th and 13th harmonic, a resonance is probably the cause of this [Cob 07].

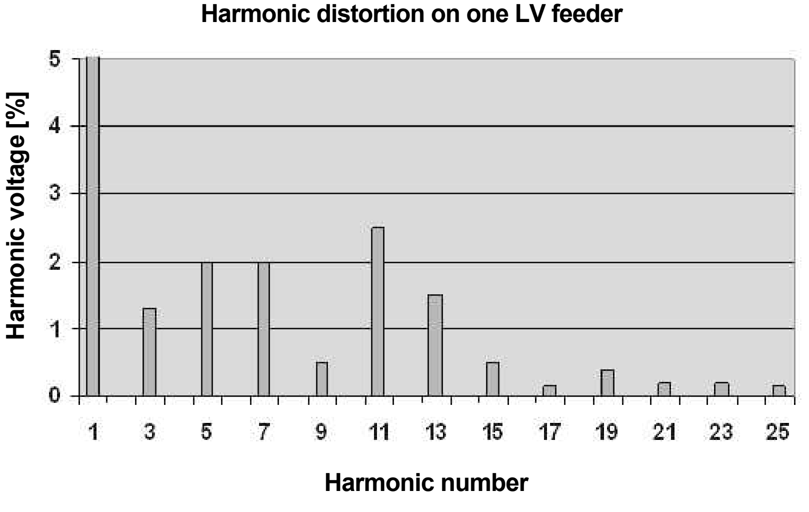

Figure 2.3: Measured harmonic voltage level caused by resonances in the electricity grid.

2.2 Reduction of harmonics

In this section three main ways of harmonic voltage reduction are discussed. The main focus is on harmonic reduction techniques that can be implemented into inverters of power electronics based DG as an ancillary service. According to the standard for the quality of the voltage at the Point of Connection (PoC) [Std01], maximum levels of harmonic voltages are prescribed. A comprehensive overview of these harmonic reduction techniques is given in Figure 2.4.

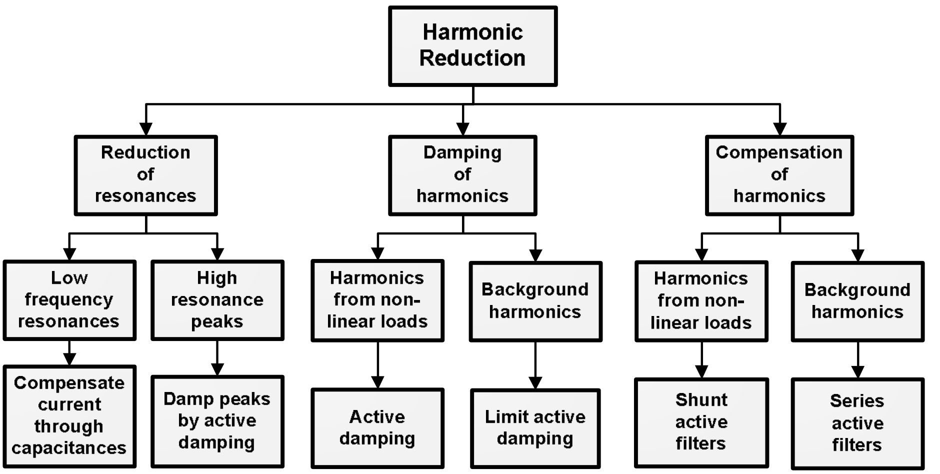

Figure 2.4: Comprehensive overview of harmonic reduction techniques implemented as ancillary services in power electronics based DG.

In the sections below the three techniques for harmonic voltages reduction in LV distribution grids, are discussed more in detail.

2.2.1 Reduction of resonances

The reduction of resonances contains two measures firstly to compensate the current through the capacitances and secondly damping the resonance peak to a lower level, as shown in the lower level of Figure 2.4. Small grid coupled inverters for DG often show a high output capacitance for filtering out switching frequency currents towards the electricity grid, i.e. filtering out conducted EMI. In the simplified grid model of Figure 2.5 resistive loads and parallel capacitances are lumped together as one RC load. This lumped load then is connected to the Point of Common Coupling (PCC), the substation busbar, as shown in Figure 1.1. The effect of cables in this simplification is not taken into account. The impedance Z_{grid} here is the sum of the total impedance of the MV grid and the transformer, simplified as a series connection of a resistance and an inductance.

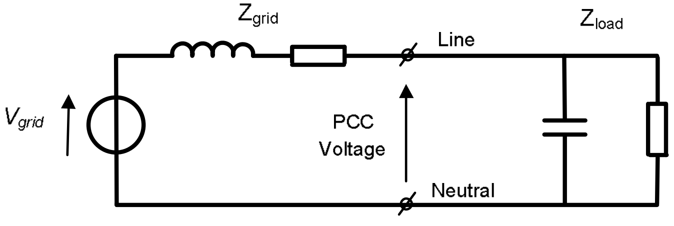

Figure 2.5: Simplified grid model with a lumped large number of resistive loads and parallel capacitances.

2.2.1.1 Virtual shift of resonances

The first method mentioned in Figure 2.4 “compensation of current through capacitances” has as effect that a resonance is virtually shifted towards a higher frequency range where the propagation is limited, preferably above the 25th harmonic. In this thesis, this ancillary service is called Virtual Parallel Capacitance Reduction (VPCR) and further explored in chapter 5. In today’s situations distribution grids resonances in general are already in the frequency range above the 25th harmonic [Std 01]. In this higher frequency range harmonics will not be propagated far in the grid, because of the damping effects of cables and transformers [Sai 03].

Figure 2.6 gives the impedance at the PCC as a function of the harmonic order plot with a parallel resonance simulated with the simplified grid of Figure 2.5, where Z_{load} stands for a lumped large number of resistive loads and beside this, parallel capacitances from output filters of inverters for DG. Also the effect of VPCR of these inverters is shown in this figure. Due to the compensation of the current through the inverter’s output filter capacitances, the resonance peak is virtually shifted to a higher frequency range [Hes 07].

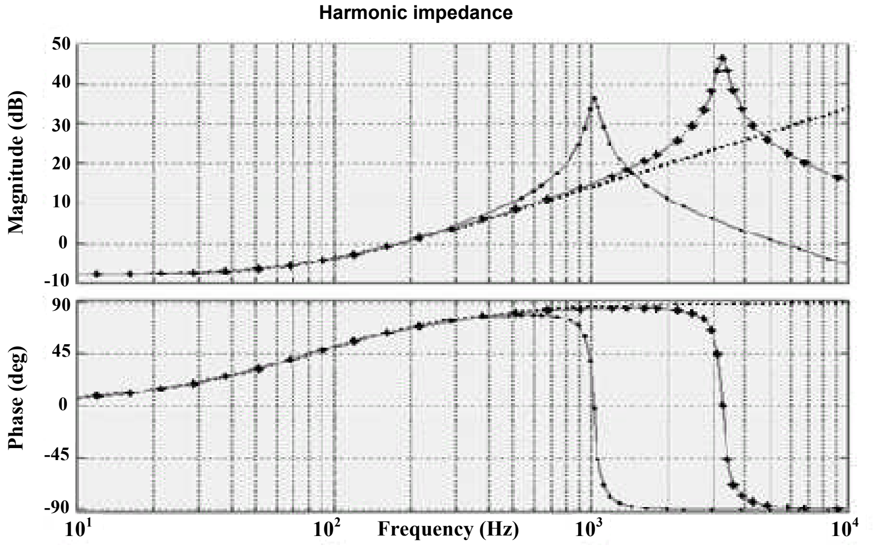

Figure 2.6: Harmonic impedance plot with a parallel resonance,

- dotted line: unloaded grid,
- line with dots: inverter load without compensated capacitor current,
- line with asterisk: inverter load with a 90% compensated capacitor current.

2.2.1.2 Damping of resonances

The second measure for the reduction of resonances is to add an extra control loop to the inverter which gives the inverter a resistive behavior for the harmonic frequency range. This will bring extra damping to resonances in the grid [Aka 96], [Ryc 05a]. In this thesis, this ancillary service is called Virtual Resistive Harmonic Damping (VRHD) and further explored in chapter 5. As can be seen in Figure 2.7, implementing both methods can be very effective.

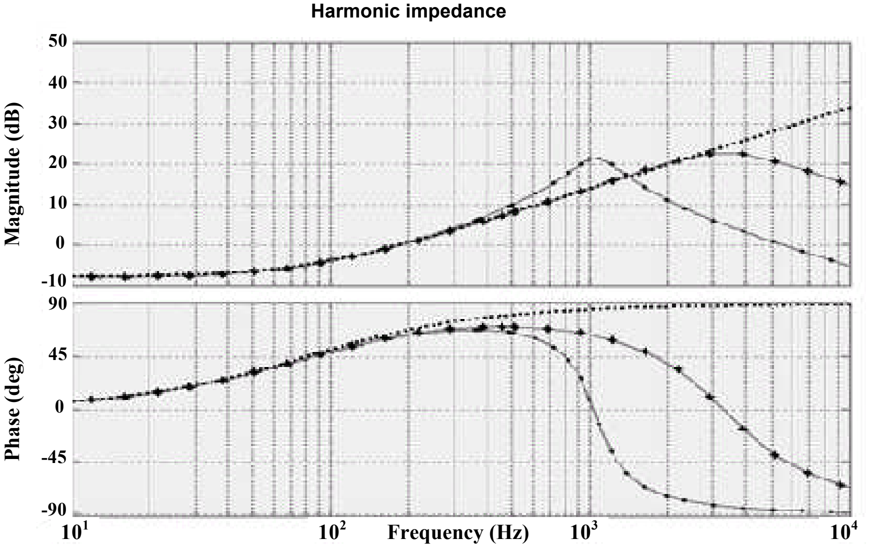

Figure 2.7: Harmonic impedance plot with a damped parallel resonance,

- dotted line: unloaded grid,
- line with dots: inverter load without compensated capacitor current,
- line with asterisk: inverter load with a 90% compensated capacitor current.

2.2.2 Damping of harmonics

Harmonics in an electricity grid can come from different origins and can be split-up in two groups that need a different approach for reduction. One group is harmonics coming from non-linear loads in the LV distribution grid itself, and the other group is harmonics coming from the MV grid, as so called background harmonics as can be seen in Figure 2.4.

Because resistive loads, like incandescent lamps, are replaced increasingly by power electronics based non-linear loads, harmonics current emissions will increase and at the same time, the resistive damping in the grid will decrease.

2.2.2.1 Harmonics from non-linear loads in the LV grid

In the model of Figure 2.8 can be seen that voltage drop over the grid impedance will affect the voltage on all the loads connected to the PCC. This holds for the fundamental as well as for harmonics.

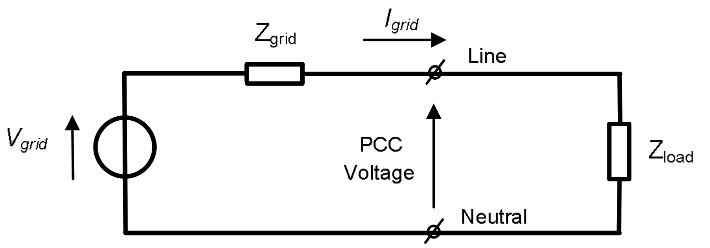

Figure 2.8: A simplified grid model.

Assume that the grid is loaded with a non-linear load, as depicted in Figure 2.9, then the harmonic currents from this non-linear load will distribute itself in the grid. The part of the harmonic currents from non-linear loads that flows through the grid impedance towards the MV grid depends on the impedance ratio between grid components on the one hand and on the type and number of loads in the grid on the other hand. The part of the harmonic currents that is flowing through the grid impedance is the main cause for the transfer into harmonic voltages at the PCC. As mentioned before, parallel resonances between grid inductances and large numbers of parallel connected capacitances could increase the impedance and with that the harmonic voltages.

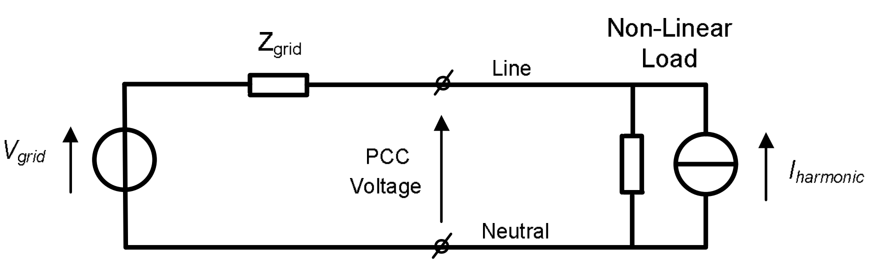

Figure 2.9: The grid loaded with a non-linear load.

If extra loads are added onto the grid, resonances can be damped, and that will reduce the harmonic voltages at the PCC. The best type of load for this damping in general is a resistive load [Ryc 02]. Figure 2.10 shows an added damping resistance in the distribution grid model. This damping resistance should only have an effect on the harmonic frequency range, to avoid dissipation at the fundamental frequency.

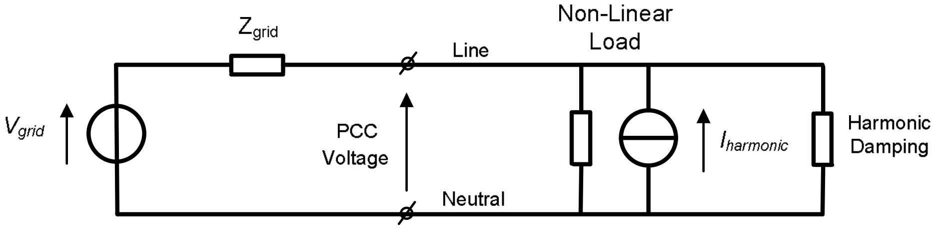

Figure 2.10: Added damping resistance in the distribution grid.

This damping can be the same damping that could be used for the damping of parallel resonances, as discussed in section 2.2.1.2, namely VRHD. Bringing this damping in the grid by means of an extra control loop in a power electronics based DG has the advantage that the damping resistance is virtual and most of the damping energy will be stored in the energy buffer capacitor of the power electronics inverter. Only a small part of the energy will be dissipated because of losses in the power electronics inverter.

2.2.2.2 Harmonics coming from the MV grid

Harmonics in the LV grid coming from non-linear loads in the MV grid (background harmonics) can be modeled as an added voltage source in series with the fundamental voltage [Std 03], as can be seen in Figure 2.11 and section 2.1.1.1. This can be done because the impedance of the MV grid, seen from the LV grid, is much lower than the impedance of the LV grid. Background harmonics can be significant with large non-linear loads like railway rectifiers, and generators like wind turbines.

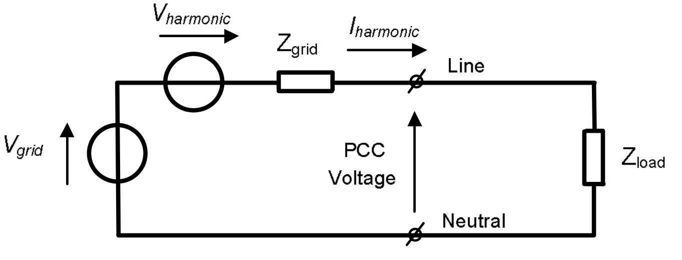

Figure 2.11: A simplified grid model with harmonic background pollution.

In case of background harmonic voltages pollution, all loads in the LV grid will draw current from this harmonic voltage source. As mentioned before, the total current towards the LV grid then will flow through the grid impedance of

Figure 2.11, which can bring a number of unwanted effects in the distribution transformer and cables.

If an extra harmonic damping is added to the distribution grid, then this damping would on the one hand reduce possible series resonances, but on the other hand could draw more harmonic current from background harmonic voltages, and with that would not guarantee an optimal effect. Figure 2.12 gives a drawing of this situation.

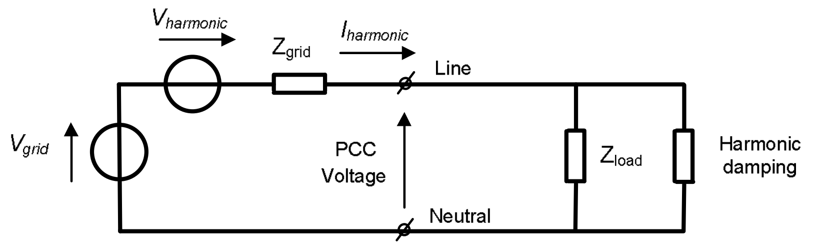

Figure 2.12: Harmonic damping added to the simplified grid with harmonic background pollution.

Therefore bringing extra damping loads onto the LV distribution grid, to reduce resonance effects, is in contradiction with the effect that this damping draw more harmonic current from background harmonic voltages.

The best solution for the reduction of background harmonics is to tackle the problem at the source, for example a harmonic compensator nearby the disturbing load in the MV grid. But assume that compensating the disturbing load locally, e.g. with harmonic shunt filters, cannot be performed, a possible solution could be the implementation of a series active filter at substation level. This kind of filter compensates harmonic voltages by adding compensation voltages to the grid voltage; as a result no harmonic currents from the disturbing MV load will flow to the LV grid [Aka 05].

2.2.2.3 Location for harmonic damping

The best location for harmonic damping is the end terminal of a distribution feeder (line or cable), acting as a harmonic termination resistor, however when the grid situation is not known and loads can vary, a good choice for a location is somewhere between the middle and the end of the line or cable [Wad 02], [Aka 99], [Aka 97], [Ryc 04].

2.2.3 Compensation of harmonics

Compensation of harmonics also contains two measures, firstly a measure for the group of harmonics coming from non-linear loads in the LV distribution grid itself, and secondly a measure for the group of harmonics coming from the MV grid, the background harmonics. This can be seen in the overview of Figure 2.4.

Modern active harmonic filters can have several features on harmonic reduction, like: harmonic filtering, damping, isolation and termination. Beside this also other services can be provided, like: reactive-power control, voltage regulation, voltage-flicker reduction [Aka 05].

In contrast with damping of harmonics, compensation of harmonics by active harmonic filters can reduce harmonic currents to an almost zero remainder level, but harmonic compensators need to be adapted to each particular situation and VRHD does not.

2.2.3.1 Active filters

Series active filters are connected in series with the grid and compensate harmonic voltages by adding voltages to the grid as a counter measure. This kind of filter is often placed at a central point to isolate two areas; this means that the grid voltage at one side of the filter can be of a different pollution then the other side. However this can only work well if the non-linear loads in the grid find a current path nearby. As explained before, non-linear loads can be modeled as linear loads with a parallel current source for each harmonic, as can be seen in section 2.1.1.1. If there is no path provided for these harmonic currents in the surrounding area, the current will propagate through the series filter to a wider area. For a good control of harmonics therefore, series active filters can be best combined with shunt active or passive filters.

Shunt active filters are connected in parallel with the grid and compensate harmonic currents by injecting currents to the grid as a counter-measure as can be seen in Figure 2.4. For this function, the best location of the shunt active filter is nearby the polluting load.

2.2.4 Combination of reduction techniques

The combination of a series active filter on substation level, together with a number of shunt active filters in the distribution grid can bring a total package of mitigation [Fuj 98a], [Fuj 98b], [Aka 96], [Jin 03].

Passive filters in general are shunt filters. Shunt passive filters compensate harmonic currents by creating a conductive path for these currents. These filters can be a single-tuned series resonator with a high quality-factor for one harmonic or a band-pass filter for a whole frequency band. The best location is nearby a polluting load. One disadvantage of passive filters is that beside the wanted resonance also unwanted resonances can show up as interaction with other grid components.

The shunt active filter can be integrated in power electronics based DG.

Table 2.1 gives a summary of the cause of harmonic problems in the distribution grid and a possible measure that falls into the research area of this thesis.

Table 2.1: Harmonic problems and possible measures.

Problem	Measure
Harmonics in the LV distribution grid, coming from non-linear loads in the LV grid itself	VRHD as ancillary service of power electronics based DG
Harmonics in the LV distribution grid, coming from non-linear loads in the MV grid	Central series active filter to isolate the LV distribution grid from the MV grid for harmonics
High grid impedance because of parallel resonances in the LV distribution grid	VPCR and VRHD as ancillary service of power electronics based DG
Low impedance path from the MV grid to the LV distribution grid because of series resonances in the LV grid	Central series active harmonic filter and/or limited VRHD

2.3 Conclusion

Harmonic voltages in a LV distribution grid can be reduced by harmonic damping or compensation. Harmonic compensation is difficult to achieve, but in contrast with harmonic damping it can reduce harmonics to even lower levels. The great advantage of harmonic damping is that it can have effect on a whole range of harmonics. With this technique there is no need for estimating the actual level of harmonics or fear of instabilities in the grid. Harmonic damping can be integrated as an ancillary service for power electronics based DG, the damping resistance is then virtual, and the energy involved is limited to the losses in the power electronics inverter. Another advantage of this damping is that the only effort to be taken is an inexpensive extension of the control system of the inverter.

A disadvantage of harmonic reduction in a LV distribution grid is that there is a contradiction in the needed measure for harmonics from the MV grid, i.e. background harmonics. Harmonic reduction must be limited to avoid wrong compensation of background harmonics, resulting in excessive currents through the distribution transformer and cables. A combination of a series active filter on substation level and harmonic damping dispersed over the distribution grid can avoid the wrong compensation for background harmonics, and therefore can be an optimal solution for harmonic mitigation.

Parallel and series resonances in the LV grid are a real threat for the power quality, because they can amplify harmonic voltage and current levels. Measures to minimize these effects are VPCR and VRHD services. The effect is that a resonance peak is virtually shifted to a higher frequency range and damped to a lower level. Both measures can be provided by ancillary services of power electronics based DG.

Chapter 3

Impedance measurement for PQ indication

In this chapter an impedance measurement system is proposed based on Fourier transformation of the time domain signals, voltage and current, together with a lock-in principal. It estimates the complex harmonic impedance spectrum for a range of harmonic frequencies up to the 40^{th}. The system is able to locate possible resonances in the grid, in order to minimize the impact. The injected stimulus for the measurement is a current waveform which contains a number of frequency components. The measurement system is developed for implementation in Digital Signal Processor (DSP) based control systems of grid-connected power electronics based converters.

This chapter discusses the measurement system and gives results from Matlab/Simulink computer simulations and laboratory measurements.

3.1 Introduction

Because today's modern home appliances and small inverters for Distributed Generators (DG) use front-end capacitances, the effect on the grid impedance in the Low Voltage (LV) distribution grid can be significant (see Chapters 1 and 2). As explained in Chapter 2, parallel capacitances and grid impedances in the LV grid can come into resonance. This resonance can make the impedance around the resonance frequency rise to a much higher level. In this way harmonic currents that lie in the same frequency range can be transferred into problematic high harmonic voltages. Harmonic impedance spectrum information could be used to locate possible resonances in the grid and furthermore to develop measures to minimize the impact of resonances.

To locate possible resonances in the grid, the measurement system must be able to estimate the complex small signal grid impedance for a range of harmonic frequencies up to the 40^{th}. Because the measurement system will be integrated into a small grid-connected power electronics converter, the injected current for the measurement must be small to comply with the standard for current emission of home appliances [Std 02]. This implies that the system must be able to extract the complex grid impedance from very small signals, often lower than the noise levels. A method that can handle these demanding specifications is based on a lock-in method [Vis 05]. However a disadvantage of this method is that it estimates only one frequency component. A Discrete Fourier Transformation (DFT) system can give the same result with a whole spectrum as output. The results of both systems are comparable, because the basis of the DFT and the lock-in method is the same.

A problem during the measurement is that the lower the signal to noise ratio of the measured signal is, the more difficult it is to do the measurement accurately. Another problem is that the closer the measurement frequency is near the frequency of a large not correlated signal, the more difficult it is to do the measurement accurately. Harmonic currents and voltages not correlated to the injection signal will disturb the measurements and make it more difficult to extract the spectrum.

Measurement systems, based on Fourier transformation or based on a lock-in principle can only work well if during the averaging time the input signal is constant and periodical. In practice for electricity grids where voltage and current harmonics are time-variant because of continual changes in load conditions and to some extent in system configuration, this can only be true for a short time [Bag 02], [Bag 98].

3.2 Basis of the measurement

To understand the reason why a combination of the DFT and the lock-in method is used for the measurement system, both methods are firstly discussed and after that compared in this section.

The basis of the extraction of spectral components lies in phasor multiplication. Because this holds for DFT as well as for the lock-in method, only the first one is discussed more in detail.

The comparison of both methods will be based on implementation of the system in a DSP. Because in practice a DSP is already loaded with several tasks like control and protection, the additional processor loading for the measurement system is focused on. The most power consuming operations during the analysis are complex multiplications. Therefore the number of complex multiplications is used as a measure for comparison of both methods.

3.2.1 Fourier series method

With Fourier series, a periodic time function $f(t)$ can be expressed as the summation of a number of harmonically related complex rotating phasors $c_n e^{j\omega nt}$, see Equation (3.1). Below the most important steps to calculate the Fourier series will be given. More details can be found in study books like [Arr 04], [Bur 85], [Her 85].

$$f(t) = \sum_{n=-\infty}^{\infty} c_n e^{j\omega nt} \tag{3.1}$$

The method to calculate c_n, is to multiply both sides of (3.1) with the conjugate of the phasor $e^{j\omega nt}$, namely $e^{-j\omega nt}$. This action will cause that a phasor component in the signal $f(t)$ that rotate at ωn, will then rotate at $\omega = 0$, i.e. it stops rotating and becomes a constant component. All phasor components in the signal $f(t)$ that rotate different from ωn will still rotate then but with a different ω.

$$f(t)e^{-j\omega nt} = \sum_{n=-\infty}^{\infty} c_n e^{j\omega nt} e^{-j\omega nt} \tag{3.2}$$

The next step is the integration of both sides over a period of time. This action will cause that all the still rotating phasors in the product $f(t)e^{-j\omega nt}$ will be averaged out. What remains is the coefficient of the phasor that has stopped rotating and has become a constant component, see (3.3) to (3.5).

$$\int_{-T/2}^{T/2} f(t)e^{-j\omega nt}\,dt = \int_{-T/2}^{T/2} \sum_{n=-\infty}^{\infty} c_n e^{j\omega nt} e^{-j\omega nt}\,dt \tag{3.3}$$

$$\int_{-T/2}^{T/2} f(t)e^{-j\omega nt}\,dt = T\sum_{n=-\infty}^{\infty} c_n \tag{3.4}$$

$$c_n = \frac{1}{T}\int_{-T/2}^{T/2} f(t)e^{-j\omega nt}\,dt \tag{3.5}$$

Each phasor now can be found by calculating the complex factor c_n , and can be plotted in a polar diagram or harmonic impedance plot by calculating the magnitude $|c_n|$ and phase angle Φ_n of the phasors.

$$c_n = |c_n|e^{j\Phi_n} \tag{3.6}$$

To implement this analysis method into a DSP, a step from continuous time to discrete time is necessary. With this step, the time function $f(t)$ will be now a function of small discrete time steps $f(kT_s)$ and for the calculation of the complex factors c_n , the DFT is used. k is the number of the sample and N stands for the total number of samples used for the DFT. The DFT coefficients can be expressed as:

$$c_n = \frac{1}{N}\sum_{k=0}^{N-1} f(kT_s)e^{-j\omega nkT_s} \tag{3.7}$$

The frequency F_0 is the fundamental frequency of the transformation and depends on the sample time and the total number of samples used for the transformation. F_0 is a measure for the resolution of the DFT.

$$F_0 = \frac{\omega}{2\pi} = \frac{1}{T_s N} \tag{3.8}$$

All the frequencies of the calculated Fourier components F_n are an integer multiple of F_0.

$$F_n = nF_0 \tag{3.9}$$

To find some specific frequency components from a time domain signal, the first thing to do is to choose F_0 in a way that the division of the specific frequency by F_0 is an integer number. Therefore it is common to express the DFT coefficients as integer multiples of F_0, called c_{F_n}.

$$c_{F_n} = \frac{1}{N} \sum_{k=0}^{N-1} f(kT_s) e^{-j2\pi \frac{n}{N} k} \tag{3.10}$$

Fast Fourier Transformation (FFT) is a DFT with a special calculation algorithm, to reduce the number of complex multiplications of the DFT. The FFT method is a generally used approach for DFT in digital signal processing [Coo 65].

3.2.2 Lock-in method

With the lock-in method the coefficient c_n of a “buried in noise” signal can be measured. For this extraction, a reference phasor of exactly the same frequency as the signal to be estimated is applied to the system. The method is based on a combination of a complex multiplier and a time averaging filter, as can be seen in Figure 3.1 and the same Equations (3.1) to (3.10) as with the calculation of Fourier Series and DFT. Details can be found on many internet sites of manufacturers of lock-in amplifiers, often explained in a non-complex way using cosine functions.

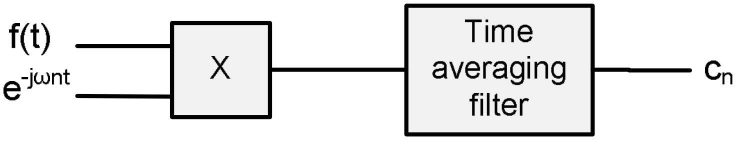

Figure 3.1: Calculation process of the lock-in measurement system.

With the lock-in method, only one Fourier coefficient for only one specific frequency is calculated, often with an optimal chosen time averaging. This method therefore is most useful if our interest is focused on one particular frequency. The optimization of the time averaging process can result in a faster averaging to zero of the rotating phasors, compared to the averaging process used in normal DFT processes. For the calculation of a spectrum or transfer function in the frequency domain for a number of frequencies chosen on beforehand, the lock-in method is a candidate.

3.2.3 Limitations of the Fourier-based methods

When a Fourier based method is used to analyze time series of measured voltages and currents, then these time series must be periodical. Beside this, the time series must be measured in a grid situation with only linear impedances, otherwise the results are not reliable and might have no value. In practice these conditions will not be met, because the impedance will change all the time in an electricity grid by switching on and off of loads and distributed generators. Therefore, the first limitation is that the measurement must take place during a period of time with a constant grid load. In practice this means that the measurement time must be as short as possible. Furthermore, most of the impedances are non-linear, like diode capacitor rectifiers. So, the second limitation is that the results are only valuable for small deviations round the operating point during the measurement. To estimate the value of this analysis method in a practical electricity grid, with combinations of loads like linear loads, non-linear loads and phase-angle controlled loads, further study on this subject will be needed. Another subject for study is that a number of these impedance measurement systems must be able to work in parallel, a solution for this is proposed in this chapter.

Grid impedance measurements are done on a simulated reduced electricity grid for which the two assumptions of periodicity and linearity are valid. Under the same conditions, also laboratory measurements are done.

Fourier-based methods can only detect integer multiples of its fundamental frequency F_0, see Equation (3.8), and therefore it loses accuracy by projecting non-integer multiples of F_0 into integer multiple components. In other words, if the resolution is too low, compared to the spectrum to be analyzed, frequency components that fall in between the measured spectrum will cause an error, also called "smearing". Another risk off inaccurate results is the estimation of small components which are contiguous to large components. Beside this, noise in the same frequency range will also reduce accuracy [Kar 05]. However increasing the resolution and enlarging the averaging time, will improve the result of the DFT.

Another cause of error is aliasing. Aliasing will take place if the sampled time signal contains frequencies that are higher than half the sample frequency [Bur 85]. To reduce the error of Aliasing, the time signal to be sampled, must be filtered by a low-pass filter first, taking into account the sample frequency.

Fourier-based systems with limited time series length only work well if the analyzed signal is periodic. Due to continue changes in load conditions and system configuration, grid parameters in practice are only constant for a short time, e.g. less than a few minutes [Bag 02]. For the development of a reliable impedance spectrum measurement system, the time variation of relevant grid parameters should be known first. The second step is to estimate the effect of these changes on the measurement system. From recorded data at two different industrial sites, it can be seen that the total harmonic distortion (THD) can be constant for about a few minutes [Bag 98], this also indicates a stable complex impedance for that period. This time is long enough for a complex impedance spectrum measurement (simulation results further in this chapter show that a measurement of 4 seconds gives a good result), however sudden changes can happen, therefore statistical analysis need to be done on successive results to filter out invalid measurements.

3.2.4 Lock-in and DFT comparison

Older lock-in measurement systems are based on analogue techniques and therefore mostly operate in a continuous time domain while modern systems often use a processor that operates with discrete time series. For comparison, both the lock-in and DFT method are assumed to work with discrete time series of the same length and sample frequency.

The difference between the two methods is that with the lock-in method basically only one arbitrary Fourier coefficient is calculated, and with the DFT method all coefficients are being processed. For the calculation of a spectrum or a transfer function in the frequency domain with the lock-in method, a number of coefficients need to be calculated successively.

An interesting measure for comparison is the processor load needed to achieve a specific result. The greatest power consuming operations during the analysis are the complex multiplications. This number of complex multiplications is an indication to compare the processor load of both methods, although there are of course a number of other actions needed. For the calculation of a single component in the frequency domain all samples will be used, therefore the number of complex multiplications for this single component is N. To calculate the total spectrum in the frequency domain, all N components need to be calculated, thus N^2 complex multiplications are required. However making use of the Cooley-Tukey Radix-2 FFT method, the number of complex multiplications can be reduced to $\frac{N}{2}\log_2 N$ because a great number of calculations in the DFT process turn out to be the same or the inverse [Coo 65].

For example, the response needs to be extracted on the injection of a series of 40 harmonic frequencies to the electricity grid. During the measurement a time series is taken of $N = 4096$ samples. The number of complex multiplications with a discrete lock-in method will be $40N = 163.840$. The DFT however, only ask for $\frac{N}{2}\log_2 N = 24.576$ complex multiplications if the FFT algorithm is used. Thus from this point of view the FFT method is superior.

Because the DFT calculation must be implemented in a processor structure, the most optimal method of calculating DFT components may depend also on processor architecture and characteristics of the compiler. Manufacturers of DSPs offer special written FFT libraries, adapted for both the hardware and compiler architecture. In general it is recommended to use these FFT libraries [Fri 05].

3.3 The complex impedance measurement system

The complex impedance measurement system is expected to measure a harmonic impedance spectrum of 40 harmonic frequencies including the fundamental in the LV distribution grid. The system injects a signal with a number of frequency components into the grid and measures the response on that. The frequency components of the injection signal that is used for the measurement must not be exactly equal to the fundamental and harmonic frequencies of the grid during the measurement. If the measured signal is a summation of the response on injected currents and currents from harmonic sources in the grid, the correlation with the injection is poor and this influences the result. Therefore, the grid fundamental frequency and the 40 harmonics need to be avoided as measurement frequencies. To cope with this, the injected and measured frequencies will be shifted slightly above the harmonics of the actual grid frequency, as can be seen in Figure 3.2.

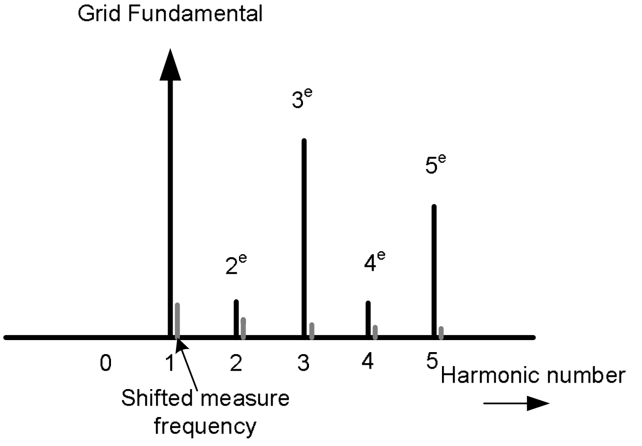

Figure 3.2: The measurement frequencies will be shifted slightly above the harmonic frequencies.

The actual grid frequency is estimated by means of a Phase Lock Loop (PLL) system. Normally the resulting impedance spectrum is a continuous function, this means that the small shift in measurement frequencies can bring good results. Figure 3.3 gives a drawing of the basis of the measurement system, which is further explained in section 3.3.2 and section 3.3.3.

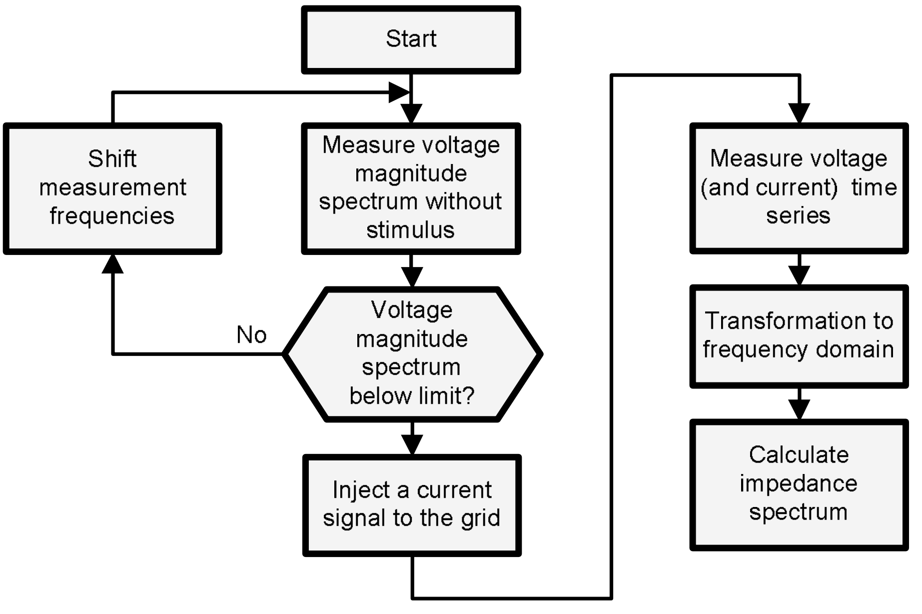

Figure 3.3: The basis of the measurement system.

3.3.1 Spectrum calculation

For the estimation of the total complex harmonic impedance spectrum, there is one frequency component that needs special attention, namely the grid fundamental frequency. The measured voltage response on the lowest frequency of the injected current is very contiguous to the relatively very large grid fundamental voltage component. Therefore the length of the time series for the DFT needs to be adjusted to estimate this fundamental impedance correctly. Harmonic components are however much lower in amplitude than this fundamental, therefore, such large time series length is not necessary for the harmonic components. For this reason the calculation part of the measurement system could be split in two, namely a lock-in system to estimate the fundamental impedance and an adapted FFT system to estimate the harmonic impedances (see Figure 3.4).

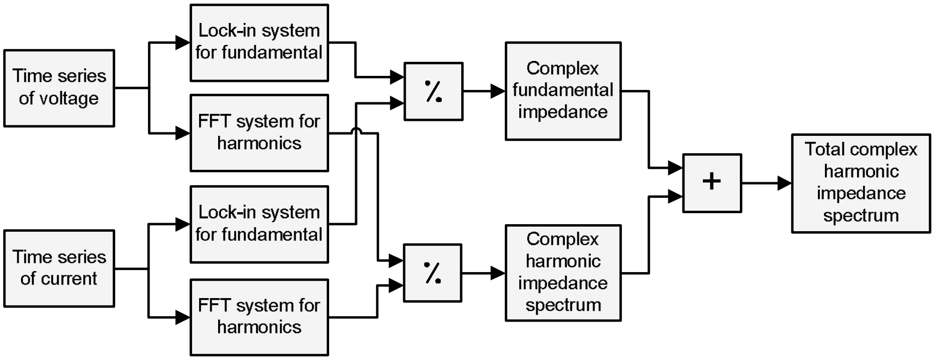

Figure 3.4: An impedance spectrum estimation that uses the two calculation methods.

3.3.2 Choosing the stimulus

For the complex impedance spectrum measurement of a LV distribution grid, the injected stimulus is a current with the spectrum of 40 harmonic frequencies including the fundamental. The injection can be seen as a current emission of an appliance that is connected to the electricity grid. Therefore, the limits of the standard for current emission of a home appliance [Std 02] are observed. To comply with this standard, the injected amplitudes of harmonic components must descend with the harmonic order, as can be seen in Figure 3.5.

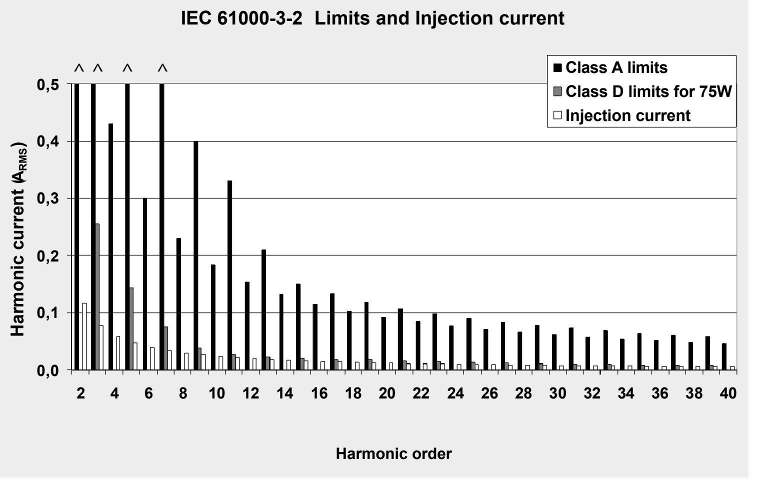

Figure 3.5 The stimulus spectrum compared to the IEC 61000-3-2 limits (the scale is limited to $0.5A_{RMS}$).

For the injection current, the frequencies F_n are a slightly shifted with F_{shift} in a way that

$$F_n = hF_{fundamental} + F_{shift} \tag{3.11}$$

This shift is done to avoid interference of the injected signal with the grid fundamental and its harmonics. Because of this small shift, the chosen measurement frequencies are not a harmonic series, but it fits well in between harmonic currents and voltages that could show up in the electricity grid. This waveform has a periodicity that depends on $F_{fundamental}$ and F_{shift}. For a fundamental frequency of 50Hz and a shift frequency of 5Hz the period of the injection signal is 0.2 seconds, as can be seen in Figure 3.6.

The advantage of this waveform, compared to step, pulse or noise stimulus, is that it only contents frequencies that are needed for the measurement.

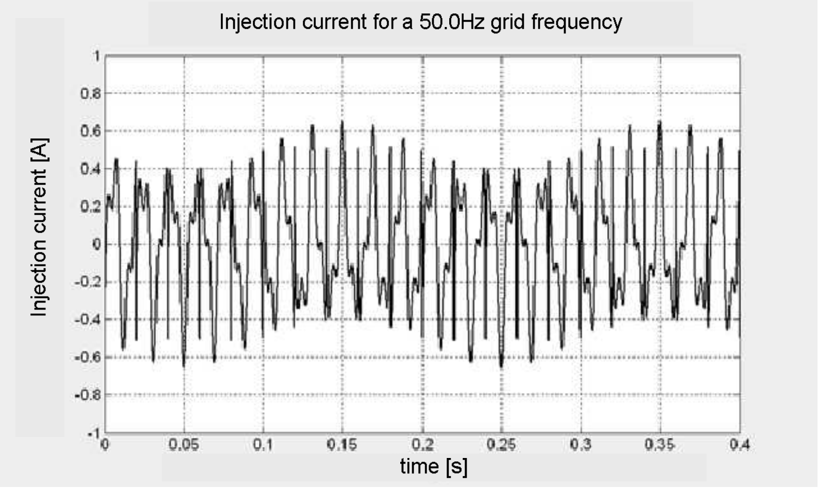

Figure 3.6: The injection current stimulus (tuned for a 50.0Hz grid).

3.3.3 Cooperation of multiple systems

Assume that multiple complex impedance measurement systems are implemented in a LV distribution grid. Interaction is possible if these systems are working at the same time on the same frequencies. To prevent this, two measures are taken. Firstly the systems will use different working frequencies by changing F_{shift} and secondly, after a successful measurement, a dead-time is taken into account, to give contiguous systems a chance. The length of this dead-time must depend on the number of active systems within a distribution area.

To be sure that the used frequencies are not used by nearby similar measurement systems, the first thing to do is to estimate the magnitude spectrum of the grid voltage, as can be seen in the right flow diagram of Figure 3.7. If the values are below a limit, the current injection starts and the harmonic impedance spectrum is calculated according to Figure 3.4.

There is always a risk that new disturbances come up during the harmonic impedance spectrum measurement or that the grid impedance is changing because of load variations. To prevent wrong measurements because of this, the deviation of the two last estimated spectra is compared to a limit. This can be seen in the left flow diagram of Figure 3.7.

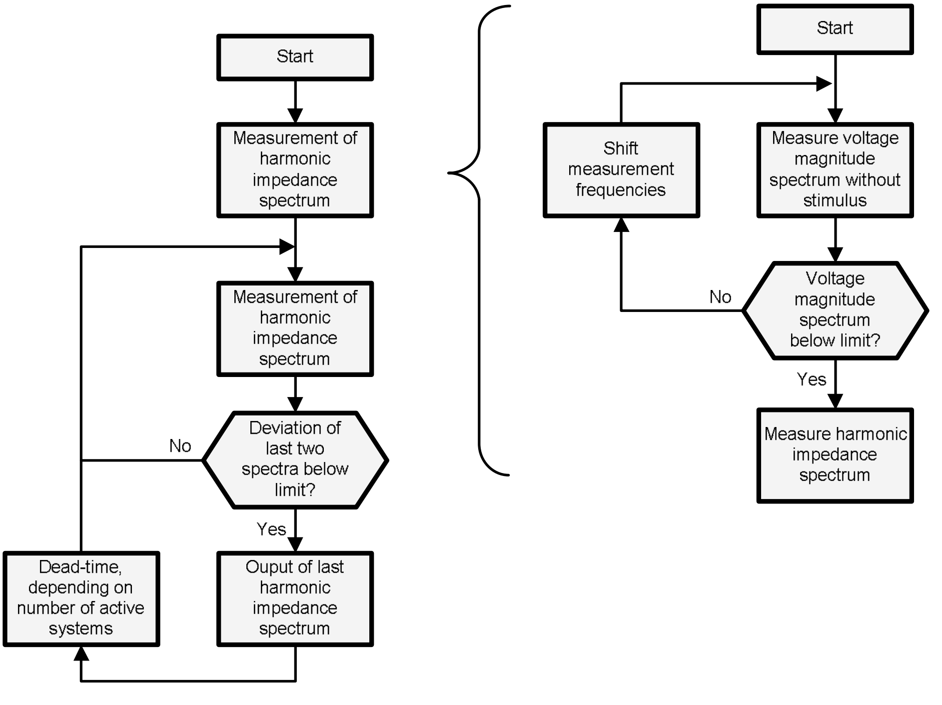

Figure 3.7: Process flow of the impedance measurement system.

3.4 Simulation of the measurement system

Computer simulations in Matlab/Simulink are done for a single measurement system. During the simulations, the pollution of the grid voltage is chosen the maximum according to the standard for the quality of the voltage [Std 01], for a number of harmonics. This means that the grid voltage is polluted to a THD of 8% as seen in Figure 3.8. Besides this, white noise with an average amplitude of 0.25% is added to the grid voltage to create a worst-case situation where measures need to be taken against insufficient averaging and aliasing. In this situation, the signals to be measured are below the noise level. A number of simulations are carried out with various fundamental frequencies of the grid voltage. The range is chosen according to the Dutch grid code that says that 99.5% of the year the frequency may vary between +1% and -1% of 50Hz [Std 05].

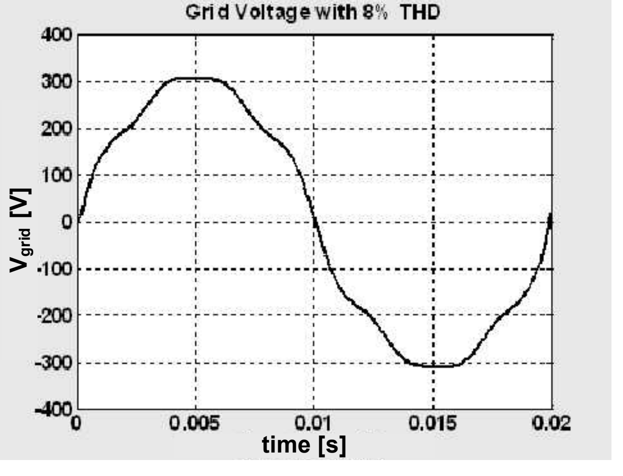

Figure 3.8: The grid voltage is polluted to the maximum to create a worst-case situation.

Figure 3.9 gives the set-up of the simulation. The measurement system is connected to a LV grid with impedances of $Z_{grid} = 0.4 + j0.25\Omega$ and $Z_{load} = 23 - j100\ \Omega$ at a frequency of 50Hz.

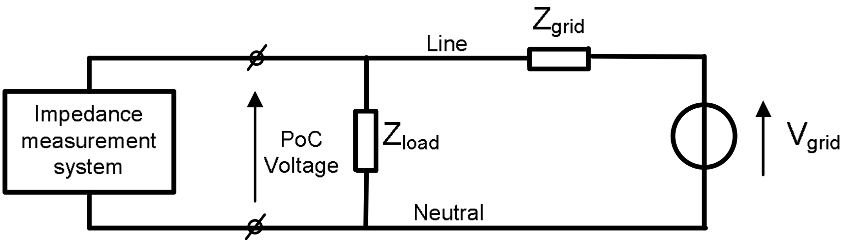

Figure 3.9: Impedance measurement of a simplified grid.

In order to be able to estimate the results, the exact harmonic impedance spectrum is calculated and plotted as a grey solid line in Figure 3.10 and in Figure 3.11, thus the grey solid line connects the exact harmonic impedances. The impedances of the harmonics from the measurement system are plotted as black dots in the figures. These figures give the impedance at the PoC as a function of the harmonic order in a harmonic impedance plot and as a Polar diagram. The harmonic impedances are calculated with the complex impedance measurement system, in a simulated 50Hz grid with a THD of 8% and also added to this 0.25% white noise. Doing measurements at various grid frequencies between 49.5Hz and 50.5Hz, showed similar results, i.e. a good match could be noticed between the exact values of the grey solid line and the measured black dots in the harmonic impedance plot or Polar diagram. To calculate the harmonic impedances from the simulated measurement system, a time series length of 1 second is used, and for the fundamental impedance 4 seconds. The time series are multiplied by a Hanning window. When multiple measurement systems are active, the latter time may be chosen longer, if F_{shift} needs to be decreased.

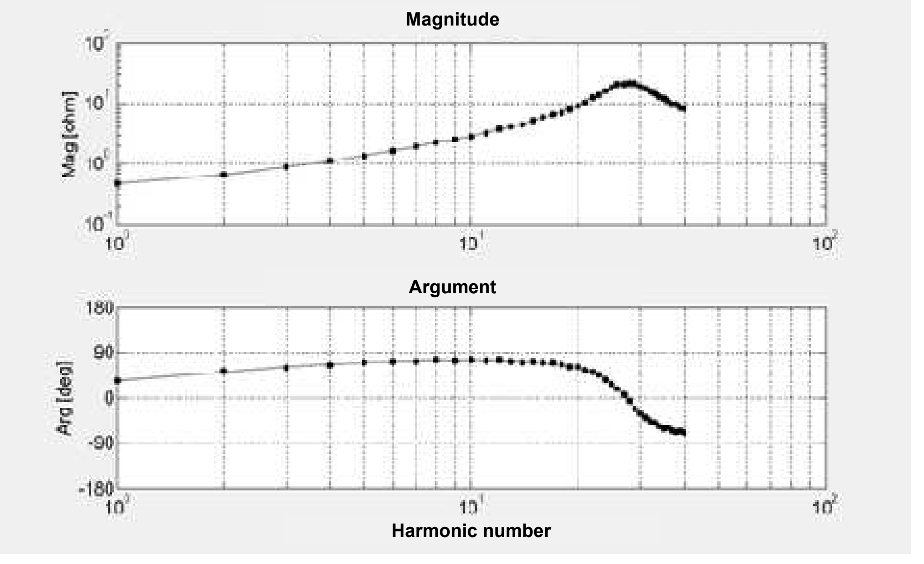

Figure 3.10: Harmonic impedance plot of the impedance at the PoC, measured in a grid with a highly polluted voltage (THD of 8% plus 0.25% white noise).

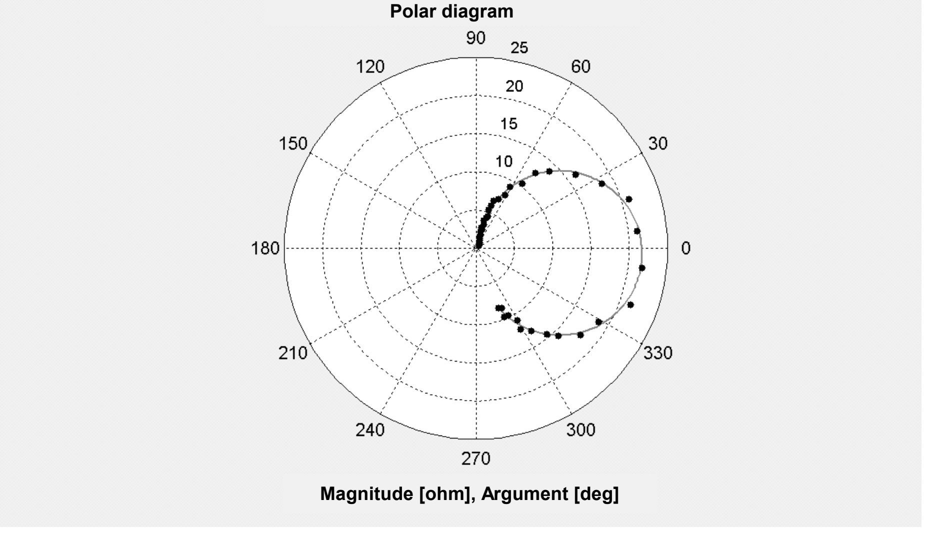

Figure 3.11: Polar plot of the impedance at the PoC, measured in a grid with a highly polluted voltage (THD of 8% plus 0.25% white noise).

3.5 Practical results

To test the system in a practical situation, a laboratory measurement set-up is made for a single measurement system as seen in Figure 3.12. The measurement system is connected to a LV grid simulator, producing a polluted grid voltage of 50Hz with a THD of 8%. The analysis of the measured voltage and current is done with Matlab software, running on a personal computer. For the stimulus the special waveform according to Figure 3.6, is amplified with a power operational amplifier, used in a current source mode. To couple the amplifier to the grid, for injecting the stimulus, a 12/230V toroid transformer is used. An analogue to digital conversion system takes samples of the grid voltage and the injection current. Time series of this data are analyzed to calculate the harmonic impedance spectrum. The used impedances are: $Z_{grid} = 0.4 + j0.25\Omega$ and $Z_{load} = 26.5 - j200\ \Omega$ at a frequency of 50Hz. For the load a resistor in parallel with a capacitor is used.

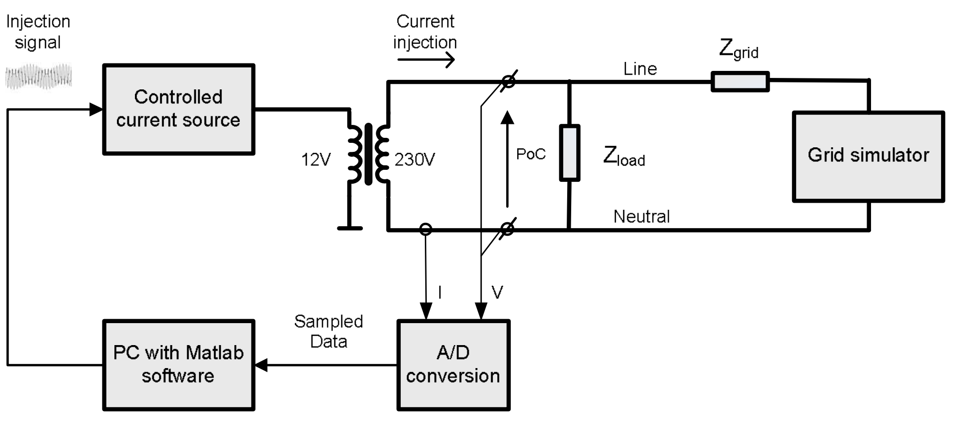

Figure 3.12: Impedance measurement in a laboratory set-up.

The exact impedance spectrum is plotted as a grey solid line in Figure 3.13 and in Figure 3.14. The measured impedances of the harmonics are plotted as black dots in the same figures. These figures give the harmonic impedance plot and the Polar diagram at the PoC, calculated with the measurement system from time series, and measured in the laboratory set-up. To calculate the harmonic impedances, a time series length of 1 second is used, and for the fundamental impedance, 4 seconds. This should be fast enough according to [Bag 98].

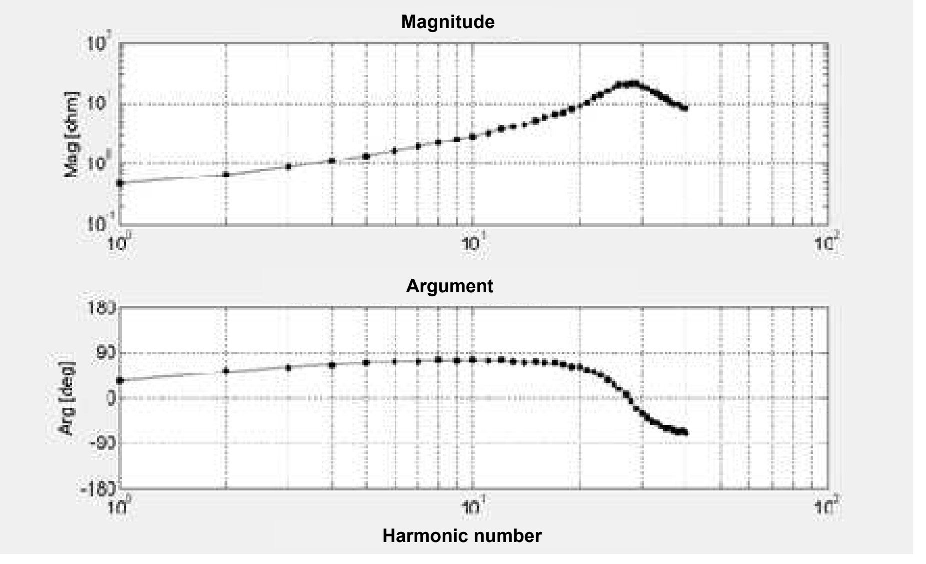

Figure 3.13: Harmonic impedance plot of the impedance at the PoC, measured in a grid with a strongly polluted voltage (THD of 8%).

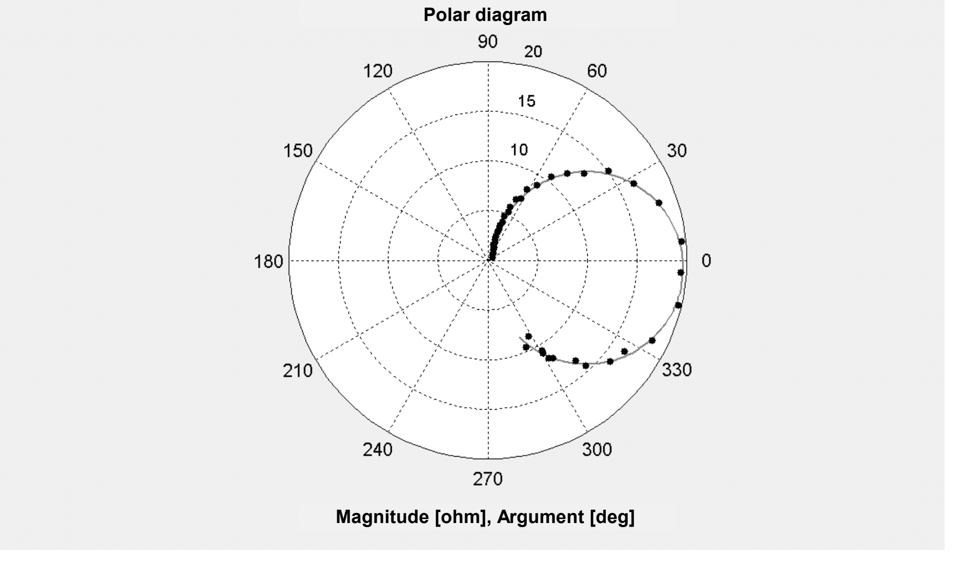

Figure 3.14: Polar plot of the impedance at the PoC, measured in a grid with a strongly polluted voltage (THD of 8%).

The purpose of the measurement system is to estimate the small signal harmonic impedance in a steady-state condition. Therefore, a Fourier based system is chosen. This impedance information can be used to locate possible resonances in the grid to take measures to minimize the impact. Another use is to make power electronics based converters automactically adaptive to various grid situations, see Chapter 5.

3.6 Conclusion

In this chapter a harmonic impedance spectrum measurement system is described, simulated with Matlab/Simulink and tested in a laboratory.

Because in an electricity grid harmonic components are much lower in amplitude then the fundamental a larger time series length is necessary for the measurement of the fundamental impedance. For this reason, the calculation part of the measurement system is split in two, namely a lock-in system to estimate the fundamental impedance and a FFT system to estimate the harmonic impedances. Another motivation for this choice is that it reduces the need for processor calculation power. Results from simulations and measurements show, that a periodical time series length of 1 second for harmonics and 4 seconds for the fundamental give good results.

Results from simulated and practical measurements show that the measurement system can work well by injecting a very low measurement current, lower than the allowed emission of a home appliance of 75W, falling in class D of the IEC 61000-3-2 standard. Besides that, the measurement system is capable of operating under polluted grid voltages with a THD of 8% and also added to this, a white noise of 0.25%. Also the grid frequency may vary between the maximum allowed steady-state conditions, i.e. between 49.5Hz and 50.5Hz.

Chapter 4

Modern appliances with constant power

This chapter focuses on the Negative Differential Impedance (NDI) of non-linear Constant Power Loads (CPLs). It is shown that stabilization against grid voltage fluctuations by a power electronics device can lead to a negative differential impedance which can bring an oscillatory grid voltage.

A laboratory measurement shows the CPL effect and computer simulations of small generator-load systems give insight in the effect of oscillatory grid voltages. It is discussed in what frequency range these voltage oscillations can be expected.

4.1 Introduction

Today's appliances increasingly are adapted and controlled by power electronics and processors. This development can bring both advantages and disadvantages for the power quality of the supply system. An advantage, for example, is the growing number of power supplies that are equipped with a power factor corrector front-end. This type of power supply behaves as a resistive load and has a very good power factor. A disadvantage is the stabilization against grid voltage fluctuations by means of power electronics, it acts as a CPL. This type of load has a NDI that can cause an oscillatory grid voltage [Mol 08], [Ema 04].

Other voltage instability effects are noticed in grids with inverters for Photovoltaic (PV) systems. They can bring a negative absolute impedance to the grid in the harmonic frequency range. This effect can reduce damping in the harmonic frequency range and with that, amplify harmonic voltages in the grid [Hes 05].

With the introduction of power electronics in home appliances years ago, the CPL effect with its NDI was introduced. An equivalent circuit of a power electronics based CPL is shown in Figure 4.1. Today the number of this kind of load is rapidly growing and will continue increasing in the future because they are less sensitive to grid voltage fluctuations. Another CPL that could show up in enormous numbers and amounts of power in the future is the battery charger for electric vehicles [Ber 09]. Automatic tap changer transformers are used today at various voltage levels and it is well known that the use of this can affect voltage stability [Aba 07], [Sal 00]. New developments in this field are transformers with power electronics to achieve instantaneous voltage regulation under load changes [Mai 09], [Kes 09]. In this case, a total low voltage distribution area could become a CPL in future grids. Although this evolution may be very recommendable to control the grid, without countermeasures it can lead to the opposite effect, namely oscillatory grid voltages.

An oscillatory grid voltage caused by the NDI of CPLs is a phenomenon that has been observed in small micro grids and isolated systems such as shipboard power systems where generators became instable because of a large share of CPLs [Riv 05]. Besides the rapidly growing numbers of CPLs, today's studies for the design of future electricity systems encompasses the possibility of isolated local distribution systems in specific situations [Cai 08]. The probability that a CPL share take the upper hand is much higher in small isolated systems. Therefore this form of instability will firstly show up in small grids. It might also show up in larger electricity grids when the CPL share remains growing.

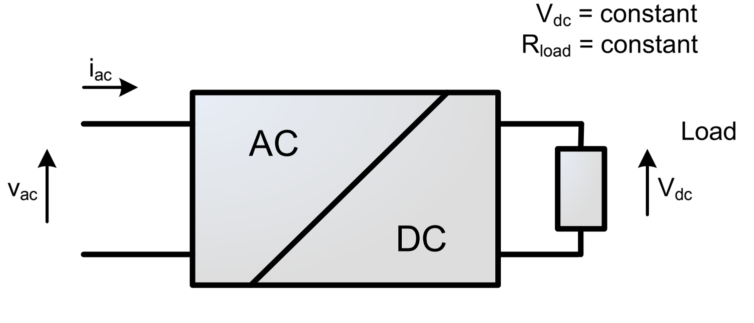

Figure 4.1: A constant power load with negative differential impedance.

4.2 Voltage stability

A CPL can cause instability as the real part of the complex impedance is negative. To get more insight in possible voltage instability a general equation for a linear transfer function in the Laplace domain is given in (4.1) [Coo 72].

$$H(s) = k \frac{\prod_{p=1}^{m} (s - z_p)}{\prod_{q=1}^{n} (s - p_q)} \tag{4.1}$$

Wherein $s = \lambda + j\omega$ is the complex frequency variable, z_p the zeros and p_q the poles of the transfer function. Due to the fact that physical systems cannot increase the response to infinite with a frequency that is rising to infinite, the order of the numerator must be equal or less than that of the denominator, so $n \geq m$ in (4.1).

The voltage instability effect can show up when the transition from one output state to a new state is not be damped to zero, but starts with an increasing oscillation. A remarkable thing is that if the transfer function is taken the opposite way, impedance will be turned into admittance, and poles will turn into zeros and the other way round, zeros will turn into poles. With this a stable system can become unstable. An example of this is the fluorescent lamp, that cannot be driven in a stable way directly (without a ballast) from a voltage source, but can be driven in a stable way directly from a current source [Den 97].

The impedance of the grid at a certain point will be determined by a number of parallel and series impedances in the surrounding area, depending on the grid structure. Assume that there are appliances in the grid that show a negative impedance value, then these particular impedances can reduce the damping in the system which results that poles are shifted towards the positive real half-plane. If the number of this kind of impedances rises significantly, poor damped resonances might occur. This phenomenon can happen when the grid voltage level goes from one state to a new state, as can be seen later in this chapter.

4.3 Impedance of appliances

The differential impedance of a grid connected appliance is the impedance that holds for deviations round an operation point, and the absolute impedance is the impedance when the appliance is working steady in that operating point. In other words, the differential impedance holds for deviations on a bias signal. The bias signal can, for example, be the grid fundamental and the deviation can be a slow variation like a flicker distortion, a sub-harmonic or an oscillation.

Non-linear grid connected appliances can have a different impedance for each operating point. Appliances that can be specified with only one impedance figure for all operating points are pure linear components without saturation effects. For example, a pure resistor has the same impedance for all frequencies in all operating points, where the absolute and differential impedance is just the resistor value. Generally this is not the case in practice; even an incandescent lamp is non-linear because of the temperature dependence of the filament resistance. This temperature effect is a slow process and its differential impedance differs from the absolute impedance at slow varying voltage levels.

Because the differential impedance of non-linear loads depends on the operation point, the differential impedance only can be seen as linear for small signals around this operating point.

4.3.1 Absolute and differential impedance

Just as with non-linear loads in general, the impedance of a CPL depends on the applied voltage. In practice a lot of home appliances are loads with AC to DC converters feeding an internal part that works on a constant direct voltage. The control system of these AC to DC converters controls the direct voltage V_{dc} in such a way that the voltage is independent of the applied grid voltage V_{ac} (see Figure 4.1). This implies that the AC power remains constant even in case the grid voltage varies. If the grid voltage increases, the grid current will decrease and also the other way round, if the grid voltage decreases, the grid current will increase. This behavior brings a NDI and as explained in section 4.2 can lead to voltage instability.

In Figure 4.2 a sketch of V_{RMS}-I_{RMS} curves of two typical loads are given. The left side figure (a) represents an incandescent lamp, where the gray dashed line is the absolute impedance for a certain operating point that depends on the applied Root Mean Square (RMS) voltage, and the gray solid line the positive differential impedance in that operating point. The right side figure (b) represents a power supply which shows a NDI.

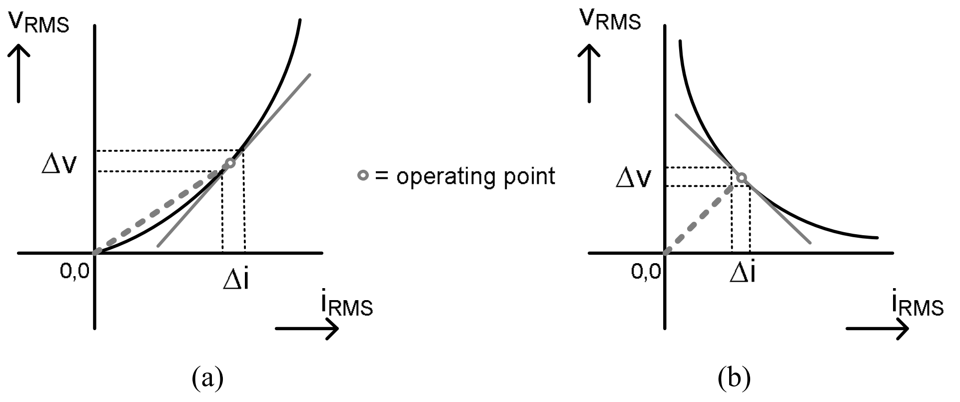

Figure 4.2: Black: v_{RMS}-i_{RMS} curve of a load, grey dashed: absolute impedance, grey solid: differential impedance – (a) incandescent lamp type load, (b) power supply type load.

The absolute impedance can also be negative [Hes 05] and shown in Figure 4.3. However, this cannot exist with a single physical component as an energy source is required.

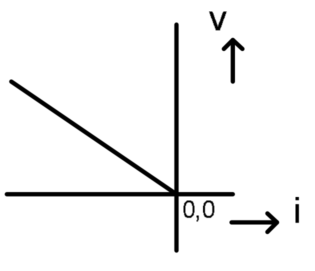

Figure 4.3: A negative absolute impedance.

In general, it can be said that loads or sources connected to the grid with power electronics interfaces have the potential to show a negative absolute impedance as well as a NDI.

4.4 Estimation of the NDI

To find the NDI effect, the operating point of a CPL must be changed. This change of operating point happens when the amplitude of the grid voltage is fluctuating slowly and in a way that the appliance is able to follow this variation with a changing operating point. This can be achieved when a low frequency distortion voltage modulates the grid fundamental voltage or when a low frequency distortion voltage is summated to the grid fundamental voltage.

4.4.1 Estimation of the NDI with a modulated distortion

Equation (4.4) gives the situation where the fundamental voltage v_f (4.2) is modulated with a small, low frequency distortion voltage v_d (4.3).

$$v_f = \hat{v}_f \cos(\omega_f t) \tag{4.2}$$

$$v_d = \hat{v}_d \cos(\omega_d t) \tag{4.3}$$

$$v_{\mathrm{mod}} = (\hat{v}_f + \hat{v}_d \cos(\omega_d t)) \cos(\omega_f t) \tag{4.4}$$

From (4.4), it can be seen that, because of the modulation, the amplitude of the applied voltage on a CPL can vary in time. Modulation brings a slow varying amplitude when the frequency of v_d is much lower than the frequency of v_f. This means that the operating point of a CPL can be changed and that the NDI effect can show up. Calculations are done with the help of Matlab/Simulink software and DFT, both from simulation on a 500W power supply model and from laboratory measurements on the aggregate load of a PC + LCD screen. Results are shown in section 4.4.5.

4.4.2 Estimation of the NDI with a summated distortion

The summation of a small distortion voltage v_d to the fundamental voltage v_f can also lead to a slow varying amplitude of the grid voltage. For summation of v_d and v_f, the following equation can be derived:

$$v_{sum} = \left(\hat{v}_f + \hat{v}_d \frac{\cos(\omega_d t)}{\cos(\omega_f t)} \right) \cos(\omega_f t) \tag{4.5}$$

From (4.5), it can be seen that because of the summation, the amplitude of the applied voltage on a CPL can vary in time. This means again that the operating point of a CPL can be changed and that the NDI effect could show up. Summation brings a slow varying amplitude when the frequency of v_d reaches the frequency of v_f. During simulations as presented in section 4.4.4 however, it was found that the NDI effect did not appear in this situation. NDI only shows up in a limited frequency range, which strongly depends on some components and the control system of the appliance.

In the simulated and measured situations below, NDI only shows up when the fundamental voltage v_f is modulated with a distortion voltage v_d.

4.4.3 NDI in the frequency domain

Figure 4.4 shows a typical control system of a power supply with a constant power load with a NDI. The frequency band where this NDI shows up depends on the transfer functions and behavior of the internal parts of the power supply.

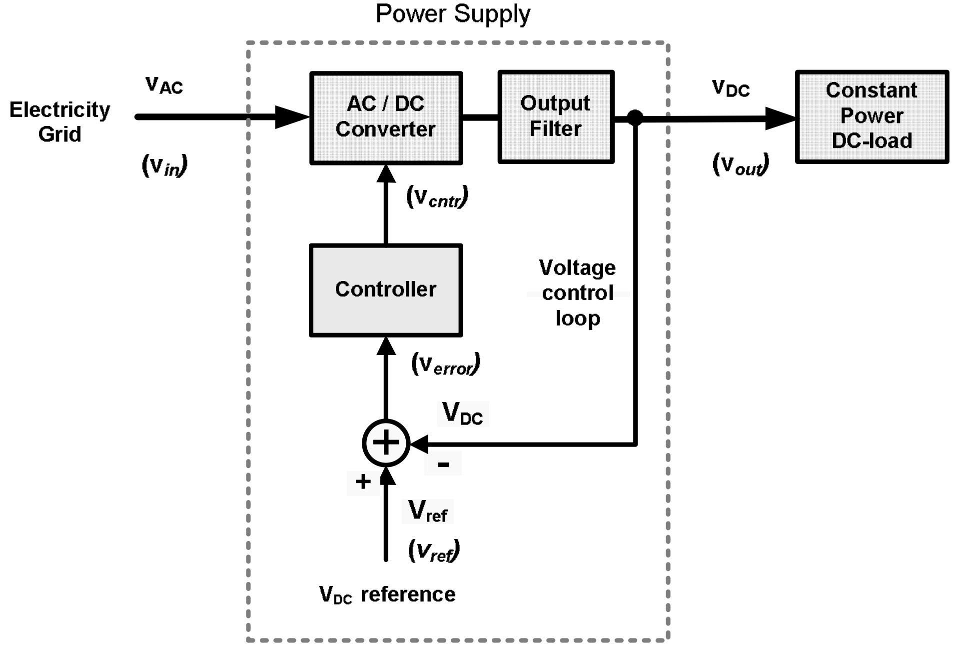

Figure 4.4: Typical control system of a CPL converter with a NDI.

The small signal transfer functions of the power supply of Figure 4.4 given in this section are simplified and counts for a Buck-converter that is operating in the continuous mode. The control system only has a voltage feed-back, no voltage feed-forward nor current-mode control is used. The output capacitor Equivalent Series Resistance (ESR) is not taken into account. Signal delay because of sampling and modulation is also not taken into account.

The closed-loop transfer function from v_{ref} to v_{out} is given in (4.10) and a Bode magnitude plot in Figure 4.5. To show the effect of the control system on the NDI, the closed-loop transfer function from v_{in} to v_{out} is given in equation (4.12) and also a Bode magnitude plot in Figure 4.6.

These transfer functions are built up as follows:

In the control system, as depicted in Figure 4.4, the controller function, v_{error} to v_{cntr} is typically:

$$H_1\left[\frac{v_{cntr}}{v_{error}}\right] = k_1 \frac{(s\tau_c + 1)^2}{s\tau_c} \frac{1}{s\tau_p + 1} \tag{4.6}$$

The time constant τ_p is very small and is only introduced to make the system physically realizable. The constant k_1 stands for a certain gain that depends on the chosen system bandwidth.

The transfer function of the AC/DC converter from v_{cntr} to v_{out} is $H_2\left[\frac{v_{out}}{v_{cntr}}\right]$. It is equal to the modulation index, k_2, times the internal bus voltage $V_{DC\ BUS}$, which depends on $v_{AC\ RMS}$. The voltage $V_{DC\ BUS}$ is here assumed to be a constant k_3, which can only be done for small signal analysis. The output filter is chosen to be of a second order type: $\frac{1}{(s\tau_f + 1)^2}$, so:

$$H_2\left[\frac{v_{out}}{v_{cntr}}\right] = k_2 k_3 \frac{1}{(s\tau_f + 1)^2} \tag{4.7}$$

If τ_c is chosen to be equal to τ_f, the round going loop-gain of the system is:

$$\overset{0}{H}\left[\frac{v_{out}}{v_{error}}\right] = k_1 k_2 k_3 \frac{1}{s\tau_f} \frac{1}{s\tau_p + 1} = k_{tot} \frac{1}{s\tau_f} \frac{1}{s\tau_p + 1} \tag{4.8}$$

Because the time constant τ_p is very small and is having no contribution to the control loop, the second term of (4.8) is further left out:

$$\overset{0}{H}\left[\frac{v_{out}}{v_{error}}\right] \approx k_{tot}\,\frac{1}{s\tau_f} \tag{4.9}$$

The closed-loop transfer function v_{ref} to v_{out} is in this case:

$$H\left[\frac{v_{out}}{v_{ref}}\right] = \frac{H_1 H_2}{1+\overset{0}{H}} = \frac{\overset{0}{H}}{1+\overset{0}{H}} = \frac{1}{s\dfrac{\tau_f}{k_{tot}}+1} \tag{4.10}$$

To estimate the frequency band where a NDI exists, presentation in the $j\omega$ domain is sufficient. This means that the λ part of the complex frequency $\lambda + j\omega$ is left out. This also means that only the steady-state modus is depicted and the damping of the system cannot be seen.

The Bode magnitude plot of Figure 4.5 shows a roll-off frequency in the $j\omega$-domain, equal to $\dfrac{k_{tot}}{\tau_f}$ from (4.10). This means that v_{out} can follow v_{ref} up to this point, roughly without reduction.

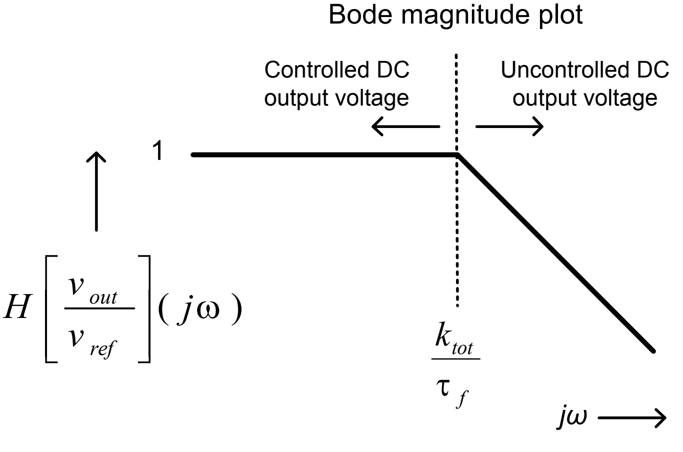

Figure 4.5: Bode magnitude plot of equation (4.10).

To get more insight of the area where a NDI exists, the closed-loop transfer function from v_{in} to v_{out} and a Bode magnitude plot is given in equation (4.12) and Figure 4.6. To get this figure, the closed-loop transfer function is derived below.

The open-loop transfer function from v_{in} to v_{out} is:

$$H'_2\left[\frac{v_{out}}{v_{in}}\right] = k_2 \frac{1}{(s\tau_f + 1)^2} \tag{4.11}$$

And the closed-loop:

$$H\left[\frac{v_{out}}{v_{in}}\right] = \frac{H'_2}{1 + H_0} = k_2 \frac{s\dfrac{\tau_f}{k_{tot}}}{s\dfrac{\tau_f}{k_{tot}} + 1} \frac{1}{(s\tau_f + 1)^2} \tag{4.12}$$

The first part of expression (4.12) shows the active filtering of v_{in} towards v_{out} by the control system and the second part shows the passive filtering of the output filter of the converter. For easy understanding, the effect of the output filter, the second part of expression (4.12), is neglected in Figure 4.6. At the frequency where the figure overturns, the control system is no longer able to limit grid voltage changes in v_{out}. It is this point where the NDI behavior stops. In this example, this equals $\dfrac{k_{tot}}{\tau_f}$.

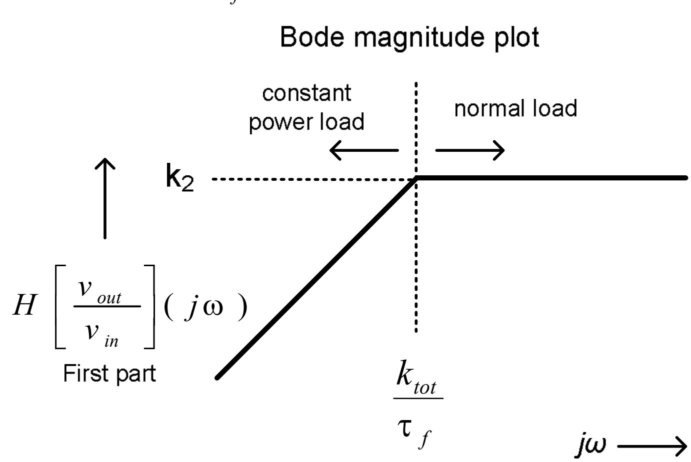

Figure 4.6: Bode magnitude plot of the first part of equation (4.12).

In this simplified figure, the large influence of the output filter and also the buffer capacitor of the AC/DC converter are not taken into account. For single-phase power supplies a large buffer capacitor is needed to guarantee a constant output power flow. Although a large buffer capacitor is not needed for three-phase power supplies, very often a large one is used for handling ride-through capability and asymmetrical voltages. This component however, has a large influence on the NDI in the frequency domain. Assuming that the differential impedance without the effect of the buffer capacitor equals $-R$, the differential impedance with this capacitor included can be modelled as a parallel circuit according to Figure 4.7.

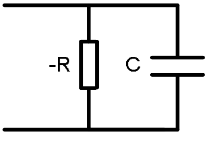

Figure 4.7: Simplified model of the differential impedance with the buffer capacitor included.

In equation (4.13) the impedance in the $j\omega$ domain of a RC parallel circuit is given.

$$Z(j\omega) = \frac{R}{j\omega RC - 1} \tag{4.13}$$

Replacing the resistance R for $-R$ in (4.13) gives the following expression for the NDI:

$$Z(j\omega) = -\frac{R}{1 - j\omega RC} \tag{4.14}$$

Figure 4.8 gives a plot of the polar diagram of (4.14).

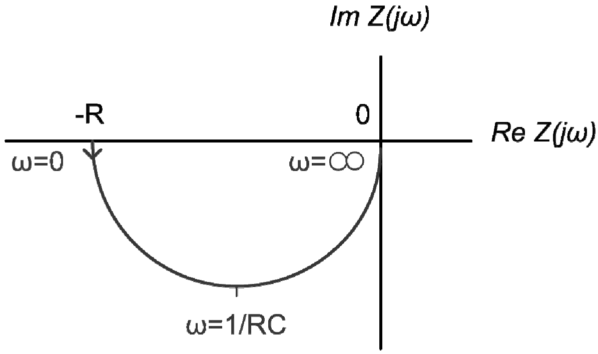

Figure 4.8: Effect of the buffer capacitor on the NDI.

In practice, this figure is not a perfect circle bow, because $-R$ is not a constant value, but depends on the converter's transfer function, for example like the one of equation (4.12).

4.4.4 Simulated NDI behavior – impact of voltage modulations

To estimate the frequency range where the NDI characteristic holds, Matlab/Simulink analysis on a simulated 230V/50Hz/500W single-phase power supply are performed. The AC input side of the power supply is driven by an ideal 230V/50Hz voltage source that has a modulation facility. The DC output side of the power supply is loaded with a 500W resistive load. During the simulation sequence, the grid voltage is modulated with a series of frequencies from 0.05 Hz to 5 Hz. Time series of the sampled input voltage and input current are stored and analyzed via DFT, to calculate the input impedance. A polar plot of the calculated differential impedance as a function of the modulated voltage is shown in Figure 4.9; this figure shows the differential impedance of a system that starts from pure resistive NDI at frequencies below 0.05Hz, towards a more capacitive-resistive system at higher frequencies.

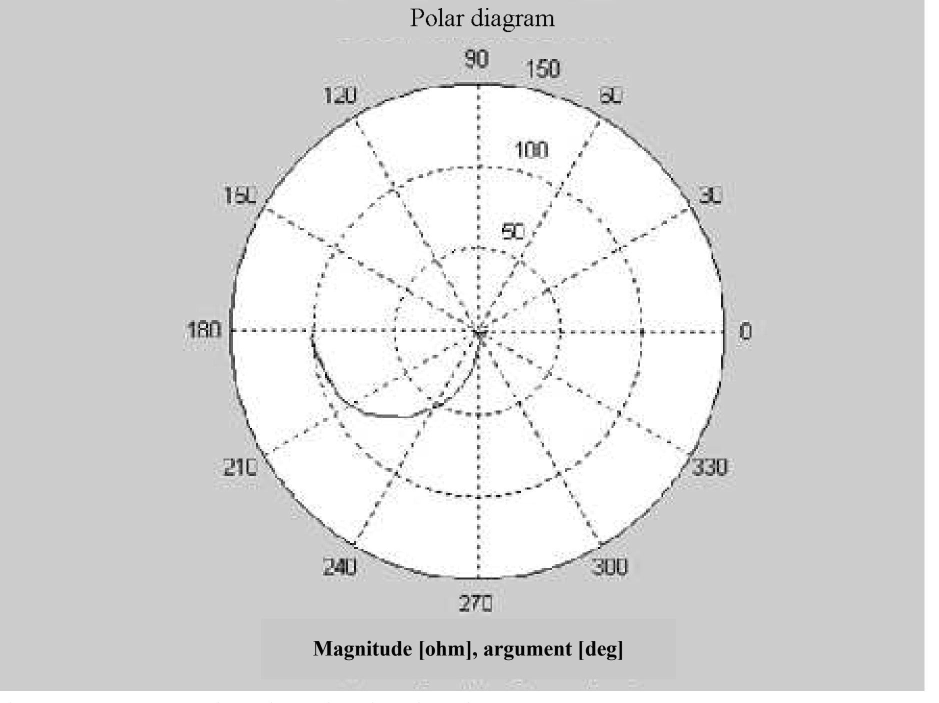

Figure 4.9: Polar plot of a simulated NDI.

4.4.5 NDI laboratory experiment

Additionally to the Matlab/Simulink experiments on a simulated 500W loaded power supply in the previous section, a real PC + LCD screen load is brought to a laboratory and subjected to a modulated 230V/50Hz single-phase grid voltage from a grid simulator. A drawing of this set-up is given in Figure 4.10 and a photograph in Figure 4.11. The first measurement with this set-up is the V_{RMS}-I_{RMS} curve of the load to show the NDI. However this does not give time nor frequency information. Therefore the time series of the sampled input voltage and input current are extracted from a Power Analyzer and stored and analyzed via DFT in a computer with Matlab/Simulink to calculate the input impedance in the frequency domain.

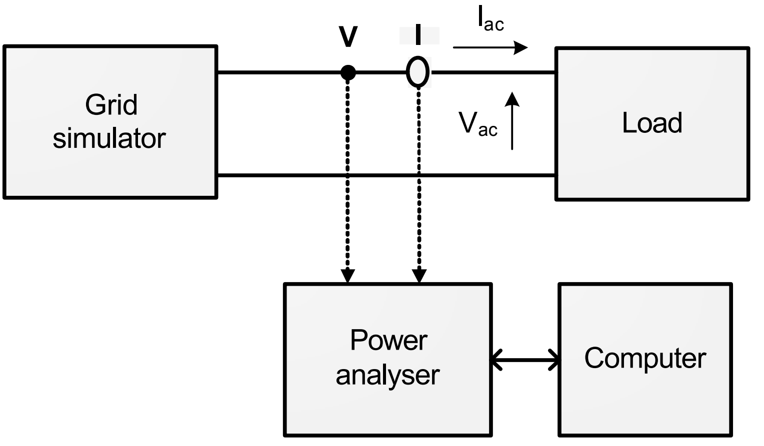

Figure 4.10: Measurement set-up for a CPL.

Figure 4.11: Laboratory measurements for a CPL.

In Figure 4.12, the V_{RMS}-I_{RMS} curve of the PC + LCD screen is plotted showing a constant power load with NDI. For this measurement the supply voltage was ramped down from 250V_{RMS} to 145V_{RMS} in 500ms time. During this ramp the RMS voltage and current were measured.

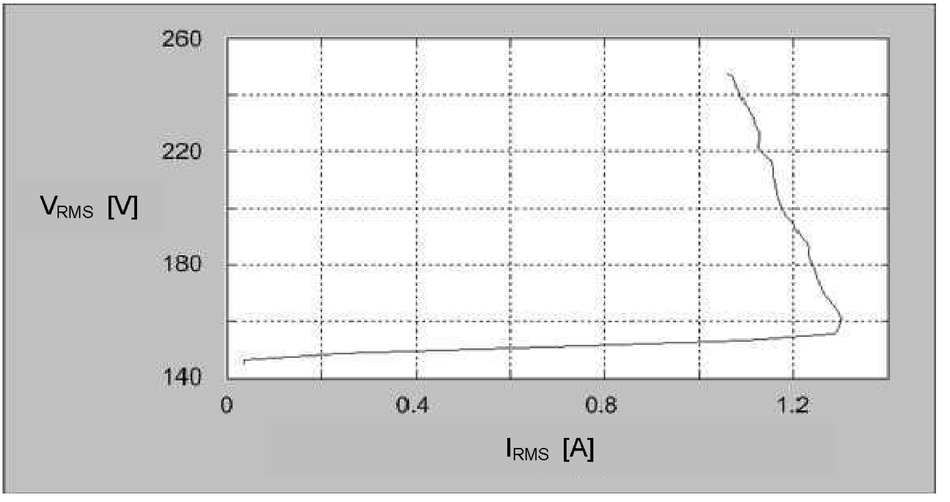

Figure 4.12: V_{RMS}-I_{RMS} curve of a PC + LCD screen, a CPL with a NDI.

As can be seen in Figure 4.12, the NDI shows up in a wide operating range. This NDI was expected because the internal electronics of the PC + LCD screen are both fed by a power supply which controls its DC output voltage. Below $160V_{RMS}$ input voltage the PC + LCD screen shuts down.

Next, the differential impedance is measured. Therefore, the grid voltage is modulated with a series of frequencies from 0.02 Hz to 5 Hz. A Polar plot of the calculated impedance of this system is shown in Figure 4.13. It shows a curve that starts from pure resistive NDI at frequencies below 0.02Hz, towards a more capacitive-resistive system at higher frequencies.

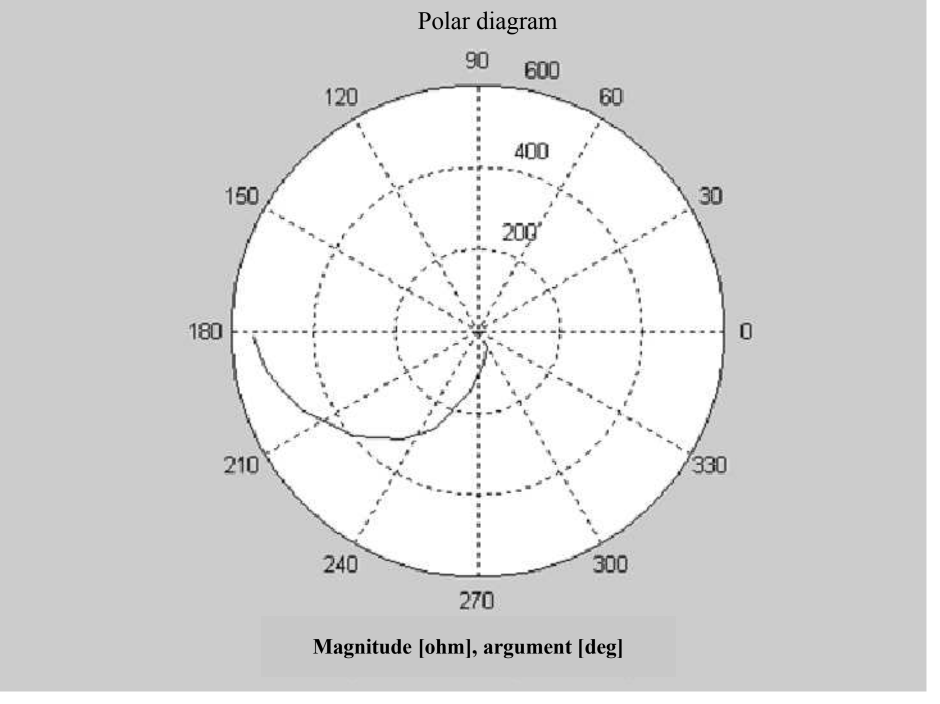

Figure 4.13: Polar plot of a measured NDI.

4.5 Generator – load simulation

In this section an oscillatory grid voltage is simulated with the help of a Matlab/Simulink computer model. The model is built up of a diesel-generator combination feeding in the first stage three loads, namely an asynchronous motor, a resistive load and a CPL (see Figure 4.14). In the second simulation, the asynchronous motor is removed from the grid and replaced by an inductive linear load (see Figure 4.16). With these simulations, the effect of various CPL shares on voltage oscillation is shown.

For the diesel-generator combination, an adapted model from the SimPowerSystems library was used. The chosen inertia constant of the diesel-generator combination has a value of H=1.5s. Further, the nominal generator power equals 120kVA. The generator speed is controlled by a governor system and the generator output voltage is controlled by a field winding control system.

The asynchronous motor model is also from the SimPowerSystems library. The motor is loaded with a constant torque in a way that the output power reaches the nominal value. Saturation effects are also taken into account in this model.

The CPL has an internal AC/DC converter loaded via a resistor at the DC output voltage. Although this converter is a three-phase type, an internal buffer capacitor of 3000µF was used in the model. The maximum power of this load is 80kW. The power of the CPL is adjusted by changing the load on the DC output side of the converter.

The loads applied to the generator do not exceed the maximum power level. With this, voltage collapse is not an issue, only oscillatory voltages.

The grid is modeled as an inductive-resistive system, the effect of capacitive grid impedances are not taken into account, because effects are suspected in frequencies far below the fundamental grid frequency.

4.5.1 Effect of a CPL in a grid with a motor and a linear load

In this simulation the generator is loaded with an asynchronous motor, with an input power of 16kW active and 32kVAr inductive, a variable 0-64kW resistive load and a variable 0-64kW CPL, as indicated in Figure 4.14. In this situation the CPL share is increased from 0 to 80% of the total active power and the total active power is kept constant by decreasing the power of the resistive load at the same time.

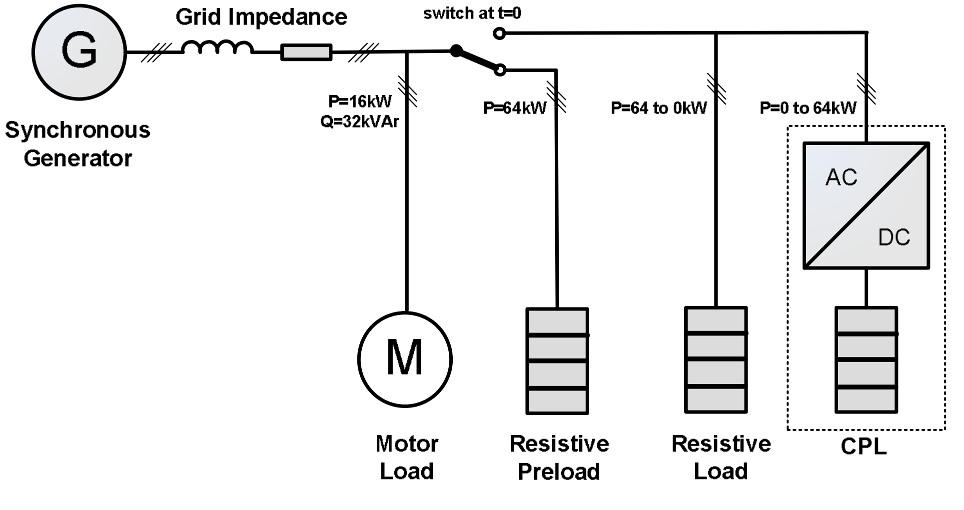

Figure 4.14: Generator-load model 1.

In Figure 4.15 the line RMS Voltage as function of time is plotted for different load situations, combined to a three-dimensional plot. Before the starting point, time = 0, the grid is in a stable condition, loaded with the motor load and a 64kW resistive preload. The resistive preload is switched off at time = 0 when its current passes through zero at the first current zero crossing. Directly hereafter at a zero-crossing of the voltage, the variable resistive load and the CPL load combination is switched on. The small delay results in a step response, which shows the damping of the system.

RMS Generator Voltage f(time, CPL share)

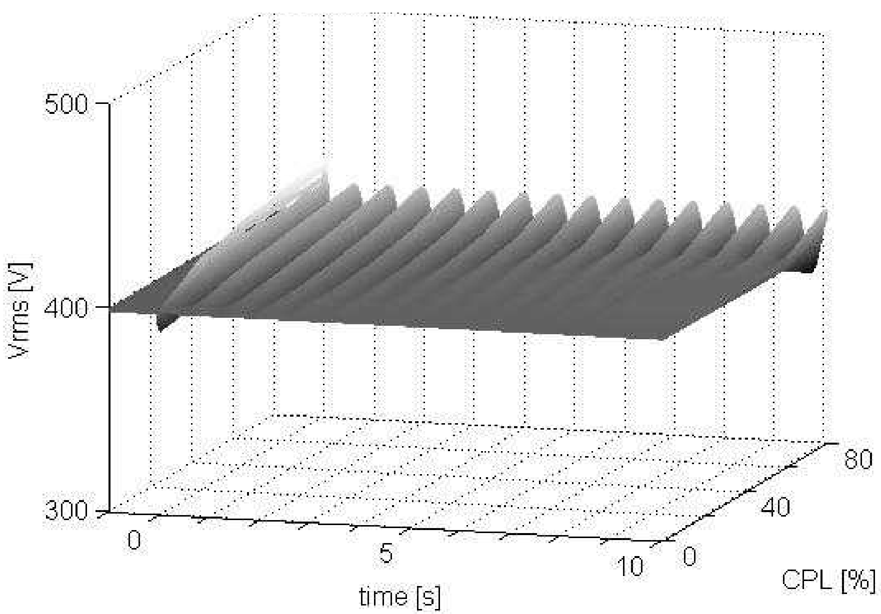

Figure 4.15: Effect of the CPL share in generator-load model 1.

In Figure 4.15, the expressed percentage of the CPL is referred to the total active load of 80kW, so 40% CPL means that the grid is loaded with 32kW CPL and 48kW from the resistive and the motor load. 80% CPL means that the grid is loaded with 64kW CPL and 16kW from the motor load. As can be noticed from Figure 4.15, at a CPL share of 80%, the voltage in this simulated set-up remains oscillating. The set-up model used shows the presence of an oscillation frequency of about 1.5Hz.

4.5.2 Effect of a CPL in a grid with only a linear load

In the second simulation the generator is loaded with a resistive and inductive linear load and a CPL. The inductive load is kept constant and while the resistive load decreases, the CPL increases. In this way the active load changes from 100% resistive and 0% CPL to 0% resistive and 100% CPL, see Figure 4.16.

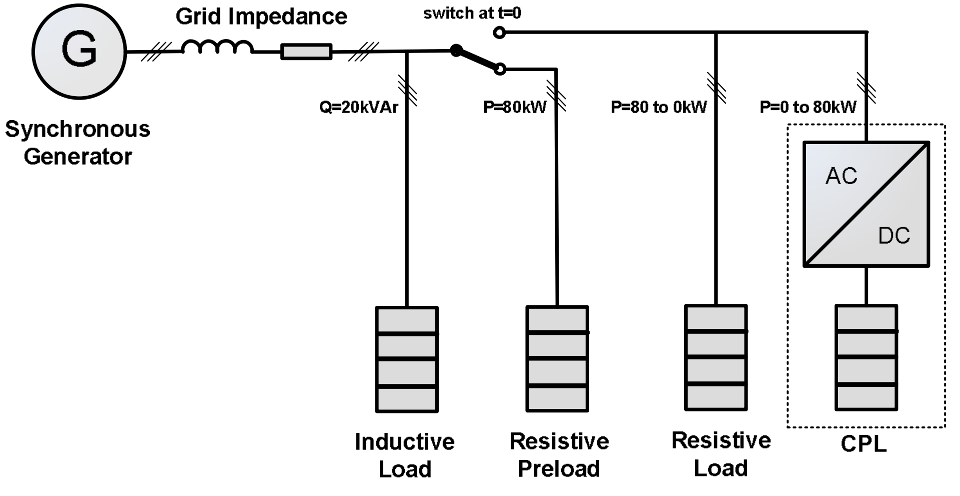

Figure 4.16: Generator-load model 2.

In Figure 4.17, the line RMS Voltage as a function of time is plotted with the different load situations combined to a three-dimensional plot. The generator is loaded in all cases with the 20kVAr inductance. Beside this, 80kW active power is drawn from the generator, by a mixture of resistive load and CPL. The expressed percentage of the CPL is referred to the total load of 80kW, so 50% CPL means that the grid is loaded with 40kW CPL and 40kW resistive load.

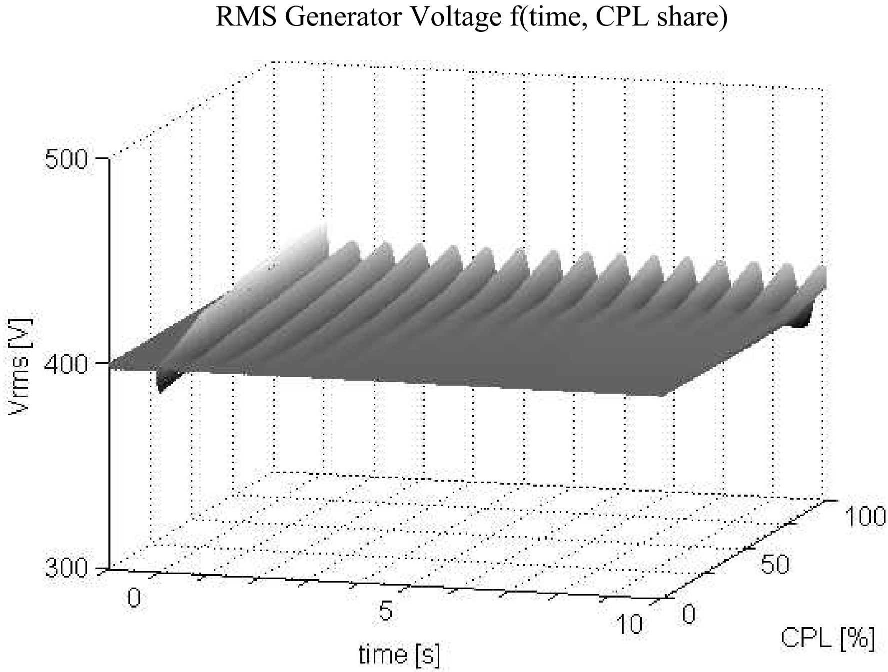

Figure 4.17: Effect of a CPL share in generator-load model 2.

Before the starting point time = 0, the grid is in a stable condition, preloaded with 80kW resistive load and 20kVAr inductive load. The resistive preload is switched off at time = 0 when its current passes through zero at the first current zero-crossing. Directly hereafter at a zero-crossing of the voltage, the variable resistive part from the linear load and the CPL load are switched on. The small delay results in a step response, which shows the damping of the system. As can be noticed from Figure 4.17, at a CPL share of about 80% and more, the voltage in this simulation remains oscillating. Also here, the set-up model used shows the presence of an oscillation frequency of about 1.5Hz.

4.5.3 Effect of the generator voltage control system

In the simulations of the previous sections, the voltage control settings of the generator model were default. The simulations show that this control system performs well without the presence of a CPL in the model. However, these simulations also show that the generator voltage control system is strongly affected by the presence of a CPL. Therefore the performance setting of the generator voltage control system is adjusted to see the effect on grid voltage oscillations. This investigation is done with the help of the generator-load model 2 of Figure 4.16. The voltage control performance is expressed in the frequency bandwidth. A bandwidth of 1 pu is the default value used in the simulations of the previous sections reducing this figure means a reduction in the voltage control speed.

In Figure 4.18, Figure 4.19 and Figure 4.20, the line RMS Voltage as function of time is plotted with different generator voltage control bandwidths from 1 pu down to 0.66 pu, combined to a three-dimensional plot. In all cases 80kW active power is drawn from the generator by a specific mixture of resistive load and CPL for each figure. The percentage of the CPL is referred to the total load of 80kW; besides this the generator is loaded in all cases with 20kVAr inductance (see Figure 4.16).

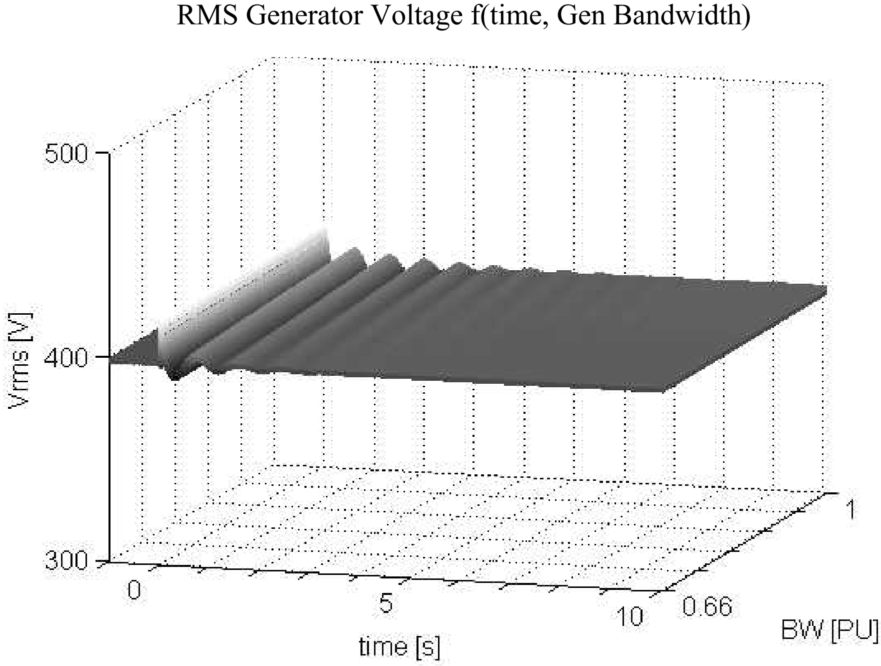

Figure 4.18: Effect of the generator voltage control bandwidth, while loaded with 50% CPL.

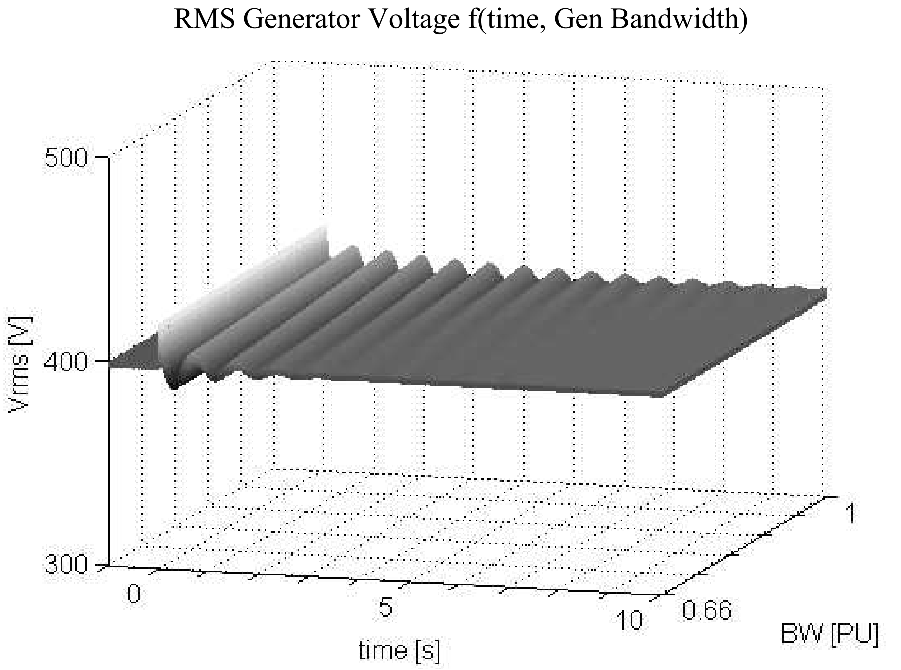

Figure 4.19: Effect of the generator voltage control bandwidth, while loaded with 75% CPL.

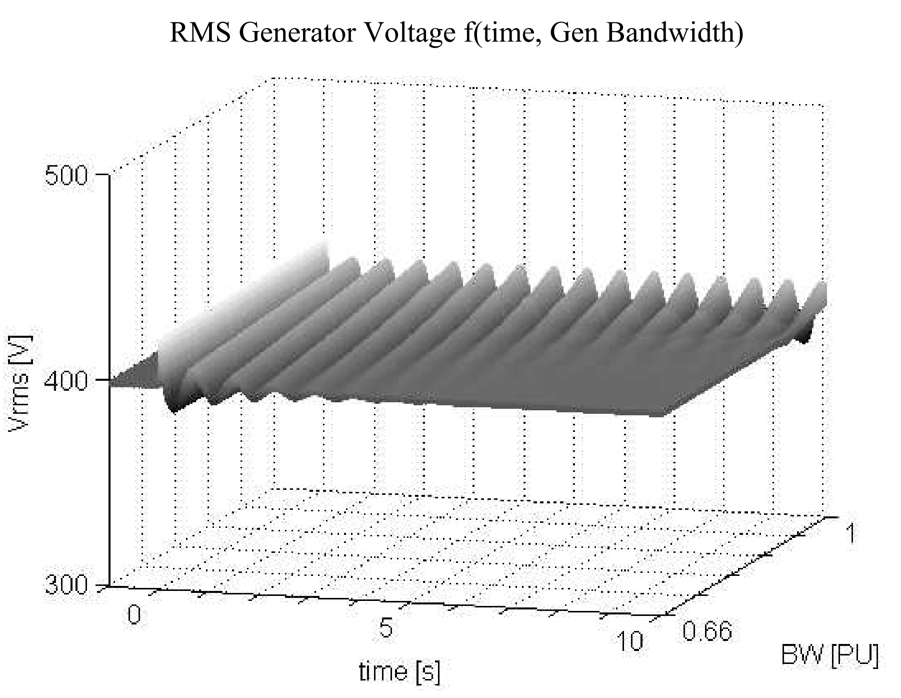

Figure 4.20: Effect of the generator voltage control bandwidth, while loaded with 100% CPL.

In Figure 4.18, Figure 4.19 and Figure 4.20, the CPL share is increased from 50% to 100%. As can be noticed from these figures, the generator voltage control bandwidth needs to be reduced only slightly to free the system from poorly damped oscillatory voltages.

4.6 Conclusion

From simulations with Matlab/Simulink and laboratory measurements, the following conclusions can be drawn for single- and three-phase power electronics based loads with a significant buffer capacitor and a CPL behavior.

The NDI effect comes up when the fundamental grid voltage is modulated with low frequency voltages in the range of about 0.02 to 5Hz, voltage oscillation is found with frequencies in this range.

A concern is the possible impact on voltage instability because of the interaction of NDI and the voltage control systems of generators, especially in small isolated grids or distribution areas that operate in island mode. This is because the energy supply is small and easily affected by a CPL fraction that takes the upper hand. However, it can also show up in larger electricity grids when the CPL share remains growing at various power/voltage distribution levels.

A possible solution for this problem can be found in adjusting the parameters of voltage control systems.

Chapter 5

Ancillary services for harmonic reduction

In this chapter computer simulations with a laboratory validated model will give insight in the two ancillary services Virtual Parallel Capacitance Reduction (VPCR) and Virtual Resistive Harmonic Damping (VRHD). These ancillary services can minimize the effect of resonances and reduce harmonic voltages in LV distribution systems. The ancillary services can be implemented in almost all appliances with a power electronics based front-end. In this work a small inverter for DG is used to implement the ancillary services VPCR and VRHD.

Simulations and validation measurements are done in the time domain as well as in the frequency domain. Time domain results show the inverter's behavior with and without the ancillary services VPCR and VRHD activated, in a situation where the grid voltage contains a harmonic pollution. Frequency domain results show the inverter's harmonic impedance measured at the output terminals under various conditions. This output impedance gives an impression of the performance of the inverter at harmonic frequencies.

The harmonic impedance is calculated from time series of measured voltage and current. The magnitude and phase of the impedance at harmonic frequencies are presented in a plot. It must be emphasized that these plots does not show impedance effects between two consecutive harmonics.

5.1 Introduction

Most small inverters for Distributed Generators (DG) of today draw a sinusoidal current with a low harmonic content which can easily comply with the applicable harmonic current emission standards. However, they can increase the harmonic distortion via resonances produced by the interaction of the output filter capacitance of the inverter and the grid impedance. As discussed in Chapter 2, grid resonances can amplify harmonic voltages and may become problematic in future grids with large numbers of power electronics based appliances. It should be mentioned that today's inverters for DG have a relatively large output capacitor up to about 3μF per kW rated output power. The equivalent capacitance of connected home-appliances can vary over a wide range from around 0.6 μF to 6μF. Therefore an inverter of a few kW can bring a large contribution to the total parallel connected capacitances at the Point of Connection (PoC) [Ens 04]. A good starting point to avoid grid resonances in the harmonic frequency range below the 25th harmonic is to let the inverter compensate the current through its output capacitance for the fundamental frequency and a number of harmonics. Because the inverter has the potential to generate such compensating currents, this feature is marked as an ancillary service.

A second measure to minimize the effect of resonances is an ancillary service that is called VRHD, which gives the inverter a resistive behavior for the harmonic frequency range. This will bring extra damping to resonances in the grid [Ryc 05a].

As made clear in section 2.2 of chapter 2, the combination of the two ancillary services VPCR and VRHD, is very effective for minimizing the impact of resonances in the LV distribution grid. This combination contains two measures, firstly VPCR is virtually shifting the resonance towards a higher frequency range where the propagation is limited, preferably above the 25th harmonic, and secondly VRHD damps the resonance peak to a lower level. VRHD will also bring damping to the harmonic currents coming from non-linear loads in the distribution grid.

Figure 5.1 shows a part of a LV distribution grid with a number of ancillary service inverters at several PoCs.

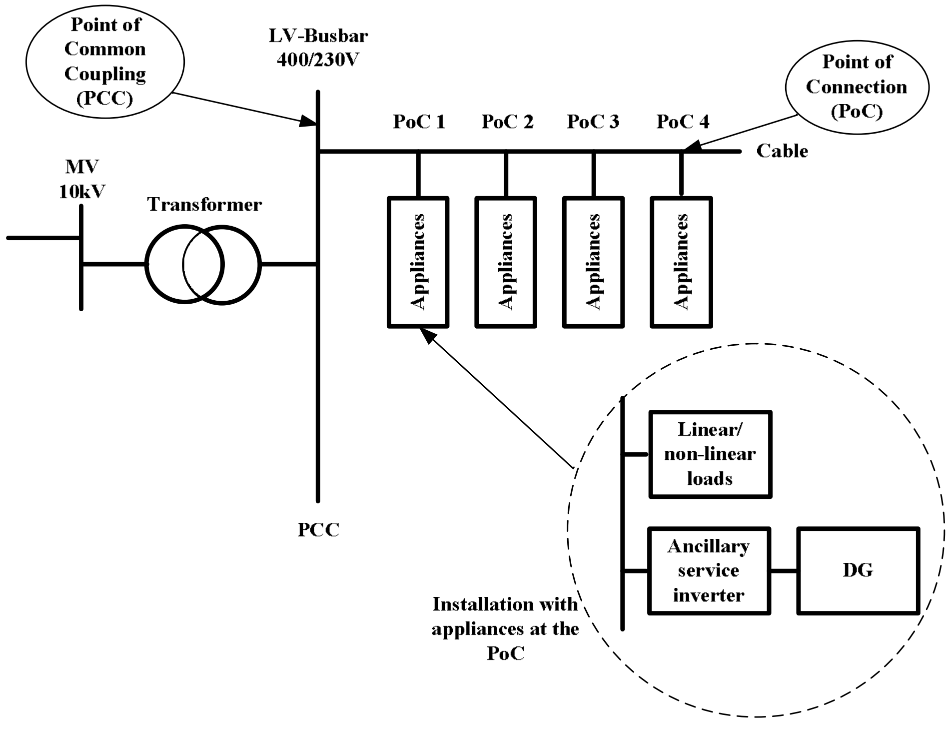

Figure 5.1: Part of a LV distribution grid with a number of ancillary service inverters.

5.2 Simulations on ancillary services

In this section the VPCR and VRHD ancillary services are firstly simulated with a Matlab/Simulink inverter model and then implemented in the Digital Signal Processor (DSP) control system of a hardware inverter by means of automatic code generation [Mat 09]. This hardware inverter is then used in laboratory experiments for the validation of the computer simulations.

To observe the effects of VPCR and VRHD, simulations are done on a network model that behaves according to the standard for the quality of voltage, for the frequency range of interest, i.e. up to the 40th harmonic [Std 01]. Only single-phase systems are studied and unbalance issues are not taken into account in this work. Because the used converter switching frequencies are much higher than the frequencies involved with the control system, an average model is used [Tao 08].

All impedances are simplified and represented as first order systems with only resistance and inductance. Capacitances of cables are not taken into account, because in this simplification, they can be neglected compared to the inverter capacitances and parallel capacitances of loads. Therefore cables are modelled as a resistive-inductive system [Old 04].

Most of the ancillary services inverter performance results are output impedances, presented in a harmonic impedance plot. The output impedance as a function of the harmonic order expresses the interaction between harmonic current and voltage, and numerous aspects and characteristics can be observed from these plots, e.g. the grid-feeding character for harmonic frequencies and the contribution to parallel resonances in the grid.

5.3 The ancillary services inverter simulation model

In this section the ancillary services inverter simulation model is discussed. This model has all the precautions, needed for automatic code generation for the DSP that is used in the hardware model for laboratory validation, see section 5.4.

The studied inverter model in this thesis is based on a grid-feeding system with small Photovoltaic (PV)-inverters. These systems inject their power into the supply system irrespective of grid conditions [Bra 06]. Because the focus of this study is on the interaction between the inverter and the grid, only the grid interfacing part of the inverter is described. Figure 5.2 shows the inverter's basic block diagram with focus on the grid interfacing part.

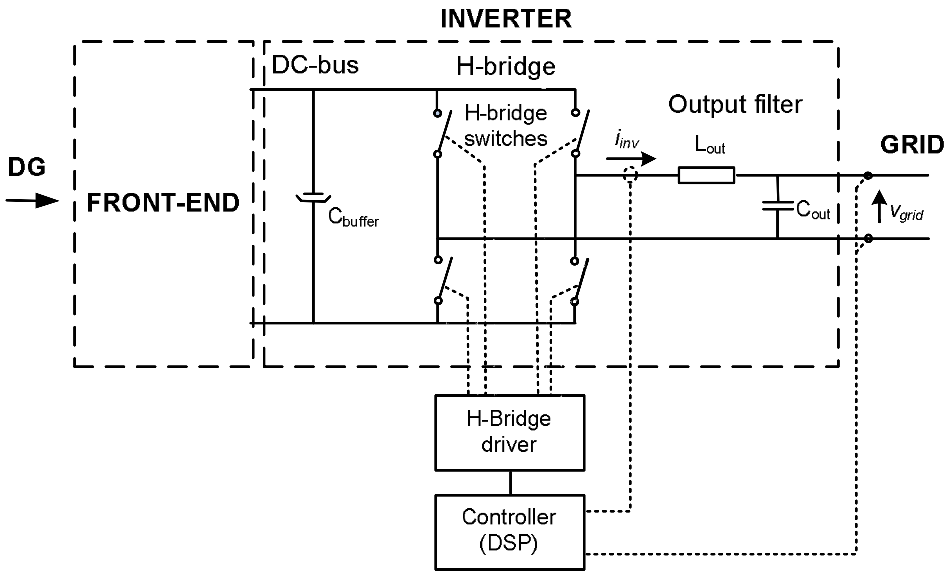

Figure 5.2: The inverter's basic block diagram with focus on the grid interfacing part.

In the following sections successively the topology, the control system, the ancillary services and the effect of large-scale implementation are discussed.

5.3.1 The inverter topology

The used topology for the ancillary services inverter simulation model is a Voltage Source Converter (VSC). A VSC characterizes itself with a low output impedance (i.e. the impedance of the converter seen from the grid). This low impedance is mainly due to the buffer capacitor and the H-bridge switching components. The output impedance is dominated by the output filter, therefore in the harmonic frequency range of interest in this thesis, the output impedance of the circuit of Figure 5.2 varies from inductive to capacitive and in between the system resonates with a high impedance, all because of the dominating effect of the output filter. In Figure 5.3 the buffer capacitor together with the inverter's H-bridge of Figure 5.2 is replaced by a controllable voltage source.

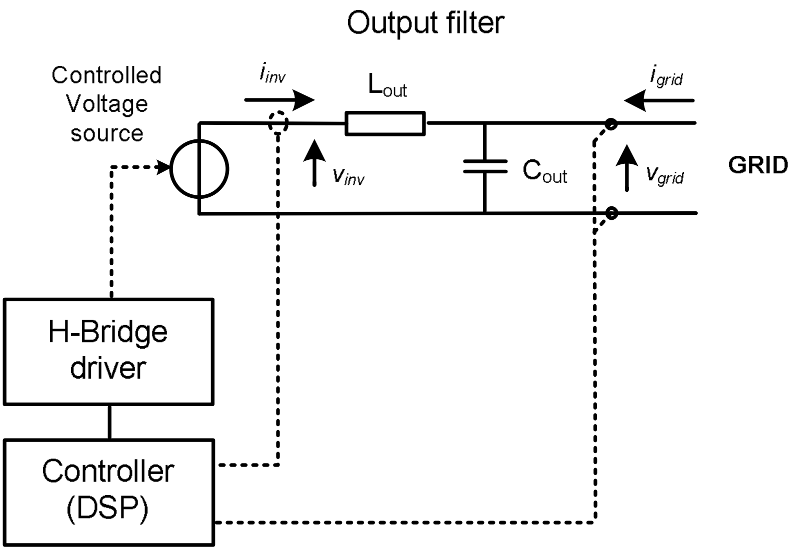

Figure 5.3: The inverter modeled as a controlled voltage source with output filter.

As mentioned before, the ancillary services inverter injects its power to the grid irrespective of grid conditions [Bra 06]. To achieve this, a high output impedance is needed for the 50Hz fundamental and to improve harmonic -and transient performance. Also for a wider frequency range that includes a number of harmonics. A current feed-back control as depicted in Figure 5.4 can provide for this high output impedance while using a VSC.

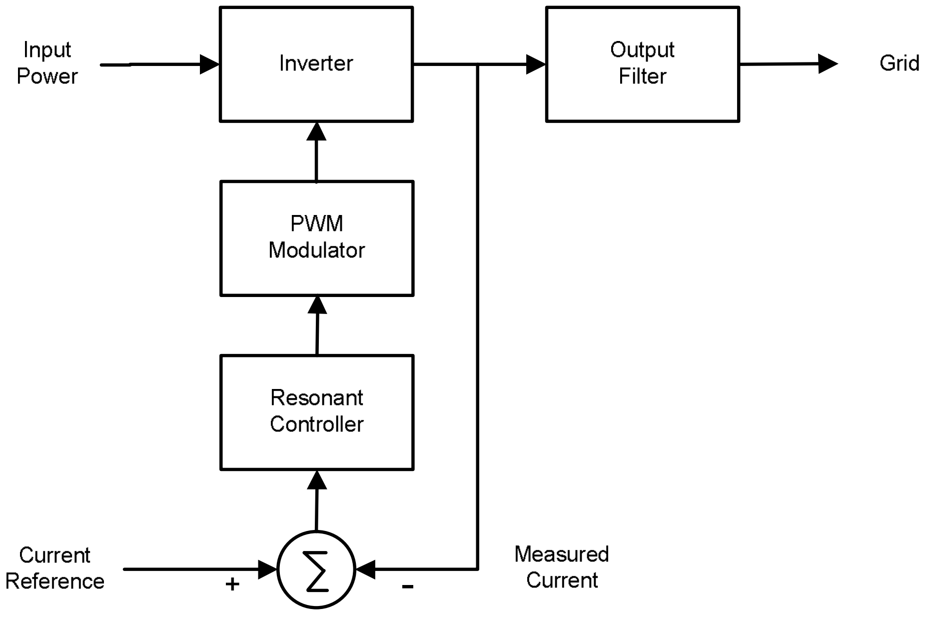

Figure 5.4: An inverter with a current feed-back control system.

Building a control system that performs well at various grid impedances, can easily be done if the only concern would be the 50Hz fundamental, however controlling also a range of harmonics is not a simple task. In today's practice, DSP based controllers are used in switching converters. Although these controllers can easily contain very complex features, the extra sample delay reduces the attainable performance in bandwidth [Tao 08], [Hol 09].

To achieve a robust system in terms of stability at various grid impedances, damping of the interaction between the output filter and grid impedance, with a special control loop is a good option [Li 09], [Lis 06].

5.3.2 The total inverter control system

The block diagram of Figure 5.5 gives the total control system of the inverter with VPCR and VRHD control. This control system measures voltage and current of the inverter system and drives the Pulse Width Modulator (PWM) (see Figure 5.6). As can be seen also in Figure 5.5, a so called "v_L-compensation" feed-forward loop is added to the system for output inductor voltage drop compensation.

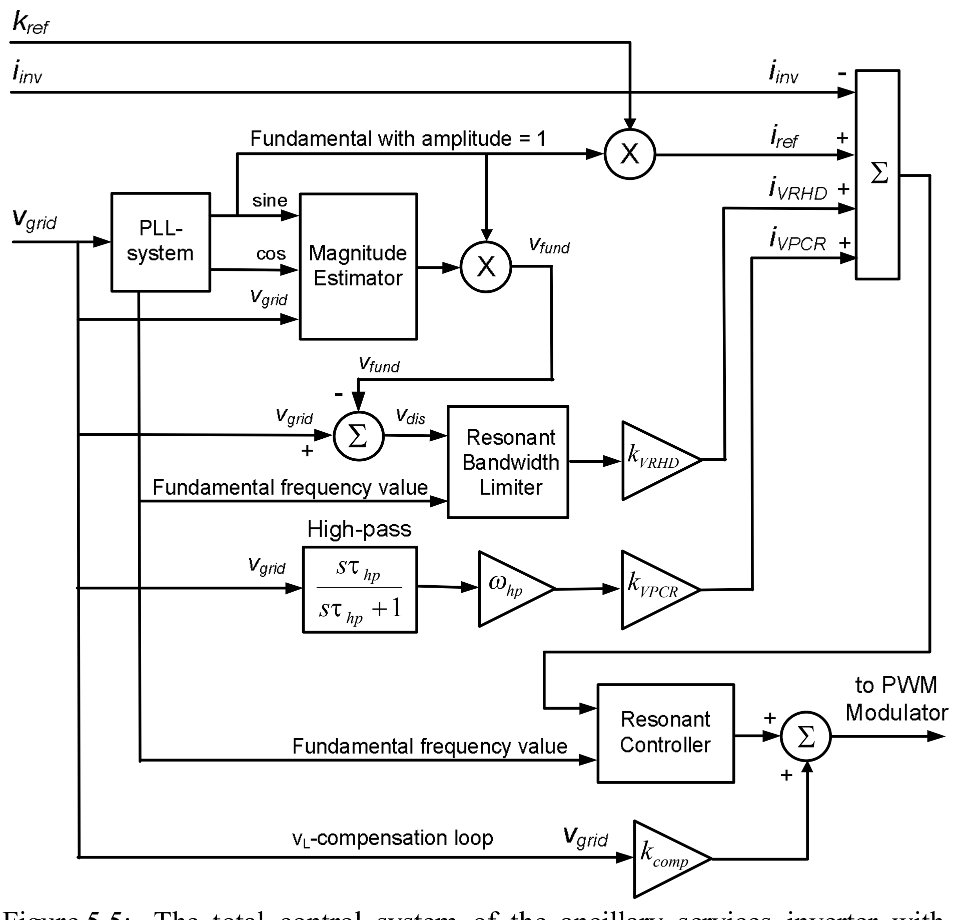

Figure 5.5: The total control system of the ancillary services inverter with VPCR and VRHD control and v_L-compensation.

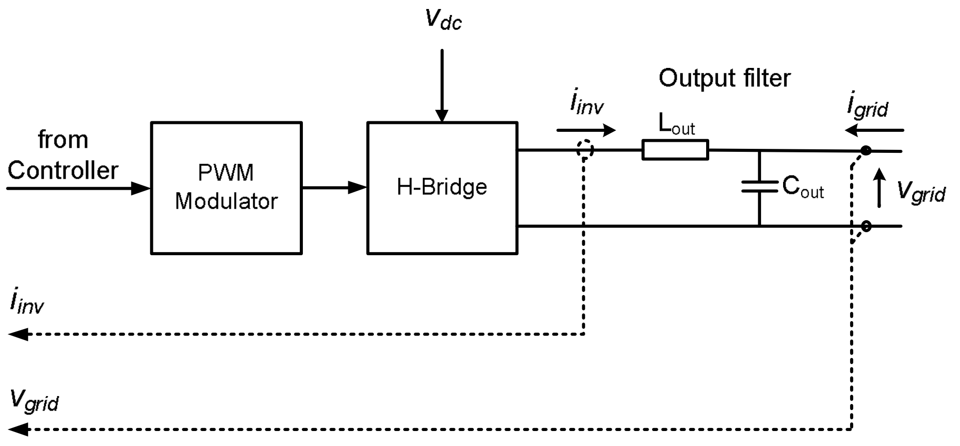

Figure 5.6: PWM modulator and the power-part (H-bridge and output filter) of the ancillary services inverter.

For the total control system, only two signals need to be measured, namely the current through the output inductor of the inverter i_{inv} and the grid voltage v_{grid}, the output of the control system goes to the PWM. A very important part of the control system is the Phase Lock Loop (PLL) system, the base of this system is a voltage controlled oscillator and a lock-in system in a loop. In chapter 3 the lock-in system is explained. The PLL system generates from a grid voltage signal with possible pollution v_{grid}, the following signals: a sine and cosine function with the same frequency as the grid voltage fundamental, and the fundamental frequency value. Sine and cosine functions are used to estimate the fundamental magnitude value from the grid voltage v_{grid}. The sine function is also used to generate a current reference signal i_{ref} that is in-phase with the grid voltage, by multiplying this sine function with k_{ref}. Giving k_{ref} is a positive value will let the inverter deliver real power to the grid. The fundamental voltage v_{fund} is used to calculate the grid voltage pollution v_{dis} by subtracting v_{fund} from v_{grid}, see equation (5.1).

$$v_{dis} = v_{grid} - v_{fund} \tag{5.1}$$

The fundamental frequency value output from the PLL is used to tune the fundamental and harmonic resonators. The used PLL system and the fundamental magnitude estimator are made of building blocks from the Matlab/SimPowerSystems toolbox library [Mat 09].

Just as in many control systems the inverter's output current i_{inv} is fed back with a negative sign and summed with the reference i_{ref} to create an error signal to drive a controller. Two additional inputs i_{VPCR} and i_{VRHD} to this summing point come from the VPCR and VRHD control.

In the following sections several functions of the total control system of Figure 5.5 are explained in more detail.

5.3.2.1 The main controller

A requirement to control a number of harmonics besides the fundamental is to build a control system with a sufficiently high gain-bandwidth product. Normally small single-phase inverters for domestic use are not designed to control harmonics, therefore a classic Proportional Integrating (PI) control system in a stationary frame, is frequently used for this kind of inverters. For the ancillary service inverter, a PI control system did not bring sufficient performance to control a reasonable number of harmonics. Thus a better approach was chosen, namely the Proportional Resonant (PR) controller [Tao 08], [Hol 09]. With the PR controller, a very high control loop-gain can be reached without too much phase shift at contiguous frequency ranges. PR controllers are often used in a stationary frame, for single-phase systems that are controlled by DSPs. PI controllers are often used in a synchronous frame, for three-phase systems. PR controllers operate in a stationary frame and are comparable to PI controllers which work in a synchronous frame [Li 09].

The main controller of the inverter model is build up of six resonators on the fundamental and the 3th, 5th, 7th, 9th and 11th harmonic. Equation (5.2) gives the transfer function for a single resonator. The characteristics of the resonator are defined by the constants k_1 and k_2 and the resonance frequency by the constant ω_{res} .

$$H_{res}\left[\frac{v_{out}}{v_{in}}\right] = \frac{k_1 s}{s^2 + k_2 s + \omega_{res}^2} \tag{5.2}$$

Figure 5.7 gives a Bode plot of the resonant controller block with multiple resonators and a added constant gain of 0dB.

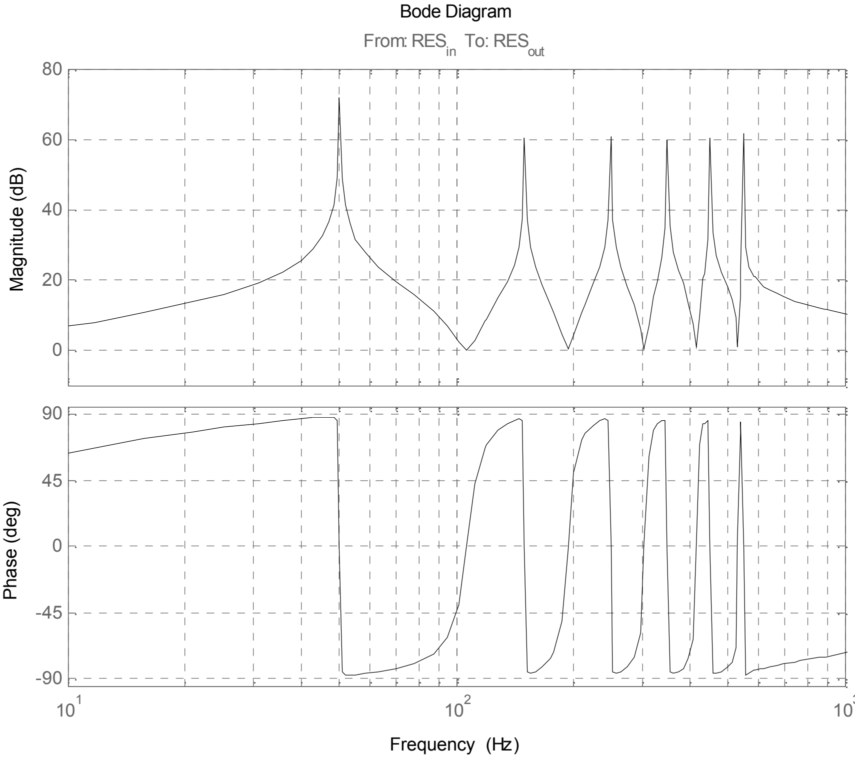

Figure 5.7: Bode plot of the transfer function of the controller block with its resonators on the fundamental (50Hz) and the 3th, 5th, 7th, 9th and 11th harmonic.

Figure 5.8 gives a Bode plot of the transfer function of the total open-loop gain of the inverter model (from i_{ref} to i_{inv}), connected to the grid with current feedback and a controller with a number of resonators. This system provides sufficient loop gain for the fundamental and the 3th, 5th, 7th, 9th and 11th harmonic.

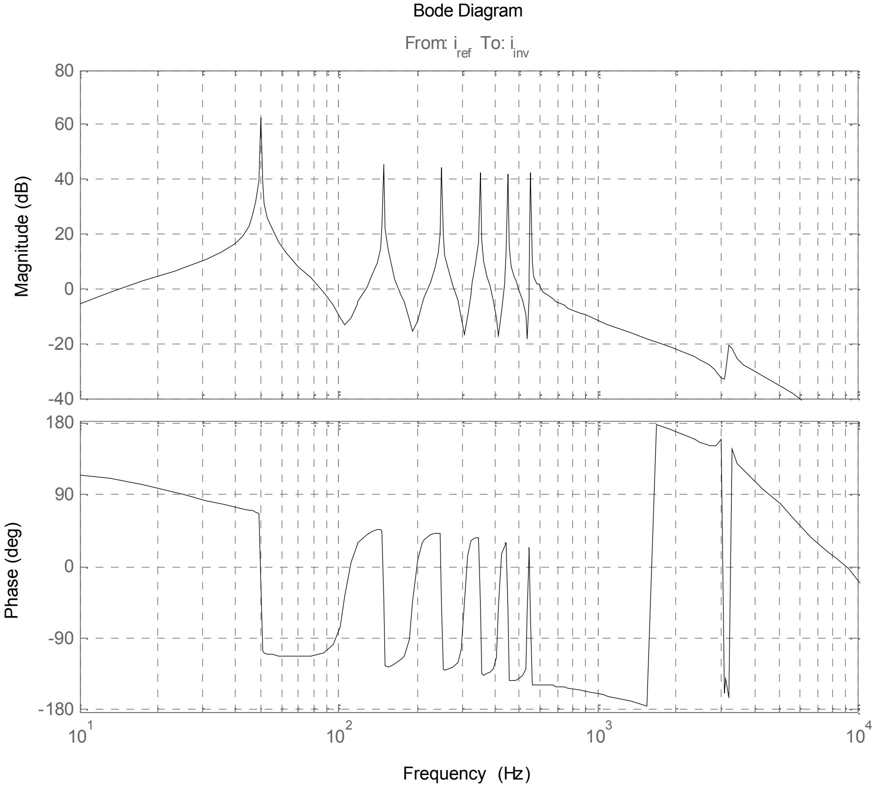

Figure 5.8: Bode plot of the transfer function of the total open-loop gain of the inverter model (from i_{ref} to i_{inv}).

5.3.2.2 Controlled and uncontrolled output impedance

The output impedance of the inverter, seen by the grid is depicted in Figure 5.9. Equation (5.3) gives the transfer function of the inverter's output impedance.

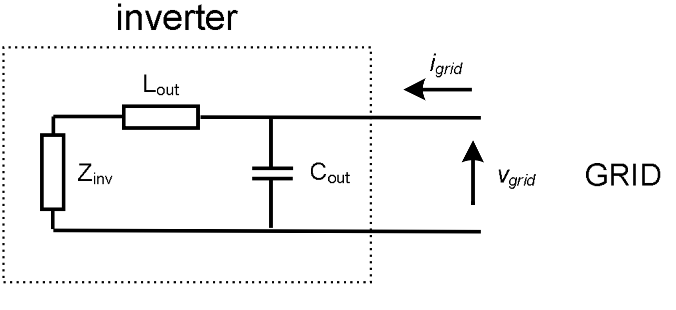

Figure 5.9: Inverter's output impedance seen from the grid.

$$H\left[\frac{v_{grid}}{i_{grid}}\right]=\frac{1}{\dfrac{1}{Z_{inv}+R_{L_{out}}+sL_{out}}+sC_{out}} \tag{5.3}$$

From Figure 5.9 and Equation (5.3) it is easy to see that the character of the impedance will be a parallel resonance. The impedance Z_{inv} has a large influence on the following:

- for an uncontrolled VSC based inverter, Z_{inv} equals a low impedance value and with that the total impedance will show a resonance between L_{out} and C_{out}, damped by resistive part of L_{out} and Z_{inv},
- for a current feed-back controlled VSC based inverter, Z_{inv} equals a high impedance value and with that the total impedance will show the impedance of only the capacitance C_{out}, see Equation (5.4).

$$H\left[\frac{v_{grid}}{i_{grid}}\right]=\frac{1}{sC_{out}} \tag{5.4}$$

However the performance of the current-controlled inverter is only excellent for the resonator frequencies of the controller, see Figure 5.8. Outside these resonator peaks, the gain-bandwidth product and the control performance is limited. To improve this limited performance, a feed-forward compensation loop is added to compensate the voltage drop over the output filter inductor L_{out}.

5.3.2.3 Output inductor voltage drop compensation

The output inductor voltage drop compensation feed-forward loop simply makes the inverter output voltage V_{inv} equal to V_{grid} and thus compensates the voltage drop over L_{out}, see Figure 5.10. This compensation loop is called "v_L-compensation".

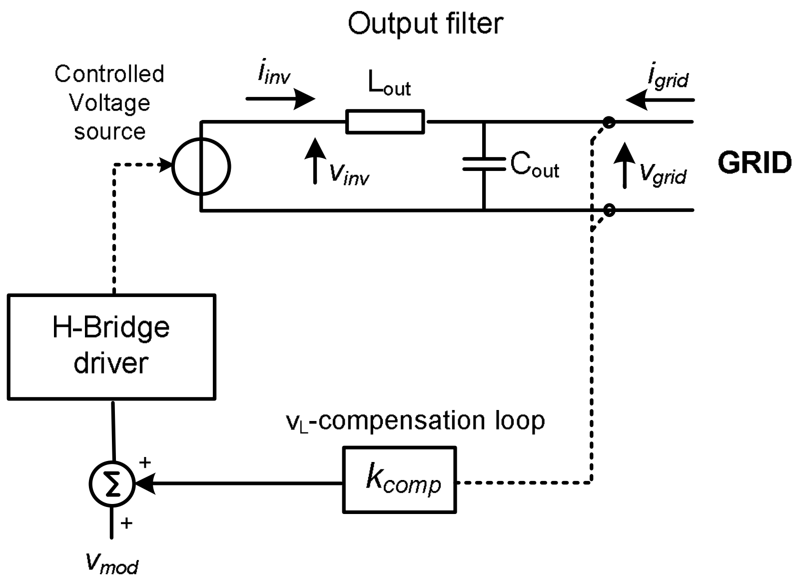

Figure 5.10: The v_L-compensation loop.

The purpose of this control loop is to increase the low output impedance of the uncontrolled inverter to a higher impedance value. This loop prevents current flowing from V_{grid} through L_{out}, see Figure 5.10, by making v_{inv} equal to v_{grid}, which implies:

$$v_{inv} = v_{grid}\, k_{comp}\, H_{\text{mod}} \tag{5.5}$$

and that:

$$k_{comp} = \frac{1}{H_{\text{mod}}} \tag{5.6}$$

For this control system H_{mod} is taken as a constant gain equal to the voltage on the buffer capacitor $V_{DC\text{-}Bus}$. The voltage drop over switching elements is not taking into account. Also the propagation delay of the switching H-bridge is not taken into account because up to the 11th harmonic this delay only brings little phase shift [Bol 05]. Equation (5.7) gives the v_L-compensation constant k_{comp}.

$$k_{comp} = \frac{1}{V_{DC-Bus}} \tag{5.7}$$

The transfer function from v_{mod} to i_{inv} of Figure 5.10, with or without v_L-compensation, strongly depends on the output filter and grid impedance. Because this transfer function has a resonance peak that affects gain and phase margin the stability of the current control loop can also be affected, as seen in Figure 5.11. This figure gives the transfer function from v_{mod} to i_{inv}, for higher and lower grid impedance, both simulated with and without 50% v_L-compensation. It can be seen that the v_L-compensation loop attenuate this resonance. In the inverter's current control system this will bring more gain margin and let the inverter cope with a variety of grid impedances. More interesting ways to minimize resonances in inverters with LC filters are presented in [Li 09].

The reason for implementing only 50% v_L-compensation and not 100% has to do with making the total control system stable for various grid impedances and also to let them operate stable in case large numbers are connected to a LV distribution grid.

Higher and lower values of grid impedances measured between the phase and neutral conductor of a typical Dutch LV outlet, from [Ber 00] are given below:

- lower grid impedance:
  - Rgrid = 0.25 Ohm,
  - Lgrid = 0.25 mH,
- higher grid impedance:
  - Rgrid = 0.70 Ohm,
  - Lgrid = 0.80 mH.

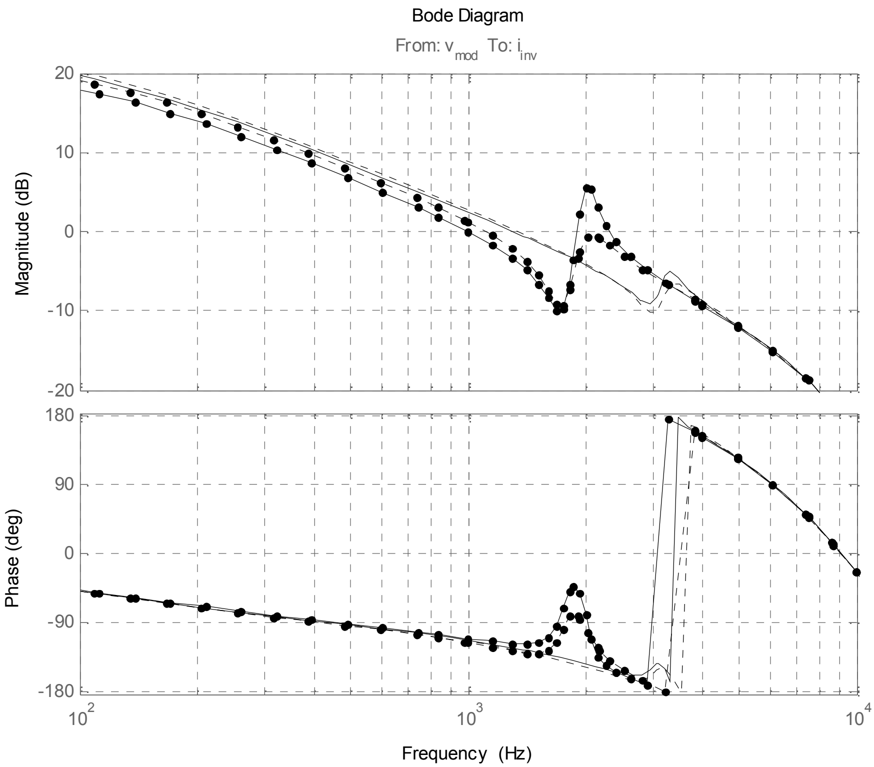

Figure 5.11: Bode transfer function plot of from v_{mod} to i_{inv}, for higher and lower grid impedances, both simulated with and without 50% v_L-compensation.

- solid line: lower grid impedance without v_L-compensation,
- dotted line: lower grid impedance with v_L-compensation,
- solid line with markers: higher grid impedance without v_L-compensation,
- dotted line with markers: higher grid impedance with v_L-compensation.

5.3.2.4 VPCR controller

The goal of VPCR is to reduce virtually the inverter's output capacitor, this is done by compensating the current through this capacitor. In Figure 5.12 the VPCR controller is copied out of the total control system of Figure 5.5. This VPCR control uses the v_{grid} signal to calculate the current through the output capacitor C_{out}, this can be done because v_{grid} equals the capacitor voltage, see

Figure 5.6. The calculated current through the output capacitor i_{VPCR} is added to the requested inverter output current i_{ref} (see Figure 5.5), with this action the capacitor current is compensated and the output capacitance virtually reduced.

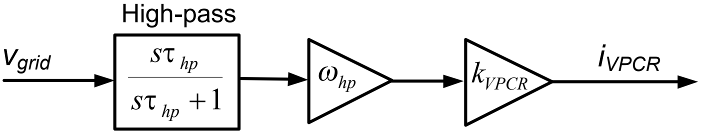

Figure 5.12: The VPCR control system of the inverter.

The relation between v_{grid} and the current through C_{out} is shown in Equation (5.11). Equation (5.12) shows how to calculate the current through C_{out}.

$$X_{C_{out}} = \frac{v_{grid}}{i_{C_{out}}} = \frac{1}{sC_{out}} \tag{5.11}$$

$$i_{C_{out}} = v_{grid} sC_{out} \tag{5.12}$$

Because building a pure differentiator is not possible and not needed, a high-pass filter is used. To give this high-pass filter a unity gain at $\omega = 1$, the filter output is multiplied with a gain that equals the value of the high-pass filter cutoff frequency ω_{hp}, see Equation (5.13). ω_{hp} is the reciprocal of τ_{hp}. The high-pass filter cutoff frequency ω_{hp} is chosen beyond the inverter's bandwidth.

$$i_{VPCR} = v_{grid} \frac{s\tau_{hp}}{s\tau_{hp}+1} \omega_{hp} C_{out} \tag{5.13}$$

Finally the constant k_{VPCR} equals the capacitor value from which the current is compensated, see Equation (5.14).

$$k_{VPCR} = C_{out} \tag{5.14}$$

5.3.2.5 VRHD controller

The goal of the VRHD control is to let the inverter behave as a (virtual) resistor at harmonic frequencies and consequently control the output impedance. Seen from the grid the output impedance is (see Figure 5.6):

$$z_{out} = \frac{v_{grid}}{i_{grid}} \tag{5.15}$$

Because the output capacitor current is compensated by the VPCR control loop, $-i_{inv}$ equals i_{grid}, and the following holds by approximation:

$$z_{out} = -\frac{v_{grid}}{i_{inv}} \tag{5.16}$$

$$i_{inv} = v_{grid} \frac{-1}{z_{out}} \tag{5.17}$$

$$i_{VRHD} = v_{grid}\, k_{VRHD} \tag{5.18}$$

$$k_{VRHD} = \frac{-1}{z_{out}} \tag{5.19}$$

The calculated current i_{VRHD} is added to the requested inverter output current i_{ref} (see Figure 5.5).

Figure 5.13 shows the VRHD control system. This VRHD control needs to minimize only the grid voltage distortion, and consequently the fundamental voltage v_{fund} is subtracted from the grid voltage v_{grid} to estimate the distortion voltage v_{dis}.

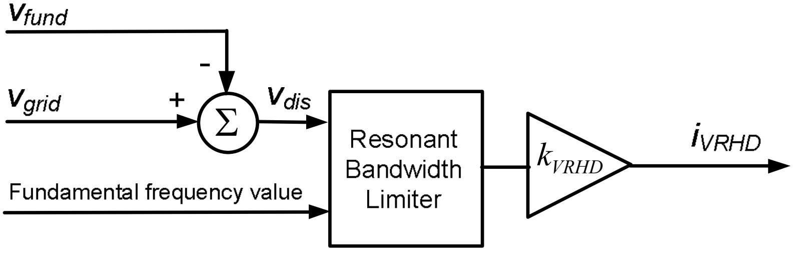

Figure 5.13: The VRHD control system of the inverter.

To avoid effects at frequencies other than the characteristic harmonics, a resonant bandwidth limiter is added to the VRHD controller, see Figure 5.13.

This resonant bandwidth limiter works with multiple resonators. At the resonant peaks the limiter has a gain of 0 dB and a zero phase shift, see Figure 5.14.

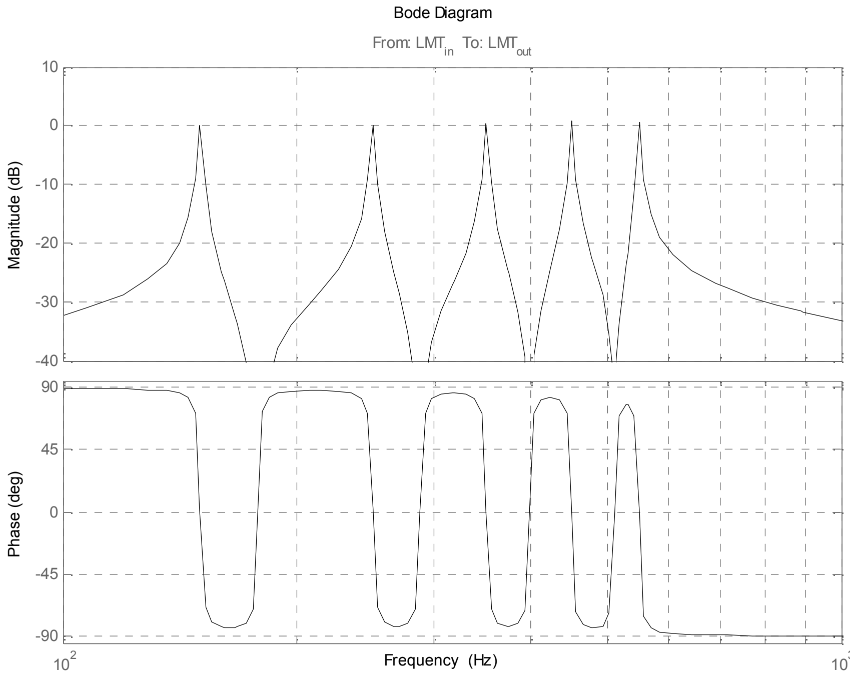

Figure 5.14: Bode transfer function plot of the resonant bandwidth limiter of the VHRD control system.

5.4 The ancillary services inverter hardware model

For safety reasons and ease of use, the used H-bridge of the ancillary service inverter hardware model was of a LV type, the system worked with an applied dc-bus voltage of $30V_{dc}$. In this work only small signal responses in a limited frequency range are analyzed and voltage drops over switching elements are not taking into account. Therefore, the transfer-function from the H-bridge PWM-input to the H-bridge average output voltage will have a linear relation with the applied dc-bus voltage, therefore scaling of the system is allowed and the presented results can be used for larger systems coupled to the LV grid.

5.4.1 The ancillary service inverter

The built inverter consists out of three sections, namely:

1. as input a DC power supply,
2. a DC-bus with 5 x 4700μF buffer capacitor,
3. a MOSFET H-bridge with an output filter, a current sensor at the output filter inductor, a current sensor at the output feeders (grid connection) and a voltage sensor over the output filter capacitor.

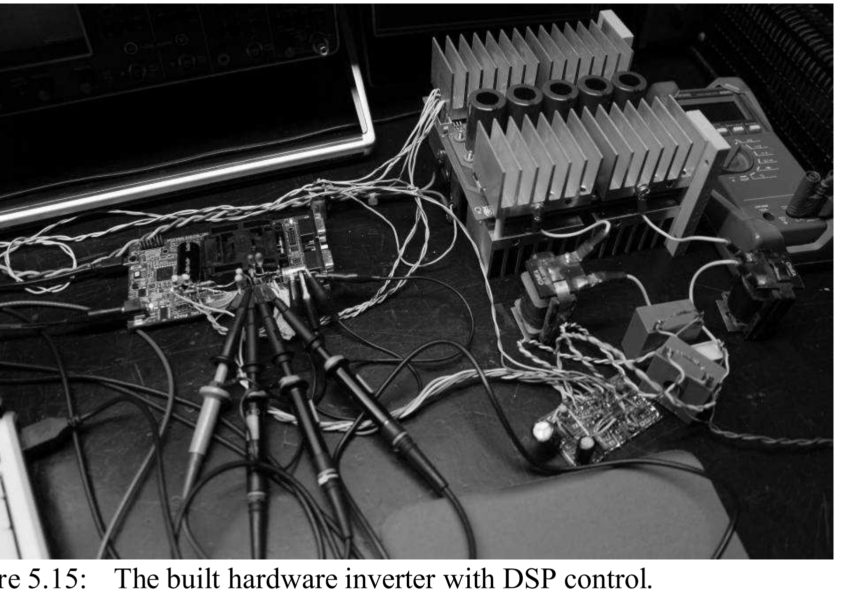

Figure 5.15: The built hardware inverter with DSP control.

Power-part specification:

- 4-leg MOSFET-bridge with high and low side drivers,
- DC input max. 40Vdc,
- output current more than $16A_{RMS}$,
- switching frequency 30kHz,
- modulation depth max. 100%,
- 5 x 4700μF/40Vdc Capacitor buffer on DC-bus,
- 2^{nd}-order output filter, cross over at 1000Hz,
- current sensors AC-type, isolated, 10kHz bandwidth,
- voltage sensor AC/DC-type, non-isolated, 10kHz bandwidth.

DSP specification:

- a F28335eZdsp DSP StarterKit (DSK) from Spectrum Digital, Inc., with TI DSP: TMS320F28335.

5.4.2 The laboratory test set-up

The laboratory set-up of Figure 5.16 represents the basic set-up for measurements in the time domain as well as in the frequency domain.

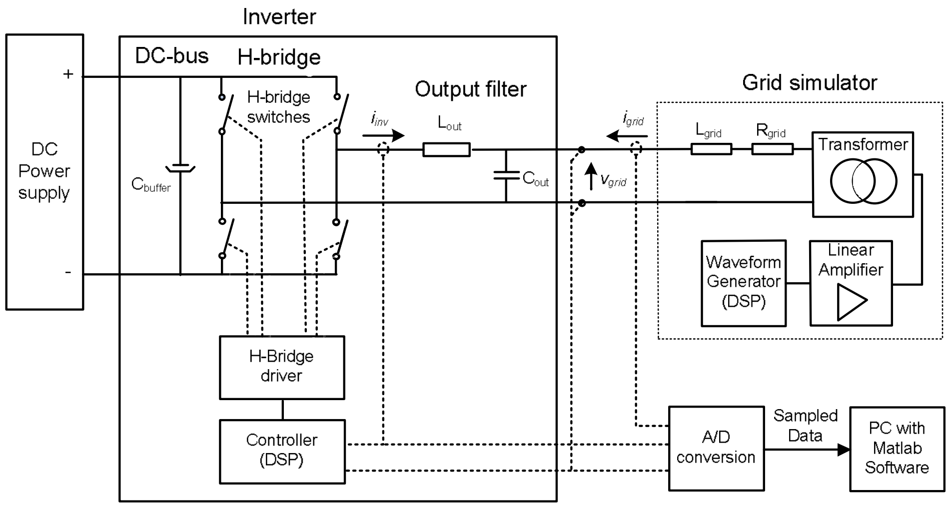

Figure 5.16: Laboratory set-up.

5.5 Validation simulations in the time domain

In this section validation simulations in the time domain of the grid voltage v_{grid}, grid current i_{grid} and the current through the inverter's output inductor i_{inv} are given. These currents show the inverter's behavior with and without the ancillary services VPCR and VRHD activated, in a situation where the grid voltage contains a harmonic pollution.

Computer simulation results with the ancillary services inverter simulation model of section 5.3 are presented as well as related laboratory experimental results for validation. Validation is done with the ancillary services inverter hardware model of section 5.4. The computer simulation model is built directly from the laboratory set-up of Figure 5.16.

In the used simulations the grid voltage v_{grid} is polluted with 10% of the 11th harmonic. In practice this would be an extremely high pollution, but this high level of pollution and high harmonic order is chosen to be able to see the effect of VPCR and VRHD clearly. The measured polluted voltage from the simulation model can be seen in Figure 5.17 and from the laboratory set-up in Figure 5.18. During all simulations the inverter is feeding 1A_{RMS} into the grid and uses an active 50% v_L-compensation as a basis. Hereafter successively the ancillary services VPCR and VRHD are activated, to notice the difference.

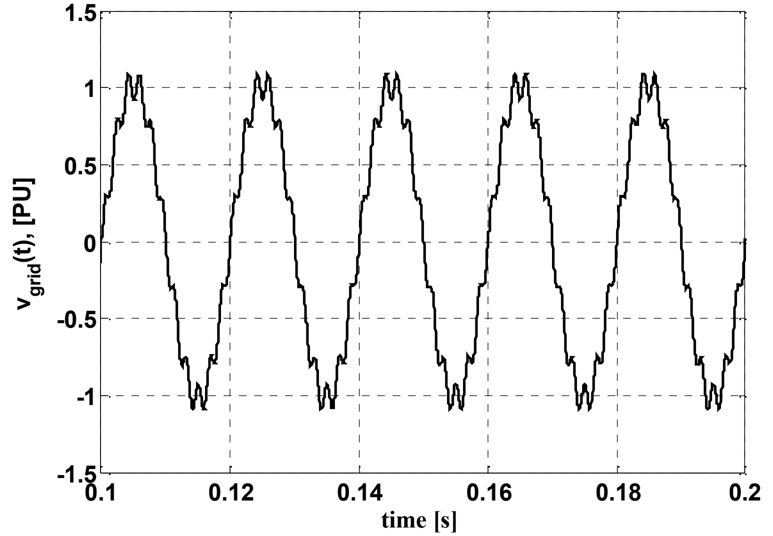

Figure 5.17: Simulation result of v_{grid} polluted with 10% of the 11th harmonic.

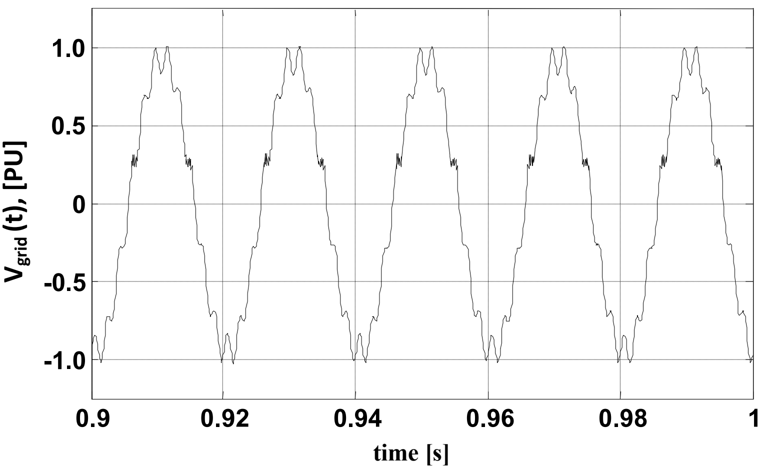

Figure 5.18: Experimental result of v_{grid} polluted with 10% of the 11th harmonic.

5.5.1 Basic inverter control

In Figure 5.19 and Figure 5.20 simulation and experimental results are given of the grid current i_{grid} and the inverter current i_{inv} under this polluted grid voltage, without activated VPCR and VRHD. As can be noticed in both figures a substantial 11th harmonic i_{grid} current is flowing through the inverter's output capacitance, because i_{grid} is polluted with this the 11th harmonic and i_{inv} has a clean sinusoidal shape.

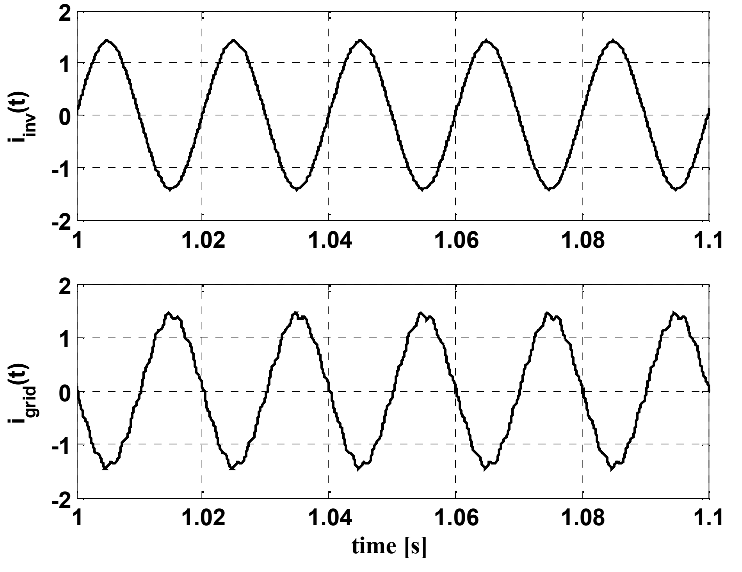

Figure 5.19: Simulated result of i_{inv} and i_{grid} without activated ancillary services.

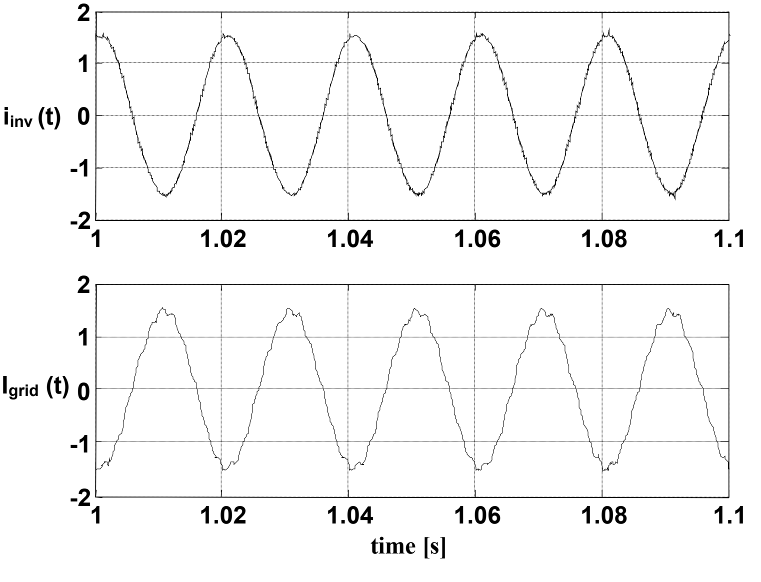

Figure 5.20: Experimental result of i_{inv} and i_{grid} without activated ancillary services.

The current i_{grid} is polluted because an 11^{th} harmonic current is flowing through the inverter's output capacitor. The reason for the almost pure sinusoidal inverter current i_{inv} is because of the current control system, see section 5.3.2.

5.5.1 Ancillary services VPCR and VRHD

In Figure 5.21 and in Figure 5.22 results are presented with activated VPCR, the effect is an almost pure sinusoidal shape of i_{grid}, this indicates that the current through the inverters output capacitor is strongly reduced. The inverter current i_{inv} now contains the 11^{th} harmonic, this indicates compensation of the 11^{th} harmonic current through the inverter's output capacitor.

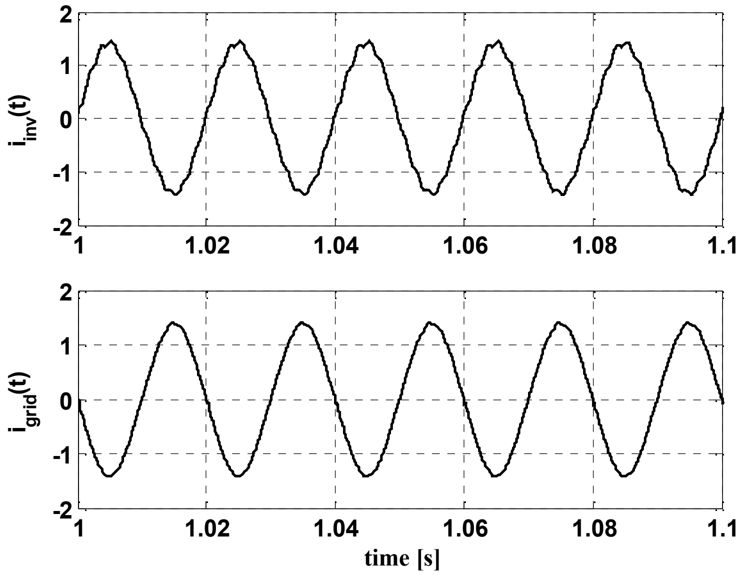

Figure 5.21: Simulated result of i_{inv} and i_{grid} with activated VPCR.

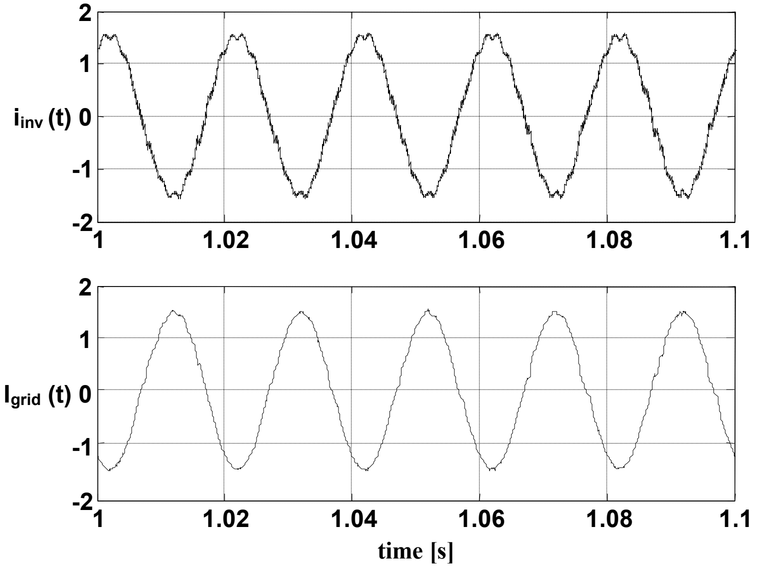

Figure 5.22: Experimental result of i_{inv} and i_{grid} with activated VPCR.

In Figure 5.23 and in Figure 5.24 results are presented with both VPCR and VRHD activated. VRHD leads an 11th harmonic current from the grid through the inverter, therefore both i_{inv} and i_{grid} strongly contain the 11th harmonic.

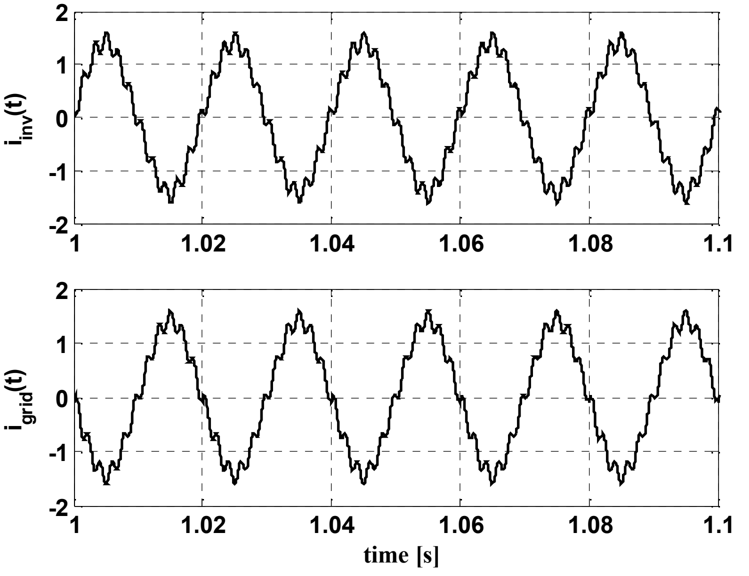

Figure 5.23: Simulated result of i_{inv} and i_{grid} with activated VPCR and VRHD.

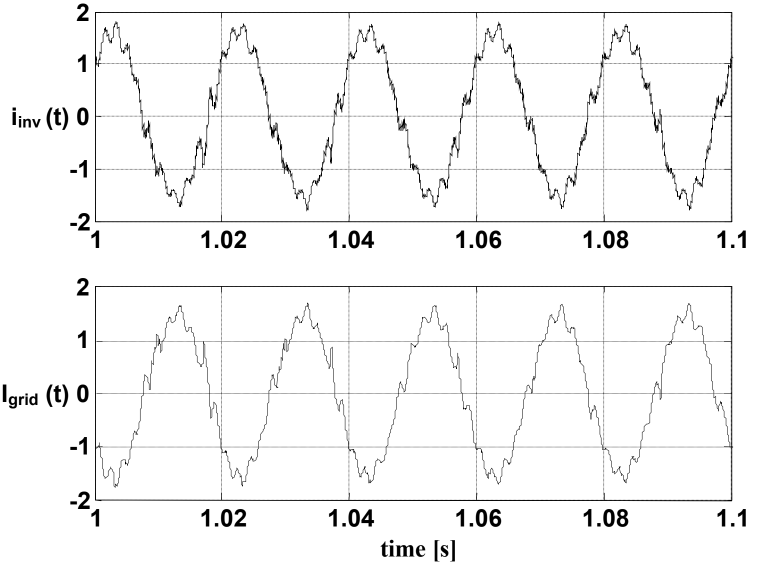

Figure 5.24: Experimental result of i_{inv} and i_{grid} with activated VPCR and VRHD.

The magnitude of the 11th harmonic current in i_{inv} and i_{grid} depends on K_{VRHD} being the conductivity of the inverter's virtual resistor. It is because of the intentionally chosen conductivity that this 11th harmonic current is led down through the inverter. This is an expected situation, just as passive harmonic filters would lead down harmonic currents, the inverter's virtual resistor also does. Both i_{grid} and i_{inv} contains the 11th harmonic current because this current is flowing through the output filter.

5.6 Validated simulations in the frequency domain

In this section simulations in the frequency domain of the inverter's output impedance as a function of the harmonic order are given, these results are presented in harmonic impedance plots. The inverter's output impedance is calculated from time series of measured voltage and current, with the laboratory set-up of Figure 5.16. The output impedance plots give an impression of the performance of the inverter's control system. Similar as in the previous section, both computer simulation results as well as related experimental results are presented in this section, for validation.

In the simulations the grid voltage v_{grid} is polluted with a flat spectrum, containing all harmonics up to the 40th. Time series of the grid voltage v_{grid} and the grid current i_{grid} are used to calculate the inverter's output impedance, only for harmonics from the 2nd to the 40th. Results from computer simulations are presented as a solid line connecting all the harmonic impedances, results from the laboratory measurements are presented as dots. For comparison both the computer simulation results and the related experimental result are presented in one figure (see next subsections).

In this work attention is paid to the inverter's controlled performance as well as the uncontrolled performance (see section 5.3.2.2).

5.6.1 Basic inverter control

In this section the effect of the basic inverter control is discussed. In the first plot the inverter's output impedance is given without any control active, hereafter the 50% v_L-compensation loop is activated. See section 5.3.2.3 for a description and explanation why only 50% compensation is used. Finally the current control loop is also activated.

In Figure 5.25 the inverter's output impedance as a function of the harmonic order is given for the situation without any control loop active. This figure clearly shows a parallel resonance between L_{out} and C_{out}, this is because the inverter impedance Z_{inv} is very low because of the VSC concept of the inverter, see also section 5.3.2.2.

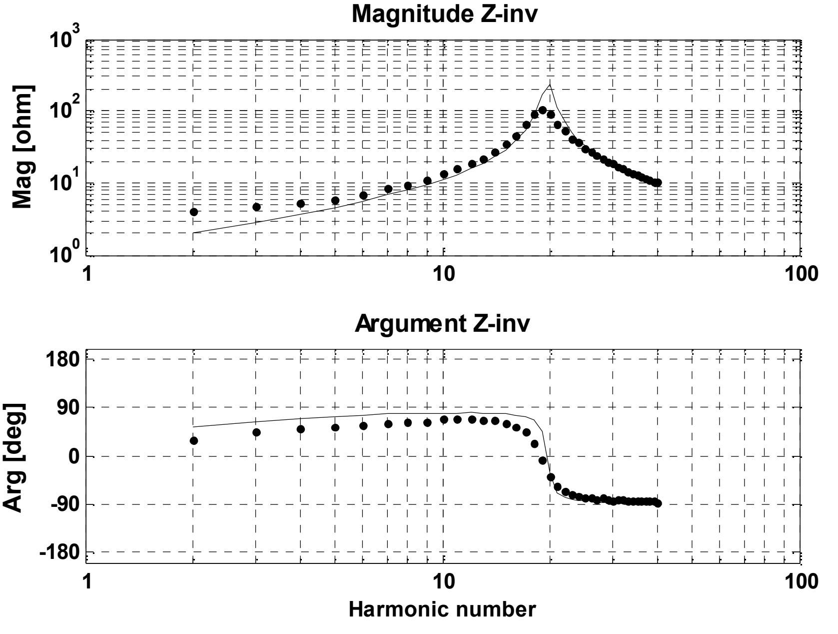

Figure 5.25: Harmonic impedance plot of the inverter's output impedance without any control.

In Figure 5.25 also can be noticed that the simulation results (solid line) differ from the experimental results (dots), because the latter one has more resistance and therefore also more damping. For frequencies lower than the 19th harmonic, the inverter's output impedance shows an inductive-resistive behavior because the phase angle tends to +90°. For frequencies higher than the 19th harmonic, the inverter's output impedance shows a capacitive behavior as this is indicated by the phase angle that goes to -90°.

In Figure 5.26 the output impedance as a function of the harmonic order is given with the 50% v_L-compensation loop active. With this loop activated, the parallel resonance between L_{out} and C_{out} is damped to a much lower peak level, compared to Figure 5.25.

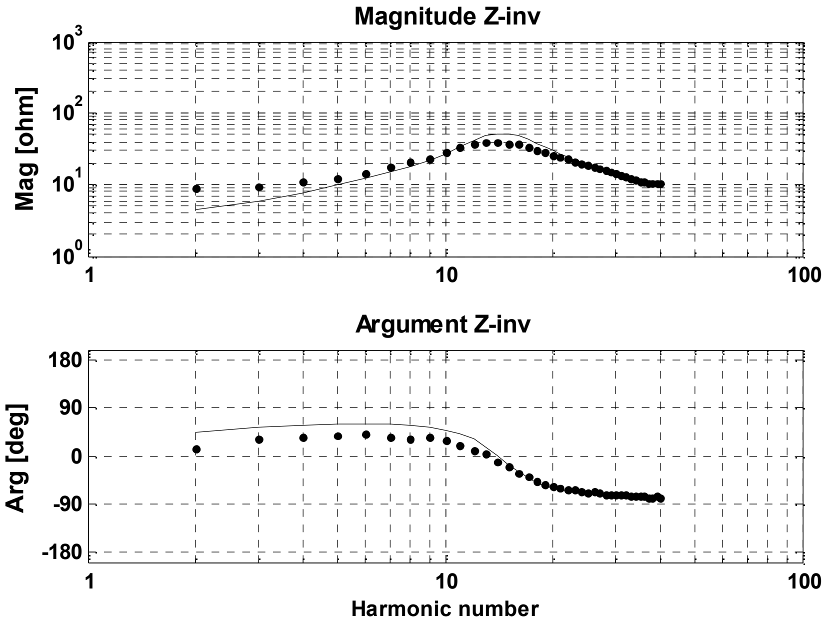

Figure 5.26: Harmonic impedance plot of the inverter's output impedance with only v_L-compensation.

The resonance frequency in Figure 5.26 is virtually shifted from about the 19th to about the 14th harmonic, this is caused by the virtual increase in inductance of L_{out} with a factor two, as a result of the activated 50% v_L-compensation loop.

In Figure 5.27 the output impedance as a function of the harmonic order is given with the current control loop activated in addition to the v_L-compensation loop. The current control loop has mainly effect on the fundamental and the 3th, 5th, 7th, 9th and 11th harmonic, because of the resonator control system, see also section 5.3.1. Because of this, the inverter has a high impedance for these harmonic frequencies. Therefore the output impedance on these harmonics equals the impedance of the output capacitor C_{out}, see also section 5.3.2.2. There is however also some effect besides these resonance peaks, therefore other harmonic impedances are affected as well.

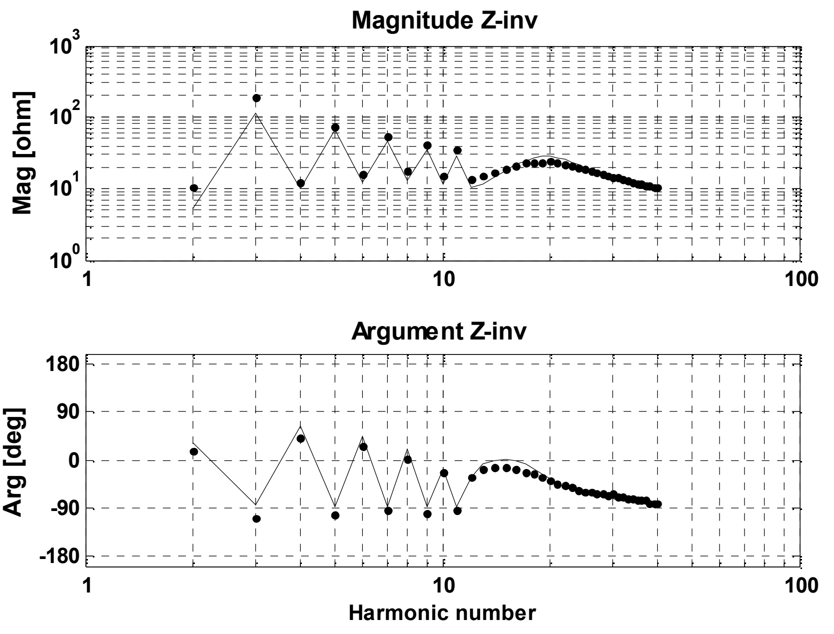

Figure 5.27: Harmonic impedance plot of the inverter's output impedance with current control and v_L-compensation.

With the activation of both the v_L-compensation and the current control loop the ancillary services inverter has its basic configuration, the harmonic impedance plot of Figure 5.27 shows thus the impedance on harmonic frequencies for this basic configuration, measured at the output feeders.

5.6.2 Ancillary services VPCR and VRHD

In this section the output impedance as a function of the harmonic order are discussed of the basic inverter with the ancillary services VPCR and VRHD activated successively.

In Figure 5.28 the inverter's output impedance as a function of the harmonic order is given with the ancillary service VPCR activated.

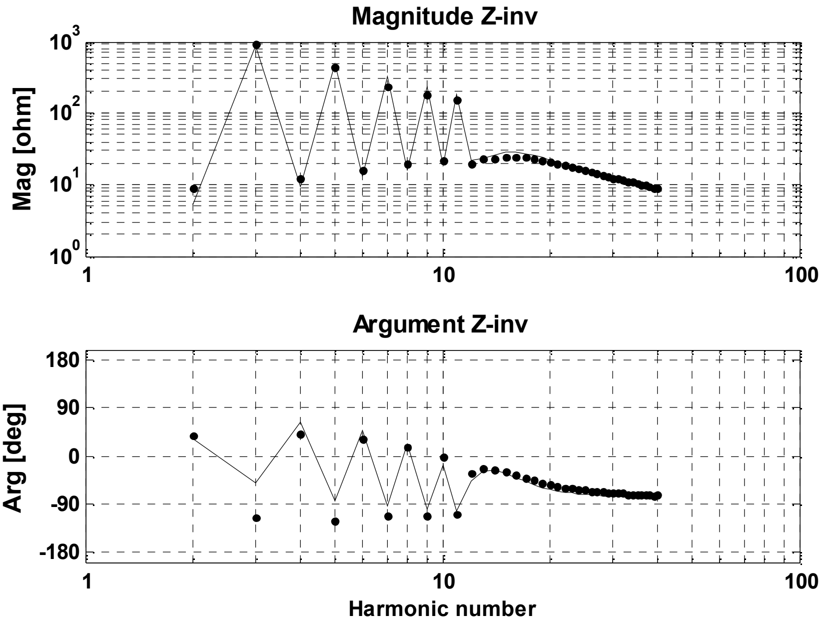

Figure 5.28: Harmonic impedance plot of the inverter's output impedance with activated VPCR.

Compared to the output impedance plot of the basic configuration (see Figure 5.27) the magnitude of the capacitive impedance has strongly increased, caused by VPRC (see Figure 5.28). This indicates a virtual reduction of the parallel capacitances. The ancillary service VPRC has mainly effect on the fundamental (not shown here) and the 3th, 5th, 7th, 9th and 11th harmonic, because the VPCR performance depends on the current control performance, see section 5.3.2.4.

In Figure 5.29 the inverter's output impedance as a function of the harmonic order is given with the ancillary service VRHD activated in addition to VPCR. The ancillary service VRHD has mainly effect on the 3th, 5th, 7th, 9th and 11th harmonic, because also the VRHD performance depends on the current control performance, besides this the VRHD controller has an extra resonant bandwidth limiter to avoid poorly defined damping at frequencies other than the harmonics supported by the resonant controller of the current control system, see also section 5.3.2.5. Because of this strongly limited effect of VRHD to the 3th, 5th, 7th, 9th and 11th harmonic, only on these harmonics, the inverter's output impedance equals the pure resistive value of 10 ohms, as adjusted.

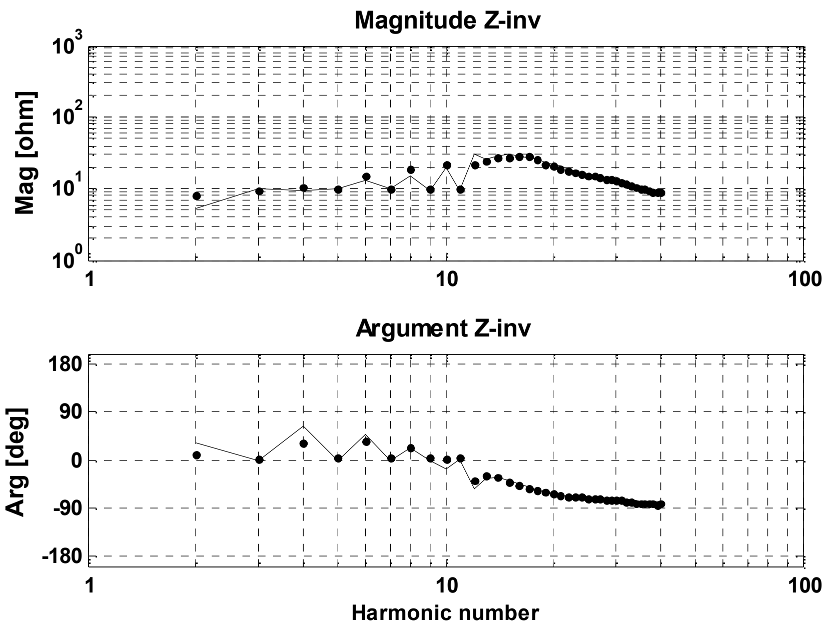

Figure 5.29: Harmonic impedance plot of the inverter's output impedance with activated VPCR and VRHD.

With the activation of both the ancillary services VPCR and VRHD, the ancillary services inverter has its full performance operation mode. The harmonic impedance plot of Figure 5.29 shows the impedance on harmonic frequencies for this operation mode, measured at the output feeders.

5.7 Discussion

An inverter for DG that offers the VPCR and VRHD can contribute to a power quality improvement, but are there any design consequences and what about the effect on efficiency and dynamic range?

Concerning the dynamic range, a certain DC-bus voltage level is needed to accurately control current while the grid voltage at the PoC is polluted with harmonics. For both services VPCR and VRHD compensation currents have to flow between the inverter and the grid, through the output filter inductor. To let this current flow, the inverter control has to superimpose compensation voltages to the PWM. Therefore, a higher dynamic range of the inverter might be needed, thus a higher DC-bus voltage might be necessary. This extra voltage strongly depends on frequency and phase angle of harmonic voltages at the inverter's output and also on the frequency and phase angle of the compensation currents through the output inductor. For the estimation of the extra voltage, the following aspects can be taken into account as a rule of thumb:

- the increase of the grid voltage peak level because of additional harmonic voltages, needs to be compensated with extra DC-bus voltage,
- the peak level of the voltage drop over the inverter's output filter inductor needs to be compensated with extra DC-bus voltage.

In the example of Figure 5.23 and Figure 5.24 about 20% extra DC-bus voltage is needed because of the added 11^{th} harmonic on the grid voltage fundamental and for the VPCR and VRHD compensation currents through the inverter's output inductor.

Concerning efficiency, the ancillary services VPCR and VRHD with its compensation current, will cause voltage drops caused by resistive losses. Although these resistive losses are expected to be small, they have to be incorporated in the efficiency calculation of the inverter. The losses caused by the ancillary services VPCR and VRHD, will slightly reduce the inverters efficiency at rated power.

In this thesis the effect off the ancillary services VPCR and VRHD on efficiency and dynamic range are not being quantified, therefore to learn more about this subject, more research need to be done.

5.8 Conclusion

In this chapter two ancillary services for minimizing the impact of resonances in the grid are studied. Both services can be implemented in power electronics based converters and are named "Virtual Parallel Capacitance Reduction (VPCR)" and "Virtual Resistive Harmonic Damping (VRHD)".

VPCR is an ancillary service that generates an additional current to compensate currents through capacitances that are placed in parallel with grid connected appliances. VPCR works in a frequency range that includes the fundamental and a number of harmonics. VRHD is an ancillary service that gives the converter a resistive behavior for a number of harmonics.

A single-phase inverter for DG with the ancillary services VPCR and VRHD is computer simulated and validated with a hardware model in a laboratory. Results of the validated simulations show that the two ancillary services perform as expected, especially the combination of the two ancillary services is very useful to minimize the effect of resonances in the LV distribution grid, because VPCR is virtually shifting the resonance towards a higher harmonic frequency range and VRHD damps the resonance peak to a lower level. VRHD will also bring damping to harmonic currents coming from non-linear loads in the distribution grid.

These two ancillary services can be implemented in power electronics based inverters for DG, as presented in this thesis. The actual working range however depends on the performance of the control system.

Chapter 6

Extended simulation of a distribution grid

In this chapter two extended computer simulation cases are discussed. In both cases multiple pieces of the validated ancillary service inverter model from the previous section are brought together in an extended simulation model. In the first model (Model 1), 200 pieces of these inverters are placed in homes and virtually compensating their own output capacitances by means of Virtual Parallel Capacitance Reduction (VPCR). In the second model (Model 2), 100 pieces of these inverters are placed in homes and virtually compensating external capacitive loads as well. The total capacitance in both models is kept the same to achieve a resonance at a frequency that roughly equals the 9^{th} harmonic frequency, to be noticed in case the VPCR is not active. All the observed homes are connected to the same phase of a Low Voltage (LV) distribution grid. This is an artificial set-up, the two other phases of the LV system and asymmetry issues are not studied. From the results the impedance of the total power system at the substation's LV busbar is presented. This impedance represents the aggregate of all impedances seen from this point, thus this includes the Medium Voltage (MV) grid via the MV/LV transformer and the complete LV grid connected to the substation. Impedances are presented as a function of the harmonic order and limited to harmonics from the 2^{nd} to the 40^{th}. In order to focus on the resonance affected by the inverters and loads with capacitive characteristics, other loads are not included in the model. Also no background pollution is present in the grid voltage.

As in the previous chapter, the harmonic impedance is calculated from time series of measured voltage and current. The magnitude and phase of the impedance at harmonic frequencies are presented in a plot. It must be emphasized that these plots does not show impedance effects between two consecutive harmonics.

6.1 The extended simulation models

Similar to the previous chapters, the purpose of the distribution grid models in this chapter is an investigation on resonances in the frequency range below the 40th harmonic. Therefore, with the extended supply system implementation of the validated inverter model all impedances are simplified and represented as first order systems with only resistance and inductance, that is, with cable capacitances ignored. In the studied models only short cable lengths are taken, it is investigated via simulation models that cable capacitance in this situation will cause a difference outside the observed harmonic range [Old 04]. Skin-effect and proximity-effect [Cob 07] are also not included as their impact on the frequency range under consideration will be negligible.

The presented results of the simulations are limited to impedance transfer function figures; only small signal analysis is done under steady-state conditions.

In Table 6.1 impedances are given of grid components used in the models, these impedances are from [Cob 07].

Table 6.1: Impedances of the grid components.

Grid component	Resistance [mΩ]	Inductance [μH]
MV-grid 50MVA (transformed to LV-grid)	0.32	10
Transformer 400kVA	4.6	48.7
Cable 50mm^2 Al (per meter length)	0.667	0.27
Home-cabling (from street to outlet)	218	180

The home-outlet impedance in the distribution grid varies in the range of Table 6.2, this complies with figures from practice, see section 5.3.2.3.

Table 6.2: Home-outlet impedance over the LV distribution grid.

Home-outlet impedance limits	Resistance [mΩ]	Inductance [µH]
Strongest outlet	250	250
Weakest outlet	310	274

This simulated distribution grid is built up in a way that the spreading of impedances between all the home connections is limited, to only find the basic resonance effects. In more practical situations resonances might appear in a harmonic range between the 25^{th} and the 40^{th}.

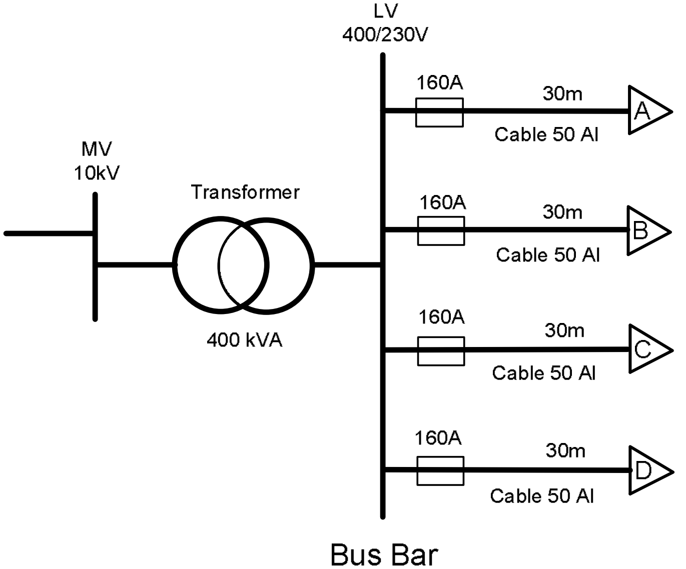

Figure 6.1: Distribution model, substation level.

In Figure 6.1 the substation part of the models is depicted by four outgoing LV feeders A to D. At the end of the 30m cable parts the feeders are connected to street level sections. In Model 1 with 200 inverters connected, all the four feeders are loaded with 50 inverters each. In Model 2 with 100 inverters as well as 100 capacitive loads, only two feeders are loaded.

In Figure 6.2 a street level section of the models is depicted. This section is connected to one of the four feeders, from this point the feeder splits-up into five cables, loaded each with 10 inverters.

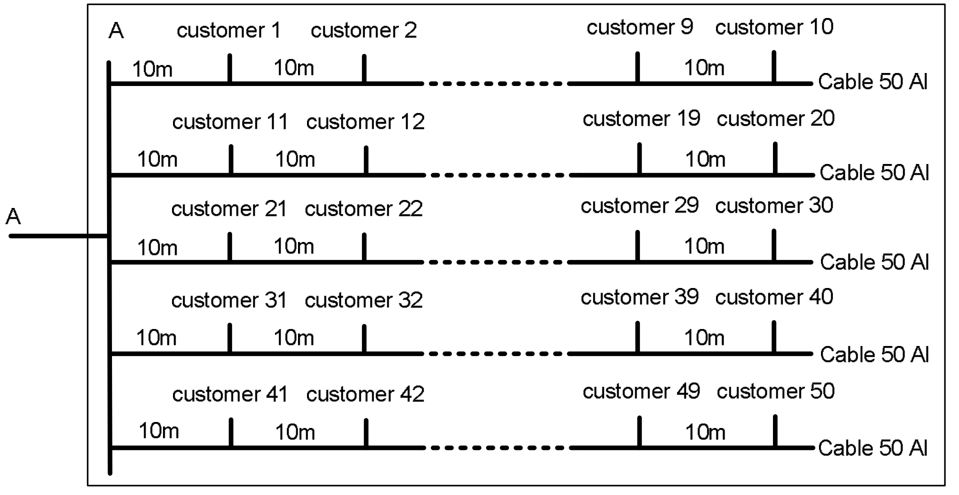

Figure 6.2: Distribution model, street level section.

The inverters are placed along these cables with equal distance in between. This street level represents a group of 50 homes with an inverter each.

In Figure 6.3 a home section of the Model 1 is depicted. This home section contains only the validated model of the ancillary services inverter.

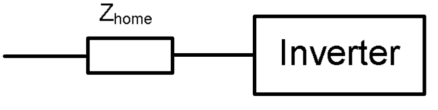

Figure 6.3: Distribution model 1, home level.

In Figure 6.4 a home section of the Model 2 is depicted. This home section contains the validated model of the ancillary services inverter and a capacitive load as well. The impedance Z_{home} represents the cabling inside the home from the PoC to the inverter connection.

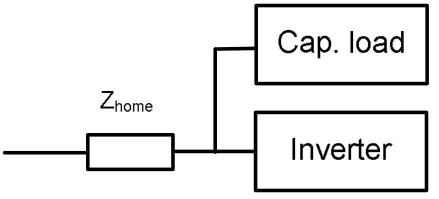

Figure 6.4: Distribution model 2; home level.

As mentioned before, all homes are connected to one phase. The other two phases are not considered in this investigation and only the connections and effects between one power line and the neutral are observed.

6.2 Understanding system resonances

Before analyzing the simulations two simplified cases are considered, based on section 5.3.2.2. First the inverters are replaced by:

1. a parallel circuit of L_{out} and C_{out} (model of a Voltage Source Converter (VSC) based inverter without current feed-back),
2. only the capacitor C_{out} (model of a VSC based inverter with current feed-back).

In the first case the output filter is driven by an uncontrolled VSC based inverter and Z_{inv} is neglected (see Figure 5.9). Figure 6.5 shows the basic circuit that generates the resonance effect in the aggregate impedance, measured at the LV busbar.

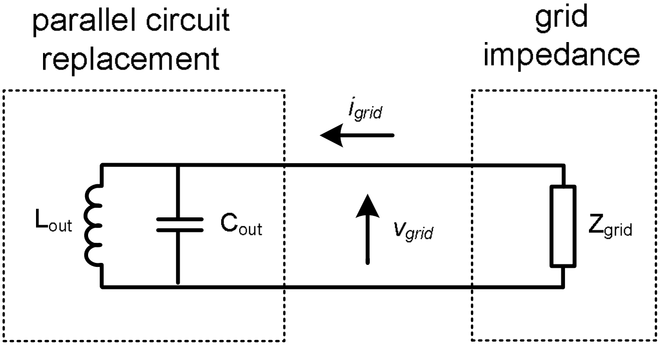

Figure 6.5: Basic impedance circuit when the inverter is replaced by the parallel circuit of L_{out} and C_{out} (VSC based inverter without current feed-back).

In the second case the output filter is driven by a current feed-back controlled VSC based inverter. Figure 6.6 shows the basic circuit that generates the resonance effect in the aggregate impedance, measured at the LV bus-bar.

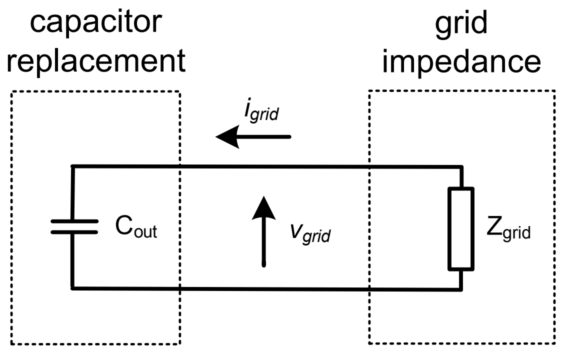

Figure 6.6: Basic impedance circuit when the inverter is replaced by only C_{out} (VSC based inverter with current feed-back).

6.2.1 VSC without current feed-back

As stated in section 5.3.2.2 for an uncontrolled VSC based inverter, Z_{inv} equals a low impedance value and with that the total impedance will show a resonance between L_{out} and C_{out}, damped by resistive part of L_{out} and Z_{inv}. In Figure 6.7 the harmonic impedance is shown, measured at the substation LV busbar in the extended distribution grid model (see Figure 6.1) with the inverters replaced by the parallel circuit of L_{out} and C_{out}. Respectively 20, 40, 80 and 200 parallel resonance circuits are connected.

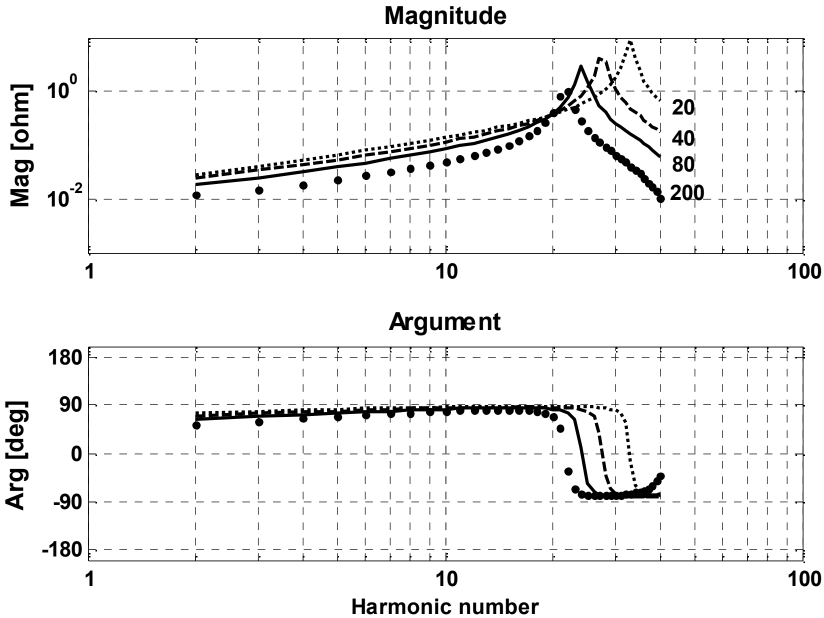

Figure 6.7: Harmonic impedance measured at the substation busbar with the inverter replaced by the parallel circuit of L_{out} and C_{out}, respectively 20, 40, 80 and 200 pieces.

At 20 pieces of parallel resonance circuits placed in the model the resonance frequency is about on the 33th harmonic. While increasing the number of parallel circuits up to 200 pieces, the resonance frequency decreases up to about the 22th harmonic, see Figure 6.7. This frequency approaches that of one single resonance circuit of L_{out} and C_{out} decoupled from the grid that lies on the 20th harmonic. In general, connecting a number of parallel resonance circuits in parallel does not change the resonance frequency as seen from Equations (6.1) to (6.4).

$$C_{out\_n} = n\,C_{out} \tag{6.1}$$

$$L_{out\_n} = \frac{L_{out}}{n} \tag{6.2}$$

$$\omega_{res} = \sqrt{\frac{1}{L_{out} C_{out}}} \tag{6.3}$$

$$\omega_{res\_n} = \sqrt{\frac{1}{L_{out\_n}\ C_{out\_n}}} = \sqrt{\frac{1}{\frac{L_{out}}{n}\,n\,C_{out}}} = \sqrt{\frac{1}{L_{out} C_{out}}} \tag{6.4}$$

But when the L_{out} and C_{out} circuits are placed in the extended distribution grid model, the resonance will shift with the number of circuits in the model. The explanation of this is that the inductive grid impedance is connected in parallel to the circuits (Figure 6.5 gives an explanation of this situation) and reduces the total inductance in the aggregate impedance, this reduction shifts the resonance to a higher frequency. The higher the number of L_{out} and C_{out} circuits in the model, the lower the aggregate impedance magnitude of these circuits is. Therefore with 200 parallel circuits in the grid model the effect of the paralleled grid impedance is limited and the resonance frequency approaches the inverters output filter resonance ω_{res} that lies on the 20th harmonic.

6.2.2 VSC with current feed-back

As stated in section 5.3.2.2 for a current feed-back controlled VSC based inverter, Z_{inv} equals a high impedance and with that the total impedance will show the impedance of only the capacitance C_{out}. In Figure 6.8 the harmonic impedance is shown, measured at the substation LV busbar in the extended distribution grid model (see Figure 6.1) with the inverters replaced by its output capacitance C_{out}. Respectively 20, 40, 80 and 200 capacitors are connected.

While increasing the number of capacitors placed in the extended distribution grid model, the resonance frequency decreases as seen in Figure 6.8. At 20 pieces of capacitors the resonance frequency is at the 26th harmonic and at 200 pieces the resonance frequency is at the 9th. Basically this resonance is an interaction between the grid impedance and the connected capacitors (Figure 6.6 gives an explanation of this situation).

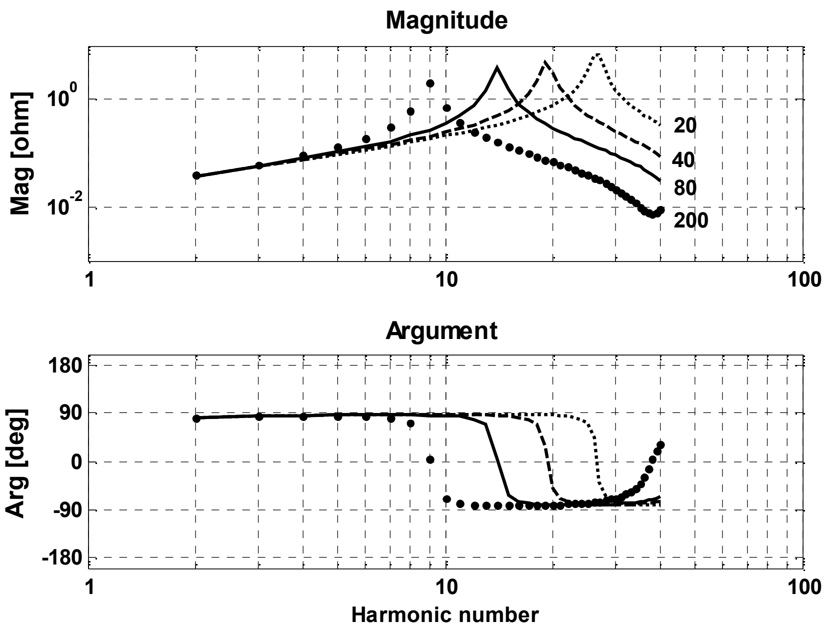

Figure 6.8: Harmonic impedance measured at the substation busbar with the inverter replaced by only C_{out} , respectively 20, 40, 80 and 200 pieces.

6.3 Implementing the validated inverter model

Similar results as in section 6.2 can be expected with the validated ancillary services inverter simulation model from section 5.3 implemented in the extensive distribution grid models, in case the inverter's ancillary services are not activated. In the frequency range where the current control system is active (3^{th}, 5^{th}, 7^{th}, 9^{th} and 11^{th} harmonic), Z_{inv} equals a high impedance value and for other frequencies Z_{inv} equals a low impedance value, see section 5.3.2.2. This low impedance effect of Z_{inv} is strongly limited because of the (50%) v_L-compensation loop (see section 5.3.2.3). Therefore resonances will be on frequencies somewhere in between the worst-case situations described in the previous sections 6.2.1 and 6.2.2. Because the current control system only works on a limited number of harmonics (3^{th}, 5^{th}, 7^{th}, 9^{th} and 11^{th}) and also the effect of the (50%) v_L-compensation loop phases out above the 13^{th} harmonic frequency, the effects of all the described situations can be expected, at the same time.

6.4 Simulation results from model 1

In this section impedance values as a function of the harmonic order are given for the aggregate grid impedance measured at the transformer substation busbar under various conditions. All simulations are done with a number of validated ancillary services inverter simulation models, connected in the extensive distribution grid model, as discussed in section 6.1. During all simulations, the 50% v_L-compensation loop is active, only the effects of activated and not activated ancillary services VPCR and Virtual Resistive Harmonic Damping (VRHD) are compared, this is done in the following order:

- VPCR and VRHD not active (basic inverter control),
- only VPCR active,
- both VPCR and VRHD active.

The effect of only VRHD is not a subject of study in this thesis, this was already done in [Ryc 05a].

6.4.1 Basic inverter control

In Figure 6.9 the impedance as a function of the harmonic order measured at the substation busbar is given with only 40 inverters connected in the grid model. In this figure a damped resonance can be noticed at the 26th harmonic, this is caused by the combination of the paralleled inverters output filters L_{out} and C_{out} together with the grid impedance, as explained in section 6.2 and 6.3.

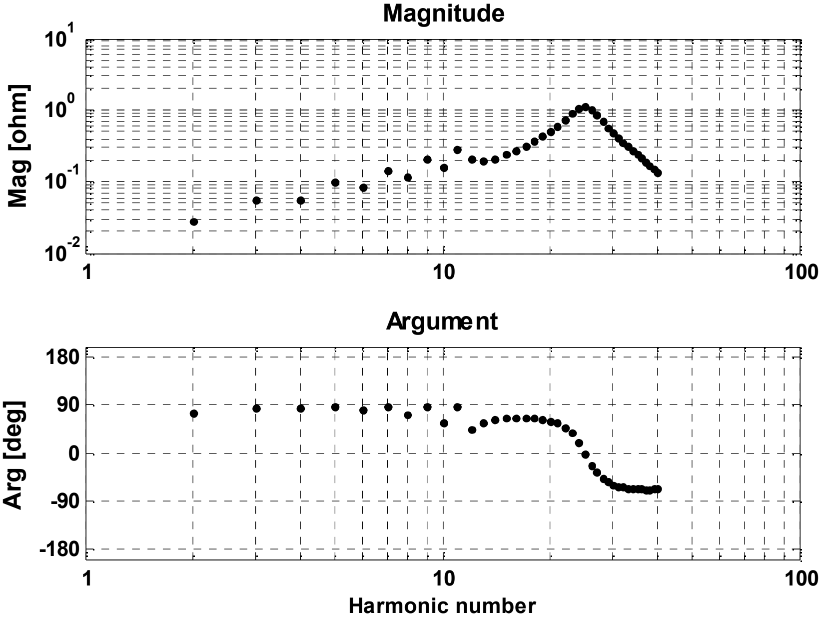

Figure 6.9: Harmonic impedance measured at the substation busbar with only 40 inverters connected.

In Figure 6.9, no resonance can be observed in the frequency range where the current control system is active (3^{th}, 5^{th}, 7^{th}, 9^{th} and 11^{th} harmonic).

When the number of inverters is increased to 200 pieces two remarkable effects show up. Firstly, the damped resonance from Figure 6.9 is shifted more towards the inverter's output filter resonance frequency, being the 20^{th} harmonic and secondly, a strong resonance is shown around the 9^{th} harmonic as seen in Figure 6.10. The latter resonance is caused by the aggregate of the inverter's capacitances and the grid inductance at the LV busbar and can only show up in the frequency range where the current control system is active (3^{th}, 5^{th},7^{th}, 9^{th} and 11^{th} harmonic). Both effects were explained in section 6.2 and 6.3.

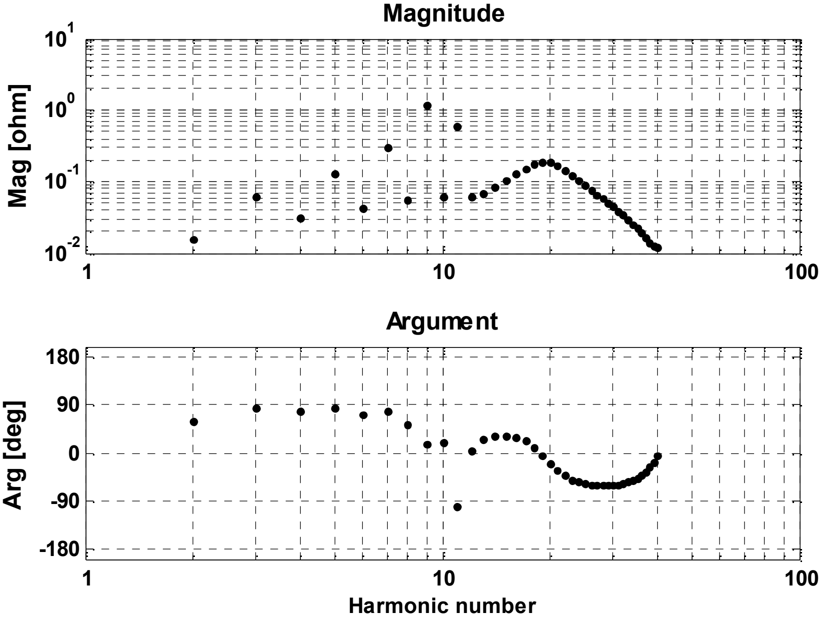

Figure 6.10: Harmonic impedance measured at the substation busbar with 200 inverters connected.

6.4.2 Ancillary services VPCR and VRHD

The VPCR ancillary service is mainly effective where the current control system is active (3th, 5th, 7th, 9th and 11th harmonic). Therefore activating VPCR means that the capacitances C_{out} are virtually reduced and the resonance at the 9th harmonic as shown in Figure 6.10 will virtually be shifted away. In Figure 6.11 no resonance can be observed anymore at the 9th harmonic and all the phase angles of the 3th, 5th, 7th, 9th and 11th harmonic are +90 degrees, this indicates a virtual inductive aggregate grid impedance in a grid with a large number of physical capacitors connected.

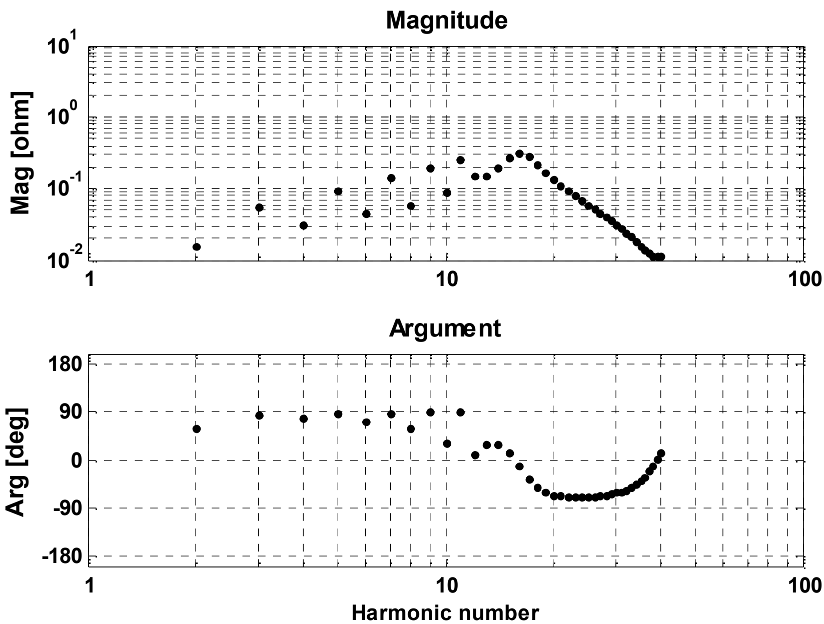

Figure 6.11: Harmonic impedance measured at the substation busbar with 200 ancillary service inverters and only VPCR active.

The VRHD ancillary service is strongly limited to only the harmonics where the current control system is active (3^{th}, 5^{th}, 7^{th}, 9^{th} and 11^{th} harmonic), because of the implementation of an extra resonant bandwidth limiter (see section 5.3.2.5). This is done to avoid a poorly defined VRHD impedance at frequencies other than the harmonics supported by the current control system. Activating this VRHD while the inverters output capacitances C_{out} are already virtually reduced by VPCR, will bring a pure resistive output impedance to each of the 200 connected inverters for the 3^{th}, 5^{th}, 7^{th}, 9^{th} and 11^{th} harmonic, see also section 5.6.2.

With both the ancillary services VPCR and VRHD active, the aggregate impedance on the 3^{th}, 5^{th}, 7^{th}, 9^{th} and 11^{th} harmonic, measured at the LV busbar, is a combination of the number of connected inverters, and the inductance- and resistive impedances. The result is given in Figure 6.12. The VRHD per inverter is set to 10Ω, this brings to total of the 200 inverters in the grid to about 0.05Ω, which can be noticed in Figure 6.12.

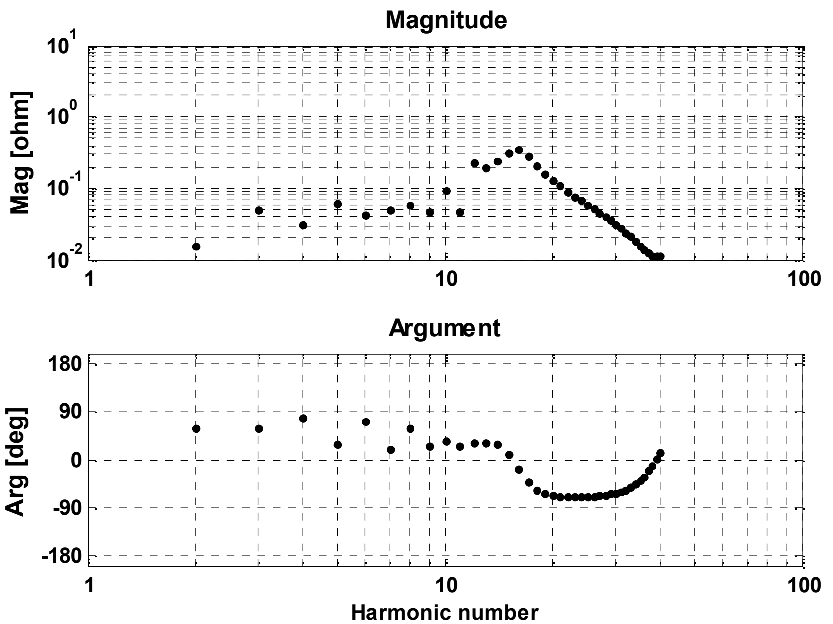

Figure 6.12: Harmonic impedance measured at the substation busbar with 200 ancillary service inverters and both VPCR and VRHD active.

6.5 Simulation results from model 2

This section gives simulation results of model 2 and the approach is similar to the previous section. The set-up of model 2 is described in detail in section 6.1. The most important difference with model 1 is that the VPCR ancillary service of the inverters of model 2 is virtually compensating also external capacitive loads besides their own output capacitances.

6.5.1 Basic inverter control

In Figure 6.13 the harmonic impedance is given with 100 inverters as well as 100 capacitive loads connected in the grid model. In the frequency range where the current control system is active (3^{th}, 5^{th}, 7^{th}, 9^{th} and 11^{th} harmonic), a strong resonance around the 9^{th} harmonic can be observed. Because in model 2 the total capacitance equals that of the model 1, the resonance is also around the same harmonic.

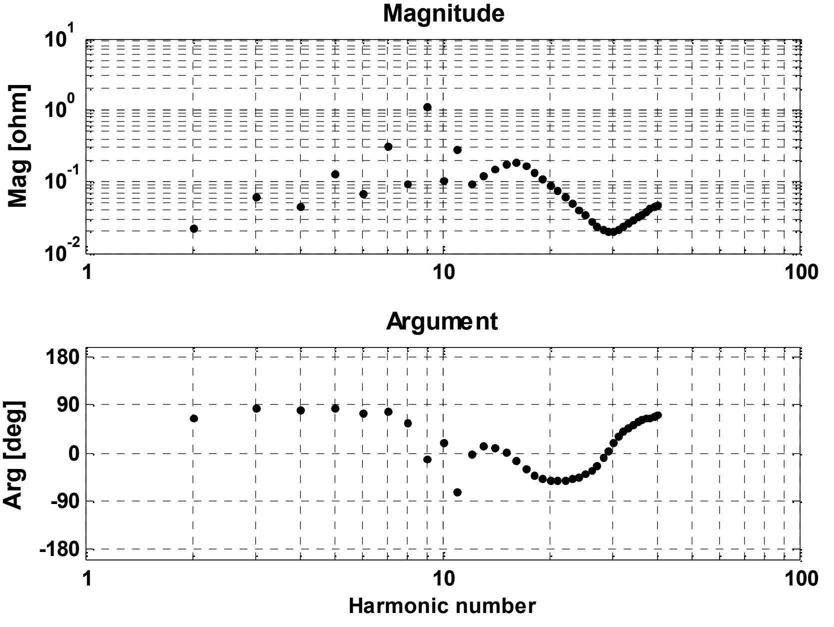

Figure 6.13: Harmonic impedance measured at the substation busbar with 100 inverters as well as 100 capacitive loads connected. A strong resonance around the 9th harmonic can be observed

6.5.2 Ancillary services VPCR and VRHD

In Figure 6.14 the VPCR ancillary service is activated in a limited way, namely only the current through the inverter's output capacitance is compensated. The aggregate capacitance now has virtually become about half the value, this should have the effect that the resonance virtually shifts with the square root of 2, that would be about the 13th harmonic, however this cannot be found since the VPCR control stops above the 11th harmonic. It can be noticed that the resonance virtually has shifted up, and that the phase angle at the 11th harmonic is about +55 degrees, this means that at the 11th harmonic, the resonance peak has not yet been reached.

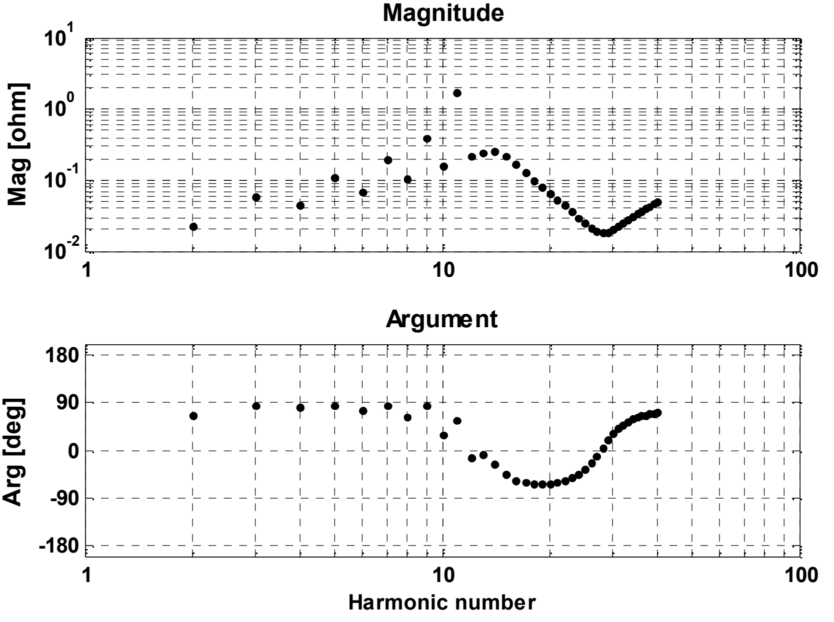

Figure 6.14: Harmonic impedance measured at the substation busbar with 100 inverters as well as 100 capacitive loads connected and a limited VPCR active.

In Figure 6.15 the VPCR ancillary service is fully activated and all the currents through the capacitances in the grid are compensated. As a result no resonance can be observed anymore at the 9th harmonic and all the phase angles of the 3th, 5th, 7th, 9th and 11th harmonic are +90 degrees, this indicates a virtual inductive aggregate grid impedance in a grid with a large number of inverters with large physical output capacitances and also a large number of physical capacitive loads connected.

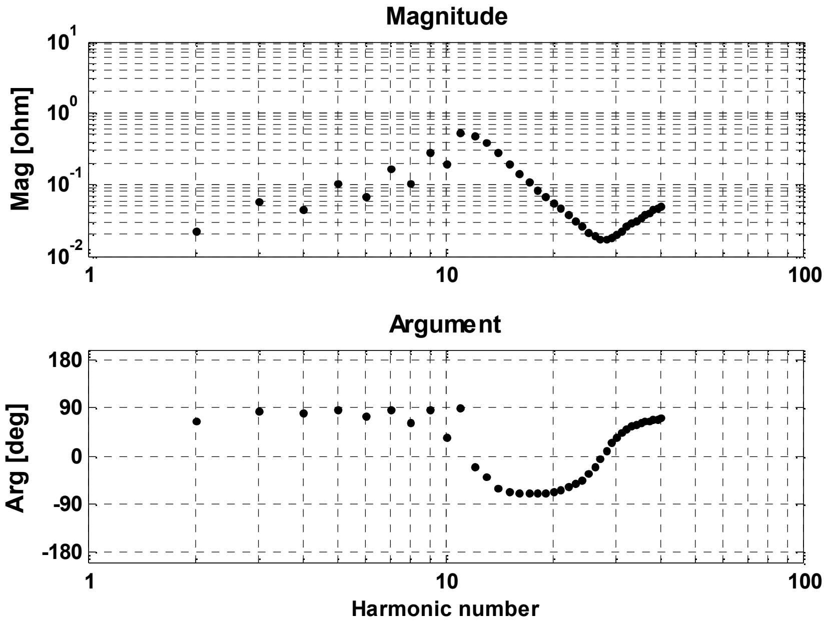

Figure 6.15: Harmonic impedance measured at the substation busbar with 100 inverters as well as 100 capacitive loads connected and full VPCR active.

With both the ancillary services VPCR and VRHD active, the aggregate impedance on the 3th, 5th, 7th, 9th and 11th harmonic, measured at the LV busbar, is a combination of the number of connected inverters, and the inductance- and resistive impedances. The result is given in Figure 6.16. The VRHD per inverter is set to 10Ω, this brings to total of the 100 inverters in the grid to about 0.1Ω, which can be noticed in Figure 6.16.

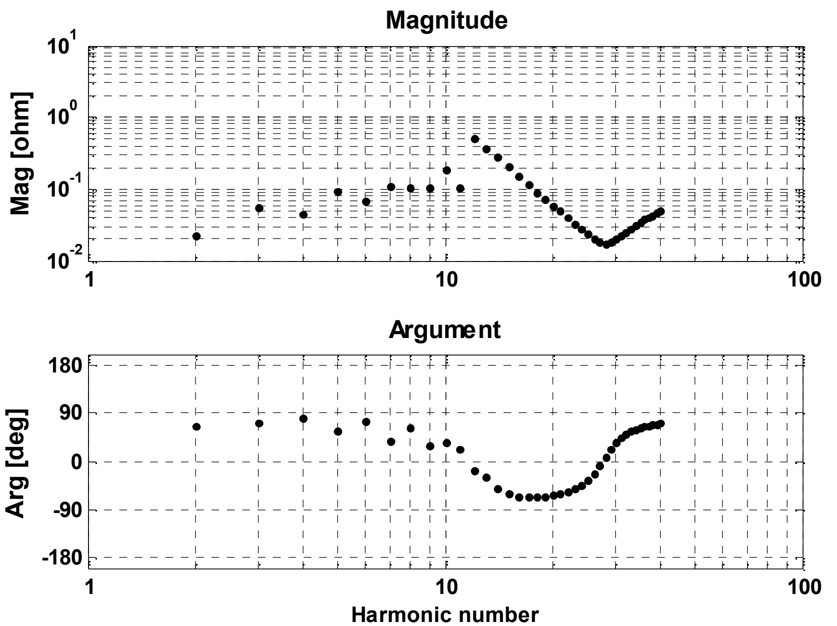

Figure 6.16: Harmonic impedance measured at the substation busbar with 100 inverters as well as 100 capacitive loads connected and both VPCR and VRHD active.

6.6 Discussion

From the simulations performed and discussed in this chapter, it was noticed that the ancillary service VPCR not only works in situations where a parallel capacitance is placed directly at the inverter's output feeders, but also in situations where capacitances are placed on other locations in the distribution grid. It must be emphasized that compensation of the current through the inverter's own output capacitance can be done without the risk of instability of the inverter's control system, because overcompensation can lead to instability. In practical situations, compensating currents through capacitors of other in parallel connected loads can bring this instability if these loads are switched off from the grid. Therefore an adaptive system will be necessary to avoid this situation. This system should be able to estimate the total parallel capacitance in the distribution area around the inverter that offers VPCR, the impedance measurement system of chapter 3 can be the basis for that. It is however recommended to do more extended simulations, but then with more detailed models of grids and an adaptive system for this VPCR ancillary service.

Another approach is that appliances that bring in more than a certain parallel capacitance per unit of power (see section 5.1), must compensate the current through their own output capacitance. Although this action will help to minimize the effect of the growing number of parallel capacitances in the grid, it should be investigated of this solution solely will be sufficient on the long term. A combination of this and converters that offer a VPCR ancillary service will possibly bring a more optimal solution.

6.7 Conclusion

In this chapter the effect the ancillary services VPCR and VRHD on two extended computer simulation models is discussed. Both models use multiple pieces of the validated ancillary service inverter model developed in this thesis. In the first model, 200 pieces of these inverters are placed in homes and compensating the current through their own output capacitances by means of VPCR. In the second model, 100 pieces of these inverters are placed in homes and compensating currents through external capacitive loads as well.

In the situation with the inverter's ancillary services not activated, a strong resonance on the 9^{th} harmonic in the aggregate impedance, measured at the LV busbar, can be observed. Activating the ancillary service VPCR effectuates that this aggregate impedance becomes virtually pure inductive, this while a large number of physical capacitors are connected. Activating both the ancillary services VPCR and VRHD, effectuates that the aggregate impedance becomes a combination of virtual inductive- and resistive impedances. The ancillary services VPCR and VRHD only work on a number of harmonics, because of the resonant control system.

These results show that both the ancillary services VPCR and VRHD perform as expected, this means that they can minimize the effect of resonances in the grid.

Chapter 7

Conclusions, contribution and recommendations

The main goal of the work presented in this thesis is to minimize the impact of resonances in low voltage distribution grids. To be able to achieve measures that can work in practice, first the phenomenon of harmonic interaction is studied and besides this a resonance assessment method is developed. This method is able to estimate the complex harmonic impedance spectrum at a certain point in the grid or to estimate the output impedance spectrum of an appliance. The method is used during the laboratory measurements but could be also used in adaptive control systems, to adjust control parameters. Computer simulation models are created to simulate possible future grid situations where resonances can occur in order to develop measures for minimizing the effect of these resonances. Laboratory experiments are done with a grid simulator and a generic hardware power electronics based inverter. With these laboratory experiments the computer simulation models are validated. Finally with the validated models, extended computer simulations are done for a Low Voltage (LV) distribution grid with systems to minimize the impact of resonances.

Two possible situations that cause grid resonances are studied in this thesis. The effects of these resonances are oscillatory voltages and a high level of harmonic voltages. The first effect, oscillatory voltages, is caused by Negative Differential Impedances (NDIs) in the grid. The origin of these NDIs are Constant Power Loads (CPLs). The CPL effect shows up when an appliance is stabilized against grid voltage fluctuations by a power electronics front-end. This stabilization can cause that a load draws a constant power from the grid while the grid voltage level is fluctuating. The second effect, a high level of harmonic voltages, is caused by parallel resonances. The origin of these parallel resonances is the connection of large numbers of front-end capacitors of power electronics based appliances to the LV grid. To minimize the impact of these parallel resonances, specific (ancillary) services are implemented to power electronics based inverters for Distributed Generators (DG).

In this chapter the main conclusions of this work, contributions to engineering and recommendations for future work are presented.

7.1 Conclusions

In this section the main conclusions of the thesis work are presented.

Measurement system for resonance assessment

Grid resonances caused by a large number of parallel capacitances in a LV grid, can increase the impedance around the resonance frequency to a much higher level. The impedance spectrum of the grid shows these resonances and therefore can be used to assess the potential to pollute the grid. In this thesis a special impedance measurement system is developed, built up and tested. The proposed measurement system can locate these possible resonances in an operating grid, to make it possible to take measures on beforehand. Measuring the impedance spectrum of the grid can be also useful to make power electronics converters automactically adaptive to various grid situations.

The measurement system is Fourier based, thus the use is limited to small signal impedance spectra that are taken under a steady-state condition. The system has a two-fold calculation part, namely a lock-in system to estimate the fundamental impedance and a Fast Fourier Transformation (FFT) system to estimate the harmonic impedances. Good simulation and measurement results are achieved with a time series length of 1 second for harmonics, and 4 seconds for the fundamental.

The system is developed and tested to be able to operate well in a practical situation. Therefore, it injects a very low measurement current, lower than the allowed emission of a home appliance of 75W, falling in class D of the IEC 61000-3-2 standard. The measurement system is capable of operating under polluted grid voltages with a Total Harmonic Distortion (THD) of 8% and also added to this a white noise of 0.25%. Also the grid frequency may vary between the allowed steady-state conditions, i.e. between 49.5Hz and 50.5Hz.

Resonances caused by CPLs

Non-linear CPLs are characterized by appliances which are stabilized against grid voltage fluctuations by a power electronics front-end. These types of loads have a NDI that can cause an oscillatory grid voltage. Simulation results show that the voltage control system of a generator can be affected by a CPL fraction that takes the upper hand. This situation can happen in small isolated grids. However, it can also happen in larger electricity grids when the CPL share remains growing at various power/voltage distribution levels. The CPLs can bring a low frequency oscillatory grid voltage. A measure to minimize this can be found in adjusting the parameters of voltage control systems, and of course also reducing the CPL fraction.

From the work that is done in this thesis, the conclusion can be drawn that the NDI effect comes up when the fundamental grid voltage is modulated with low frequency voltages in the range of about 0.02 to 5Hz, voltage oscillation is found with frequencies in this range.

Resonances caused by parallel capacitances

Parallel capacitances of appliances and grid components can induce resonances in the LV grid and can increase harmonic distortion levels. This especially holds for resonances below the 25^{th} harmonic because the damping effects of cables and transformers are limited in this range. Resonances in a range lower than the 25^{th} harmonic may become more common in the near future.

Power electronics based loads and DGs have an Electro Magnetic Interference filter (EMI-filter) capacitor at the output terminals, and can be marked as an appliance with a so-called parallel capacitance. The parallel capacitance of a single home appliance is small, but the aggregate parallel capacitance of a large and still increasing number in a distribution grid can increase to a high level. Today the equivalent capacitance of connected home-appliances at the Point of Connection (PoC) can vary over a wide range from around 0.6 μF to 6μF. Today's inverters for DG have a relatively large output capacitor up to about 3μF per kW rated output power. Therefore an inverter of a few kW can bring already a large contribution to the total in parallel connected capacitances at the PoC.

Grid resonances caused by parallel connected capacitors of appliances can be seen as a parallel resonance for harmonic currents from non-linear loads in the LV distribution grid and at the same time they can be seen as a series resonance for non-linear loads in the Medium Voltage (MV) grid. Parallel resonances can increase the impedance around the resonance frequency to a much higher level. Harmonic currents from non-linear loads in the LV grid can be transferred into problematic high harmonic voltages. Series resonances in the LV grid can bring a low impedance path for background harmonics, i.e. harmonic voltages in the MV grid causes harmonic currents flowing into the LV grid. These harmonic currents will flow through the distribution transformer and can gain unwanted effects in this component. Besides this, at the LV side, the harmonic voltages can rise to a high level.

A combination of two measures is proposed in this thesis to reduce these harmonic currents and voltages, namely harmonic damping and a virtual reduction of parallel capacitances. Harmonic damping can have effect on the total range of harmonics without estimating the actual level of harmonics in the grid. For background harmonics, the harmonic damping must be limited to avoid excessive currents through the distribution transformer and cables. Virtual reduction of parallel capacitances is a technique that compensates harmonic currents through parallel capacitors. The effect of this combined measure is that a resonance peak is virtually shifted to a higher frequency range and damped to a lower level.

In this thesis both proposed measures are marked as ancillary services that can be implemented in power electronics based converters. These services are called “Virtual Parallel Capacitance Reduction (VPCR)” and “Virtual Resistive Harmonic Damping (VRHD)”. As presented in this thesis, these two ancillary services can be implemented in power electronics based inverters for DG as well. The affected harmonic range depends on the performance of the control systems.

A single-phase inverter for DG with the ancillary services VPCR and VRHD is computer simulated and validated with a hardware model in the laboratory. Results of the simulations show that the two ancillary services perform as expected, especially the combination of the two ancillary services is a useful measure to minimize the effect of resonances in the LV distribution grid.

It is observed that VPCR can virtually reduce the amount of parallel capacitance with a factor ten. This implicates that a possible resonance is virtually shifted with the square root of ten, i.e. to a more than three times higher frequency.

It is also observed that VRHD damps a resonance peak to a much lower level. Virtual resistance values in between 0.5 to 2 times the equivalent resistance that would draw the rated power of the inverter from the grid, performed well.

Results from a computer simulation of a large-scale LV distribution grid with 200 pieces of power electronics based DG on a single phase, indicates that also in this situation, both the ancillary services VPCR and VRHD perform as expected.

7.2 Thesis contribution

Measurement system for resonance assessment

Grid resonances (parallel or series) are suspected if harmonic voltage or current amplification is observed. To be able to separate cause and effect in situations of poor harmonic quality of the grid voltage a resonance estimation method is needed. This thesis proposed a method to locate resonances in an operating grid. A special grid impedance measurement system is developed, built and tested.

Resonances caused by CPLs

Oscillatory grid voltages caused by CPLs are up to now not experienced because the electricity grid still has a very strong normal load part, compared to the fraction of the load that has a CPL behavior. However this situation will change in future. The contribution of this thesis is that the work on this subject can be seen as an eye opener for new power quality problems that might appear. Reasons of the threat are mentioned like new types of loads, new voltage regulating grid components and the operation of isolated local distribution systems in specific situations.

Resonances caused by parallel capacitances

To master the transition towards a more decentralized generation it is very important to know the system harmonic interaction and to minimize the impact of resonances. The thesis contribution on this subject is an explanation of the phenomenon of grid voltage pollution caused by resonances and how to control this problem.

A strong combination of two measures to minimize grid resonances is proposed and added as ancillary services to an inverter of a power electronics based DG, namely VPCR and VRHD. These ancillary services are simulated and validated.

7.3 Recommendations

Measurement system for resonance assessment

An important goal of the impedance measurement system for resonance assessment is to learn more about the grid resonance phenomenon. Therefore a number of these systems need to be installed into LV distribution grids at several locations. Before this can take place, more laboratory and field tests are needed for further validation of the system. It is important to figure out, if the system's limitations are hindering the accuracy of the results, e.g. results are only valuable for small deviations round the operating condition and during the measurement the grid voltages and currents need to be constant. In a laboratory the effect of voltages and currents fluctuations and also combinations of loads like linear loads, non-linear loads and phase angle controlled loads, needs to be studied.

Another use of the impedance spectrum system is to make power electronics based converters automactically adaptive to various grid situations. An interesting study in this field would be how the described control systems in this thesis can use this impedance measurement system to perform optimal for several grid impedance conditions.

Resonances caused by CPLs

Because this part of the thesis is done with a diesel-generator model instead of that of power electronics based DG, further study on this subject is very much recommended. Research in this field could be incorporated in studies on the transition towards future Smart Grids.

Resonances because of parallel capacitances

In the field of grid resonances caused by parallel capacitances, more research is needed to assess the significance and impact of this phenomenon in future Smart Grids. Various types of appliances and power electronics based DG can be benchmarked on their potential to gain grid resonances. The proposed ancillary services in this thesis can be validated in a larger scale laboratory set-up and in a real field test. This field test could be in a distribution grid with large numbers of power electronics based DG. The sensitivity to the grid parameters can be further investigated and if necessary a more sophisticated control technique can be developed, e.g. an adaptive control system with automatic parameter adjustment by using a complex impedance spectrum measurement system.

Concerning the ancillary services VPCR and VRHD, it is recommended to perform extended simulations with more detailed models of grids. More research is needed to estimate the stability boundaries of a power electronics converter that offers these ancillary services. For example, in practical situations overcompensation of parallel capacitances can take place if loads are switched off from the grid. Instabilities can happen and measures to avoid them need to be investigated.

Bibliography

[Aba 07] K. Abaci et al, "Observing Chaotic Oscillations Induced by under Load Tap Changer in Power Systems", Journal of Applied Sciences 7(1), ANSI, pp. 66-71, 2007

[Aka 05] H. Akagi, "Active Harmonic Filters", Proceedings of the IEEE, Vol. 93, No. 12, pp. 2128–2141, December 2005.

[Aka 99] H. Akagi, H. Fujita, K. Wada, "A Shunt Active Filter Based on Voltage Detection for Harmonic Termination of a Radial Power Distribution Line", IEEE Transactions on Industry Applications, Vol. 35, No. 3, pp. 638-645, May/June 1999.

[Aka 97] H. Akagi, "Control Strategy and Site Selection of a Shunt Active Filter for Damping of Harmonic propagation in Power Distribution Systems", IEEE Transactions on Power Delivery, Vol. 12, No 1, pp. 354-363, January 1997.

[Aka 96] H. Akagi, "New trends in active power line conditioners", IEEE Transactions on Industry Applications, vol. 32, no. 6, pp. 1312-1322, Dec. 1996.

[Arr 04] J. Arrillaga, N.R. Watson, "Power System Harmonics", Second Edition, ISBN 0-470-85129-5, John Wiley & Sons Ltd, 2004.

[Bag 02] Y. Baghzouz, R. F. Burch, A. Capasso, A. Cavallini, A. E. Emanuel, M. Halpin, R. Langella, G. Montanari, K. J. Olejniczak, P. Ribeiro, S. Rios-Marcuello, F. Ruggiero, R. Thallam, A. Testa, and P. Verde, Probabilistic Aspects Task Force of the Harmonics Working Group, "Time-Varying Harmonics: Part II—Harmonic Summation and Propagation", IEEE Transactions on Power Systems, Vol. 17, No. 1, pp. 279-285, Jan. 2002.

[Bag 98] Y. Baghzouz, R. F. Burch, A. Capasso, A. Cavallini, A. E. Emanuel, M. Halpin, R. Langella, G. Montanari, K. J.

Olejniczak, P. Ribeiro, S. Rios-Marcuello, F. Ruggiero, R. Thallam, A. Testa, and P. Verde, Probabilistic Aspects Task Force of the Harmonics Working Group, “Time-Varying Harmonics: Part I – Characterizing Measured Data”, IEEE Transactions on Power Delivery, Vol. 13, No. 3, pp. 938-944, July 1998.

[Ber 09] J. van den Berg, I. Harms, J. Schroeders, S. Sondeijker, “Actieplan Elektrisch Rijden – Op weg naar één miljoen elektrische auto’s in 2020”, Stichting Natuur en Milieu, Utrecht, maart 2009.

[Ber 00] M. van den Bergh, “Public Low Voltage Supply System Impedance Tests in France - Belgium – The Netherlands – Germany”, Poway Report, CNS Inc., Sept. 2000.

[Bol 05] B. Bolsens, “EMC Problems and Possible Solutions in High Frequency Power Electronic Converters”, Ph.D. dissertation, Faculteit Ingenieurswetenschappen, Katholieke Universiteit Leuven, Belgium, Dec. 2005.

[Bos 06] A.J.A. Bosman, “Harmonic modeling of Solar inverters and their interaction with the distribution grid”, Master thesis, Eindhoven University of Technology. Department of Electrical Engineering, Electrical Power Systems, 2006.

[Bra 06] K. De Brabandere, “Voltage and Frequency Droop Control in Low Voltage Grids by Distributed Generators with Inverter Front-end”, Ph.D. dissertation, Faculteit Ingenieursweten-schappen, Katholieke Universiteit Leuven, Belgium, Oct. 2006.

[Bur 85] C.S. Burrus, T.W. Parks, “DFT/FFT and Convolution Algorithms”, Theory and Implementation, ISBN 0-471-81932-8, John Wiley & Sons Ltd, 1985.

[Cai 08] R. Caire et al, “High-level Specification of the Functionalities for Novel Electricity Distribution Grid Control”, Deliverable D2.1 of the INTEGRAL EU-Project, FP6-038576, 2008.

[Cob 07] J.F.G. Cobben, “Power Quality, Implications at the Point of Connection”, Ph.D. dissertation, Faculty of Electrical

Engineering, Eindhoven University of Technology, The Netherlands, 2007.

[Col 99] C. Collombet, J.M. Lupin, J. Schonek, "Harmonic disturbances in grids and their treatment", Cahier technique no. 152, Schneider Electric, France, Dec. 1999.

[Coo 65] J. Cooley and J. Tukey, "An Algorithm for the Machine Calculation of Complex Fourier Series", Mathematics of Computation, Vol. 19, No. 90, pp. 297-301, Apr. 1965.

[Coo 72] J.C. Cool, F.J. Schrijf, T.J. Viersma, "Control techniques", in Dutch: "Regeltechniek", Study book, Agon Elsevier, 1972.

[Cos 10] E.J. Coster, "Distribution Grid Operation Including Distributed Generation", Ph.D. dissertation, Faculty of Electrical Engineering, Eindhoven University of Technology, The Netherlands, 2010.

[Den 97] E. Deng, S. Cuk, "Negative Incremental Impedance and Stability of Fluorescent Lamps", IEEE Applied Power Electronics Conference (APEC), Atlanta, GA, USA, pp. 1050-1056, Febr. 1997.

[Ema 04] A. Emadi, "Modeling of Power Electronic Loads in AC Distribution Systems Using the Generalized State-Space Averaging Method", Transactions on Industrial Electronics, Vol. 51, No.5, Chicago, pp. 992-1000, Oct. 2004.

[End 01] W. Enders, Ch. Halter, and P. Wurm, "Investigation of typical problems of PV inverters", 17th European Photovoltaic and Solar Energy Conference, Munich, Germany, pp. 763–766, 2001.

[Ens 04] J.H.R. Enslin, P.J.M. Heskes, "Harmonic Interaction Between Large Numbers of Photovoltaic Inverters and the Distribution Grid", IEEE Transactions on Power Electronics, vol. 19, no. 6, pp. 1586-1593, Nov. 2004.

[Fri 05] M. Frigo and S.G. Johnson, "The design and implementation of FFTW3", Proceedings of the IEEE, 93(2), pp. 216-231 Febr. 2005.

[Fuj 98a] H. Fujita, H. Akagi, “The Unified Power Quality Conditioner: The Integration of Series- and Shunt-Active Filters”, IEEE Transactions on Power Electronics, Vol. 13, No. 2, pp. 315-322, March 1998.

[Fuj 98b] H. Fujita, T. Yamasaki, H. Akagi, “A Hybrid Active Filter for Damping of Harmonic Resonance in Industrial Power Systems”, IEEE/PELS PESC Conf. Rec., pp. 209-216, 1998.

[Gus 07] K. De Gussemé, W.R. Ryckaert, D.M. Van de Sype, J.A. Ghijselen, J.A. Melkebeek, “A Boost PFC Converter with Programmable Harmonic Resistance”, IEEE Transactions on Industry Applications, Vol. 43, No. 3, pp. 1621-1627, May/June 2007.

[Hes 07] P.J.M. Heskes, J.L. Duarte, “Harmonic reduction as ancillary service by inverters for Distributed Energy Resources (DER) in electricity distribution networks”, Cired, Vienna, 21-24 May 2007.

[Hes 05] P.J.M. Heskes, J.F.G. Cobben, H.H.C. de Moor, "Harmonic distortion in residential districts due to large scale PV implementation is predictable", International Journal of Distributed Energy Resources, vol. 1, no. 1, pp. 17-32, Jan./Mar. 2005.

[Her 85] O. Herrmann, J.H. Jansen, “Ontwerp en realisatie van digitale filters”, Dutch, Dictaat code 123147, THT, vakgroep BSC, 1985.

[Hol 09] D.G. Holmes, T.A. Lipo, B.P. McGrath, and W.Y. Kong, “Optimized Design of Stationary Frame Three Phase AC Current Regulators”, IEEE Trans. on Power Electronics, vol. 24, no. 11, pp. 2417-2426, Nov. 2009.

[Jin 03] P. Jintakosonwit, H. Fujita, H. Akagi, S. Ogasawara, “Implementation and Performance of Cooperative Control of Shunt Active Filters for Harmonic Damping Throughout a Power Distribution System”, IEEE Transactions on Industry Applications, Vol. 39, No. 2, pp. 556-564, March/April 2003.

[Jin 02] P. Jintakosonwit, H. Fujita, H. Akagi, S. Ogasawara, “Implementation and Performance of Automatic Gain

Adjustment in a Shunt Active Filter for Harmonic Damping Throughout a Power Distribution System”, IEEE Transactions on Power Electronics, Vol. 17, No. 3, pp. 438-447, May 2002.

[Kar 05] M. Karimi-Ghartemani, “Analysis of Harmonics and Inter-Harmonics”, 48th IEEE International Midwest Symposium on Circuits and Systems, Cincinnati, Ohio, USA, 7-10 Aug. 2005.

[Kes 09] J.C.P. Kester et al, “A smart MV/LV-station that improves power quality, reliability and substation load profile”, Paper 0776, Cired, Prague, June 2009.

[Kot 05] A. Kotsopoulos, P.J.M. Heskes, M.J. Jansen, “Zero-Crossing Distortion in Grid-Connected PV Inverters”, IEEE Transactions on Industrial Electronics, vol. 52, no. 2, pp. 558-565, 2005.

[Li 09] Y.W. Li, “Control and Resonance Damping of Voltage-Source and Current-Source Converters With LC Filters”, IEEE Trans. on Industrial Electronics, vol. 56, no. 5, pp. 1511-1521, May 2009.

[Lis 06] M. Liserre, R. Teodorescu, and F. Blaabjerg, “Stability of Photovoltaic and Wind Turbine Grid-Connected Inverters for a Large Set of Grid Impedance Values”, IEEE Trans. on Power Electronics, vol. 21, no. 1, pp. 263-272, Jan 2006.

[Mai 09] A. Maitra et al, “Intelligent Universal Transformer Design and Applications”, Paper 1032, 20th International Conference on Electricity Distribution, Cired, Prague, June 2009.

[Mat 09] The Mathworks Inc., Matlab and Simulink version R2009a, Natick, Massachusetts, USA, 2009.

[Mee 08] J.J. Meeuwsen, J.M.A. Myrzik, G.P.J. Verbong, W.L. Kling, J.H. Blom, “Electricity networks of the future: Various roads to a sustainable energy system”, Cigré conference, Paris, France, 2008.

[Mol 08] M. Molinas D. Moltoni, G. Fascendini, J. A. Suul, R. Faranda, T. Undeland, “Investigation on the Role of Power Electronic Controlled Constant Power Loads for Voltage Support in Distributed AC systems”, 39th IEEE PESC08, Rhodos, Greece, 2008.

[Old 04] H.E Oldenkamp, I. de Jong, P.J.M. Heskes, P.M. Rooij, H.H.C. de Moor, "Additional Requirements for PV inverters necessary to maintain utility grid quality in case of high penetration of PV generators", 19th European PV Solar Energy Conference, Paris, France, 2004.

[Pom 07] J.A. Pomilio, Senior Member IEEE, and S.M. Deckmann, "Characterization and Compensation of Harmonics and Reactive Power of Residential and Commercial Loads", IEEE Transactions on Power Delivery, Vol. 2, No. 2, pp. 1049-1055, April 2007.

[Rib 09] P.F. Ribeiro, "Time-Varying Waveform Distortions in Power Systems", 396 pages book, ISBN: 978-0-470-71402-7, Wiley-IEEE Press, July 2009.

[Riv 05] C. Rivetta, G. A. Williamson, and A. Emadi, "Constant power loads and negative impedance instability in sea and undersea vehicles: statement of the problem and comprehensive large-signal solution", IEEE Electric Ship technologies Symposium, Philadelphia, PA, pp. 313-320, July 2005.

[Ryc 06] W.R. Ryckaert, K. De Gussem!e, D.M. Van de Sype, L. Vandevelde and J.A. Melkebeek, "Damping potential of single-phase bidirectional rectifiers with resistive harmonic behavior", IEE Proc.-Electr. Power Appl., Vol. 153, No. 1, pp. 68-74, January 2006.

[Ryc 05a] W.R. Ryckaert, K. de Gusseme, D.M. Van de Sype, J. A. Ghijselen, J.A. Melkebeek, "Reduction of the Voltage Distortion with a Converter Employed as Shunt Harmonic Impedance", In Proceedings of the IEEE Applied Power Electronics Conference (APEC), vol. 3, pp. 1805-1810, Austin, TX, USA, March, 2005.

[Ryc 05b] W.R. Ryckaert, K. de Gusseme, D.M. Van de Sype, J.J. Desmet, J.A. Melkebeek, "Adding Damping in Power Distribution Systems by means of Power Electronic Converters", In Proceedings of the 11th European Conference on Power Electronics and Applications (EPE), Dresden, Germany, Sept. 2005.

[Ryc 04] W.R. Ryckaert, J.J.M. Desmet, J. Driesen, J.A.A. Melkebeek, "The Influence on Harmonic Propagation of the Resistive Shunt Harmonic Impedance Location along a Distribution Feeder and the Influence of Distributed Capacitors", In Proceedings of the IEEE 11th International Conference on Harmonics and Quality of Power (ICHQP), pp. 129-135, NY, USA, Sep. 2004.

[Ryc 02] W.R. Ryckaert, J.A.L. Ghijselen, J.A.A. Melkebeek, "Optimized Loads for Damping Harmonic Propagation", In Proceedings of the IEEE Power Engineering Society Summer Meeting, Chicago, USA, vol. 2, pp. 818-823, July 2002.

[Sai 03] M. Saito, T. Takeshita, N. Matsui, "Modeling and Harmonic Suppression for Power Distribution Systems", IEEE Transactions on Industrial Electronics, Vol. 50, No. 6, pp. 1148-1158, Dec. 2003.

[Sal 00] S.K. Salman and I.M. Rida, "ANN-Based AVC Relay for Voltage Control of Distribution Grid with and without Embedded Generation", International Conference on Electric Utility Deregulation and Restructuring and Power Technologies, Aberdeen UK, 2000.

[Std 01] EN50160, European Standard, "Voltage characteristics of electricity supplied by public distribution systems", 1999, CENELEC, Brussels, Belgium.

[Std 02] IEC 61000-3-2, International Standard, "Limits for harmonic currents emissions (equipment input current ≤ 16 A per phase", 2000, (2, Amendment 1: 2001), IEC, Geneva, Switzerland.

[Std 03] IEEE-Std-519-1992, "IEEE Recommended Practices and requirements for harmonic control in Electrical Power Systems", IEEE, Industry Applications Society and Power Engineering Society, New York, NY, USA, 1992.

[Std 04] EMC-directive (89/336/EEC), European directive, 1989.

[Std 05] DTE grid code Legislation, DTE (Dutch office for Energy Regulation), The Netherlands, April 2005.

[Tao 08] H. Tao, "Integration of sustainable energy sources through power electronic converters in small distributed electricity generation systems", Ph.D. dissertation, Faculty of Electrical Engineering, Eindhoven University of Technology, The Netherlands, 2008.

[Vis 05] K. Visscher, P.J.M. Heskes, "A method for operational grid and load impedance measurements", International Conference on Future Power Systems (FPS), Amsterdam, Nov. 2005.

[Wad 02] K. Wada, H. Fujita, H. Akagi, "Considerations of a Shunt Active Filter Based on Voltage Detection for Installation on a Long Distribution Feeder", IEEE Transactions on Industry Applications, Vol. 38, No. 4, pp. 1123-1130, July/August 2002.

[WEC 04] World Energy Council (WEC), "Energy End-Use Technologies for the 21st Century", A report of the WEC, ISBN 0 946121 15 X, 2004.

List of symbols and abbreviations

Symbols

c_n	complex factor [-]
C_p	parallel capacitance [F]
C_s	series capacitance [F]
F	frequency [Hz]
F_0	fundamental frequency of the Fourier transformation [Hz]
$f(t)$	function in the time domain [-]
$H(s)$	transfer function in the Laplace domain [-]
$H[v_{out}/v_{in}]$	v_{in} to v_{out} transfer function in the Laplace domain [-]
$\overset{0}{H}$	round going loop gain in the Laplace domain [-]
i	current [A]
i_{ac}	alternating current [A]
I_{dc}	direct current [A]
i_{RMS}	Root Mean Square current [A]
I_h	harmonic current [A]
k	constant [-]
L_p	parallel inductance [H]
L_s	series inductance [H]
N	total number of samples [-]
p_q	general pole [-]
R_p	parallel resistance [ohm]
R_s	series resistance [ohm]
s	complex frequency in the Laplace domain [-]

T	period time [s]
T_s	sample time [s]
V	voltage [V]
v_{ac}	alternating voltage [V]
V_{dc}	direct voltage [V]
V_{grid}	voltage of the grid [V]
v_{RMS}	Root Mean Square voltage [V]
v_{sum}	summated voltage [V]
Z	impedance [ohm]
Z_{grid}	impedance of the grid [ohm]
Z_{home}	impedance of cabling inside the home [ohm]
$Z_{inverter}$	output impedance of the inverter [ohm]
Z_{load}	impedance of the load [ohm]
z_p	general zero [-]
Δi	change in current [A]
Δv	change in voltage [V]
τ	time constant [s]
ω	angular frequency [rad/s]
ω_f	fundamental angular frequency [rad/s]

Abbreviations

AC	Alternating Current
A/D	Analogue/Digital
Al	Aluminum
CHP	Combined Heat and Power
CPL	Constant Power Load
DC	Direct Current
DG	Distributed Generation

DFT	Discrete Fourier Transformation
DSO	Distribution System Operator
DSP	Digital Signal Processor
EMI	Electro Magnetic Interference
ESR	Equivalent Series Resistance
FFT	Fast Fourier Transformation
H	Henry
Hz	hertz
kVAr	kilo Volt-Ampere reactive
kW	kilo Watt
LCD	Liquid Cristal Display
LV	Low Voltage
MPP	Maximum Power Point
MV	Medium Voltage
MVA	Mega Volt-Ampere
NDI	Negative Differential Impedance
PC	Personal Computer
PCC	Point of Common Coupling
PFC	Power Factor Corrector
PI	Proportional Integrating
PLL	Phase Locked Loop
PoC	Point of Connection
pu	per unit
PV	Photovoltaic
PWM	Pulse Width Modulation
RMS	Root Mean Square
THD	Total Harmonic Distortion

VA	Volt-Ampere
VPCR	Virtual Parallel Capacitance Reduction
VRHD	Virtual Resistive Harmonic Damping
VSC	Voltage Source Converter

Acknowledgement

From the start to the finish of this four years Ph.D. work I have been supported by many people from which I like to address some in particular.

First of all, I would like to thank Gerrit Jan Schaeffer who was at the Energy Research Centre of the Netherlands (ECN), he convinced me that I could obtain a Ph.D. and gave me support for this route. I like to thank Martin Scheepers of ECN for continuing this support after changing situations at ECN. I want to express my appreciation to professors Ton Backx, Jan Blom, Wil Kling and Johanna Myrzik, for accepting me as a Ph.D. student at the Technical University of Eindhoven.

My special thanks goes to my professor Wil Kling for his great help and confidence in me. I will always remember his valuable thoroughly review of this thesis. I thank my copromotor Johanna Myrzik for her review and the discussions I had with her about this work. My special thanks goes also to Paulo Ribeiro for his valuable support in helping me to improve this work. I also thank all the Ph.D. students for their interest and fellow-feeling.

I am grateful to Paulo Ribeiro, Antonello Monti and Pavol Bauer for being a member of the core committee for this thesis and for their review. Also I thank the other members Elena Lomonova and Martin Scheepers.

Thanks to my ECN colleagues of the Engineering and Service (E&S) department to help me solving a software problem.

The work presented in this thesis was part of the research project ‘Voltage quality in future infrastructures’ (‘Kwaliteit van de spanning in Toekomstige Infrastructuren (KTI)’ in Dutch). I thank all the members of the steering committee for their feedback during the half year meetings.

Finally, I want to thank my life partner Edith van Wolferen for her support throughout the years.

List of publications

Journal articles

[1] P.J.M. Heskes, J.M.A. Myrzik, W.L. Kling, "Impact of Distribution System's Non-Linear Loads with Constant Power on Grid Voltage", John Wiley European Transactions on Electrical Power (ETEP) Journal, vol. 21, Issue 1, pp. 698-711, 2011.

[2] P.J.M. Heskes, J.M.A. Myrzik, W.L. Kling, "A Harmonic Impedance Measurement System for Reduction of Harmonics in the Electricity Grid", International Journal of Distributed Energy Resources, vol. 5, no. 4, pp. 315-331, Oct./Dec. 2009.

[3] S. Islam, A. Woyte, R.J.M. Belmans, P.J.M. Heskes, P.M. Rooij, R. Hogedoorn, "Cost effective second generation AC-modules: Development and testing aspects", Science Direct, Elsevier, Renewable Energy 31, pp. 1897–1920, 2006.

[4] S. Islam, A. Woyte, R.J.M. Belmans, P.J.M. Heskes, P.M. Rooij, "Investigating performance, reliability and safety parameters of photovoltaic module inverter: Test results and compliances with the standards", Science Direct, Elsevier, Renewable Energy 31, pp. 1157–1181, 2006.

[5] A. Kotsopoulos, P.J.M Heskes, M.J. Jansen, "Zero-Crossing Distortion in Grid-Connected PV Inverters", IEEE Transactions on Industrial Electronics, vol. 52, no. 2, pp. 558-565, 2005.

[6] P.J.M. Heskes, J.F.G. Cobben, H.H.C. de Moor, "Harmonic distortion in residential areas due to large scale PV implementation is predictable", International Journal of Distributed Energy Resources, vol. 1, no. 1, pp. 17-32, Jan./Mar., 2005.

[7] J.H.R. Enslin, P.J.M. Heskes, "Harmonic Interaction Between Large Numbers of Photovoltaic Inverters and the Distribution Grid", IEEE

Transactions on Power Electronics, vol. 19, no. 6, pp. 1586-1593, Nov. 2004.

Conference papers

[1] P.J.M. Heskes, J.M.A. Myrzik, W.L. Kling, "Ancillary Services for Minimizing the Impact of Resonances in Low Voltage Grids by Power Electronics based Distributed Generators", IEEE Power Energy Systems General Meeting, Detroit, Michigan, USA, July 24-29, 2011, *accepted*.

[2] P.J.M. Heskes, J.M.A. Myrzik, W.L. Kling, "Harmonic Distortion and Oscillatory Voltages and the Role of Negative Impedance", IEEE Power Energy Systems General Meeting, Minneapolis, USA, July 25-29, 2010.

[3] P.J.M. Heskes, J.M.A. Myrzik, W.L. Kling, "Power Electronic Loads with Negative Differential Impedance in a Low Voltage Distribution System", 20th International Conference on Electricity Distribution, Cired, Prague, 8-11 June 2009.

[4] E. de Jong, E. de Meulemeester, P.J.M. Heskes, "Design and realisation of a unique MV converter implemented in a new power electronic equipment test laboratory for emerging MV applications", IEEE PES General Meeting - 2008.

[5] P.J.M. Heskes, J.M.A. Myrzik, W.L. Kling, "Survey of Harmonic Reduction Techniques Applicable as Ancillary Service of Dispersed Generators (DG)", IEEE Young Researchers Symposium, Technical University of Eindhoven, The Netherlands, February 7-8, 2008.

[6] P.J.M. Heskes, J.L. Duarte, "Harmonic reduction as ancillary service by inverters for Distributed Energy Resources (DER) in electricity distribution grids", Cired, Vienna, May 2007.

[7] K. Visscher, P.J.M. Heskes, "A method for operational grid and load impedance measurements", International Conference on Future Power Systems, FPS, Amsterdam, Nov. 2005.

[8] J.F.G. Cobben, W.L. Kling, P.J.M. Heskes, H.E. Oldenkamp, "Predict the level of harmonic distortion due to Dispersed Generation", Cired, Prague, June 2005.

[9] H.E Oldenkamp, I. de Jong, P.J.M. Heskes, P.M. Rooij, H.H.C. de Moor, “Additional Requirements for PV inverters necessary to maintain utility grid quality in case of high penetration of PV generators”, 19th European Photovoltaic Solar Energy Conference and Exhibition, Paris, France, June 2004.

[10] P.J.M. Heskes, P.M. Rooij, H.H.C. de Moor, S. Islam, A. Woyte, J. Wouters, “Development, Production and Verification of the Second Generation of AC-modules (PV2GO), increasing life time and lowering cost-price by reducing the number of components significantly”, 19th European Photovoltaic Solar Energy Conference and Exhibition, Paris, France, June 2004.

[11] J.H.R. Enslin, W.T.J. Hulshorst, A.M.S. Atmadji, P.J.M. Heskes, A. Kotsopoulos, J.F.G. Cobben, P. Van der Sluijs, “Harmonic Interaction Between Large Numbers of Photovoltaic Inverters and the Distribution Grid”, IEEE Proceedings, Powertech Extended Digest, 2003.

[12] J.H.R. Enslin, P.J.M. Heskes, an adapted version of: “Harmonic Interaction between a Large Number of Distributed Power Inverters and the Distribution Grid”, Power Electronics Specialists Conference (PESC-2003), Acapulco, Mexico, 2003.

[13] J.H.R. Enslin, P.J.M. Heskes, another adapted version of: “Harmonic Interaction between a Large Number of Distributed Power Inverters and the Distribution Grid”, presented at PELS, 2003.

[14] J.H.R. Enslin, W.T.J. Hulshorst, J.F. Groeman, P.J.M. Heskes, “Grid Interaction Considerations of Photovoltaic Rich Grids”, Cigre, 2003.

[15] P.J.M. Heskes, J.H.R. Enslin, “Power Quality Behavior of Different Photovoltaic Inverter Topologies”, PCIM-2003, 24th International Conference Nürnberg, Germany, 2003.

[16] A. Kotsopoulos, P.J.M Heskes, M.J. Jansen, “Zero-Crossing Distortion in Grid-Connected PV Inverters”, IECON, 2002.

[17] A. Kotsopoulos, J.L. Duarte, M.A.M. Hendrix, P.J.M. Heskes, “Islanding Behavior of Grid-Connected PV Inverters Operating Under Different Control Schemes”, PESC, 2002.

[18] E.C. Molenbroek, P.J.M. Heskes, F. Groeman, R.J.C. van Zolingen, "PV Standardisation Activities in The Netherlands, PV in Europe, from Technology to Energy Solutions", Rome, Italy, October 2002.

[19] P.J.M Heskes, J.A. Eikelboom, P.M. Rooij, G. Bettenwort, B. Margaritas, E. Ortjohann, "A New Low-cost Modular Inverter Using Advanced ASIC Control, rigorous performance tests result in rapid adaptation to market demands", 17th European Photovoltaic Solar Energy Conference and Exhibition, Munich, Germany, October 2001.

[20] P.M. Rooij, J.A. Eikelboom, P.J.M Heskes, "Reliability testing of grid connected PV inverters", 16th European Photovoltaic Solar Energy Conference and Exhibition, Glasgow, Scotland, May 2000.

Curriculum vitae

Peter J.M. Heskes was born in The Hague, the Netherlands, in 1955. He received the Electronic Engineer degree from the HTS, The Hague, The Netherlands, in 1980. From 1980 to 1999, he was with a large Dutch electronic-product manufacturer for the military and professional market. He started there as a Product Designer and became a Product Manager of the power-electronics department. His work was related to power electronics converters. In 2000, he started as a Project Co-Coordinator on Intelligent Energy Management at the Energy Research Centre of the Netherlands (ECN), Petten, The Netherlands. His current work is related to power electronics converter technology in grid connected distributed energy systems. In 2007 he started to combine his work at ECN with a position as a Ph.D. student at the Electrical Energy Systems group of the Eindhoven University of Technology. His research interests are power quality issues related to the interaction of power electronics converters of distributed energy systems with the electricity grid.